

ACI 440.1R-15

Guide for the Design and Construction of Structural Concrete Reinforced with Fiber-Reinforced Polymer (FRP) Bars

Reported by ACI Committee 440



American Concrete Institute
Always advancing



Guide for the Design and Construction of Structural Concrete Reinforced with Fiber-Reinforced Polymer (FRP) Bars

Copyright by the American Concrete Institute, Farmington Hills, MI. All rights reserved. This material may not be reproduced or copied, in whole or part, in any printed, mechanical, electronic, film, or other distribution and storage media, without the written consent of ACI.

The technical committees responsible for ACI committee reports and standards strive to avoid ambiguities, omissions, and errors in these documents. In spite of these efforts, the users of ACI documents occasionally find information or requirements that may be subject to more than one interpretation or may be incomplete or incorrect. Users who have suggestions for the improvement of ACI documents are requested to contact ACI via the errata website at <http://concrete.org/Publications/DocumentErrata.aspx>. Proper use of this document includes periodically checking for errata for the most up-to-date revisions.

ACI committee documents are intended for the use of individuals who are competent to evaluate the significance and limitations of its content and recommendations and who will accept responsibility for the application of the material it contains. Individuals who use this publication in any way assume all risk and accept total responsibility for the application and use of this information.

All information in this publication is provided “as is” without warranty of any kind, either express or implied, including but not limited to, the implied warranties of merchantability, fitness for a particular purpose or non-infringement.

ACI and its members disclaim liability for damages of any kind, including any special, indirect, incidental, or consequential damages, including without limitation, lost revenues or lost profits, which may result from the use of this publication.

It is the responsibility of the user of this document to establish health and safety practices appropriate to the specific circumstances involved with its use. ACI does not make any representations with regard to health and safety issues and the use of this document. The user must determine the applicability of all regulatory limitations before applying the document and must comply with all applicable laws and regulations, including but not limited to, United States Occupational Safety and Health Administration (OSHA) health and safety standards.

Participation by governmental representatives in the work of the American Concrete Institute and in the development of Institute standards does not constitute governmental endorsement of ACI or the standards that it develops.

Order information: ACI documents are available in print, by download, on CD-ROM, through electronic subscription, or reprint and may be obtained by contacting ACI.

Most ACI standards and committee reports are gathered together in the annually revised ACI Manual of Concrete Practice (MCP).

American Concrete Institute
38800 Country Club Drive
Farmington Hills, MI 48331
Phone: +1.248.848.3700
Fax: +1.248.848.3701

Guide for the Design and Construction of Structural Concrete Reinforced with Fiber-Reinforced Polymer (FRP) Bars

Reported by ACI Committee 440

Carol K. Shield, Chair
William J. Gold, Secretary
Tarek Alkhrdaji
Charles E. Bakis
Lawrence C. Bank
Abdeldjelil Belarbi
Brahim Benmokrane
Luke A. Bisby
Gregg J. Blaszak
Hakim Bouadi
Timothy E. Bradberry
Gordon L. Brown Jr.
Vicki L. Brown
John P. Busel
Raafat El-Hacha
Garth J. Fallis
Amir Z. Fam
Nabil F. Grace
Mark F. Green
Zareh B. Gregorian

Doug. D. Gremel
Shawn P. Gross*
H. R. Trey Hamilton III
Issam E. Harik
Kent A. Harries
Mark P. Henderson
Bohdan N. Horeczko
Michael W. Lee
Maria Lopez de Murphy
Ibrahim M. Mahfouz
Amir Mirmiran
John J. Myers
Antonio Nanni
Ayman M. Okeil
Carlos E. Ospina
Renato Paretto
Max L. Porter
Andrea Prota
Hayder A. Rasheed
Sami H. Rizkalla

Rajan Sen
Rudolf Seracino
Pedro F. Silva
Khaled A. Soudki
Samuel A. Steere III
Jay Thomas
Houssam A. Toutanji
J. Gustavo Tumialan
Milan Vatovec
David White
Sarah E. Witt

Consulting Members
P. N. Balaguru
Craig A. Ballinger
Harald G. F. Budelmann
C. J. Burgoyne
Elliot P. Douglas
Rami M. Elhassan
David M. Gale

Russell Gentry
Arie Gerritse
Srinivasa L. Iyer
Koichi Kishitani
Howard S. Kliger
Kyuichi Maruyama
Antoine E. Naaman
Hajime Okamura
Mark A. Postma
Ferdinand S. Rostasy
Surendra P. Shah
Mohsen Shahawy
Yasuhisa Sonobe
Minoru Sugita
Luc R. Taerwe
Ralejs Tepfers
Taketo Uomoto
Paul Zia

*Subcommittee Chair.

Fiber-reinforced polymer (FRP) materials have emerged as an alternative for producing reinforcing bars for concrete structures. Fiber-reinforced polymer reinforcing bars offer advantages over steel reinforcement because they are noncorrosive. Some FRP bars are nonconductive as well. Due to other differences in the physical and mechanical behavior of FRP materials versus steel, unique guidance on the engineering and construction of concrete structures reinforced with FRP bars is necessary. Other countries and regions, such as Japan, Canada, and Europe have established design and construction guidelines specifically for the use of FRP bars as concrete reinforcement. This guide offers general information on the history and use of FRP reinforcement, a description

of the unique material properties of FRP, and guidelines for the design and construction of structural concrete members reinforced with FRP bars. This guide is based on the knowledge gained from worldwide experimental research, analytical work, and field applications of FRP reinforcement.

Keywords: anchorage (structural); aramid fiber; carbon fiber; crack control; concrete construction; concrete slabs; cover; creep rupture; deflections; design examples; durability; fiber-reinforced polymer; flexural strength; glass fiber; moments; reinforced concrete; reinforcement; serviceability; shear strength; spans; strength analysis; stresses; structural concrete; structural design.

CONTENTS

CHAPTER 1—INTRODUCTION AND SCOPE, p. 2

1.1—Introduction, p. 2

1.2—Scope, p. 3

ACI Committee Reports, Guides, and Commentaries are intended for guidance in planning, designing, executing, and inspecting construction. This document is intended for the use of individuals who are competent to evaluate the significance and limitations of its content and recommendations and who will accept responsibility for the application of the information it contains. ACI disclaims any and all responsibility for the stated principles. The Institute shall not be liable for any loss or damage arising there from.

Reference to this document shall not be made in contract documents. If items found in this document are desired by the Architect/Engineer to be a part of the contract documents, they shall be restated in mandatory language for incorporation by the Architect/Engineer.

ACI 440.1R-15 supersedes ACI 440.1R-06 and was adopted and published March 2015.

Copyright © 2015, American Concrete Institute.

All rights reserved including rights of reproduction and use in any form or by any means, including the making of copies by any photo process, or by electronic or mechanical device, printed, written, or oral, or recording for sound or visual reproduction or for use in any knowledge or retrieval system or device, unless permission in writing is obtained from the copyright proprietors.

CHAPTER 2—NOTATION AND DEFINITIONS, p. 3

- 2.1—Notation, p. 3
- 2.2—Definitions, p. 5

CHAPTER 3—BACKGROUND, p. 6

- 3.1—Historical development, p. 6
- 3.2—History of use, p. 6
- 3.3—Material characteristics, p. 8

CHAPTER 4—MATERIAL CHARACTERISTICS, p. 9

- 4.1—Physical properties, p. 9
- 4.2—Mechanical properties and behavior, p. 10
- 4.3—Time-dependent behavior, p. 11
- 4.4—Effects of high temperatures and fire, p. 13

CHAPTER 5—DURABILITY, p. 14

- 5.1—Accelerated durability testing, p. 14
- 5.2—Durability of FRP bars, p. 14
- 5.3—Durability of bond between FRP and concrete, p. 15

CHAPTER 6—GENERAL DESIGN CONSIDERATIONS, p. 16

- 6.1—Design philosophy, p. 16
- 6.2—Design material properties, p. 16

CHAPTER 7—FLEXURE, p. 16

- 7.1—General considerations, p. 16
- 7.2—Flexural strength, p. 17
- 7.3—Serviceability, p. 20
- 7.4—Creep rupture and fatigue, p. 24

CHAPTER 8—SHEAR, p. 24

- 8.1—General considerations, p. 24
- 8.2—Shear strength of FRP-reinforced members, p. 24
- 8.3—Detailing of shear stirrups, p. 26
- 8.4—Shear strength of FRP-reinforced two-way concrete slabs, p. 26

CHAPTER 9—SHRINKAGE AND TEMPERATURE REINFORCEMENT, p. 27

- 9.1—Minimum FRP reinforcement ratio, p. 27

CHAPTER 10—DEVELOPMENT AND SPLICES OF REINFORCEMENT, p. 27

- 10.1—Development of stress in straight bar, p. 27
- 10.2—Development length of bent bar, p. 29
- 10.3—Development of positive moment reinforcement, p. 30
- 10.4—Tension lap splice, p. 30

CHAPTER 11—DESIGN EXAMPLES, p. 31

Example 1—Flexural (moment) strength using equivalent rectangular concrete stress distribution (compression-controlled section), p. 31

Example 2—Flexural (moment) strength using equivalent rectangular concrete stress distribution (tension-controlled section), p. 32

Example 3—Design of a rectangular beam with tension reinforcement only, p. 34

Example 4—Design of one-way solid slab, p. 36

Example 5—Distribution of reinforcement for effective crack control, p. 39

Example 6—Deflection of a simple-span nonprestressed rectangular beam, p. 42

Example 7—Creep rupture stress check under sustained loads, p. 45

Example 8—Design for shear (members subject to shear and flexure only), p. 46

Example 9—Development of bars in tension (compression-controlled or transition zone section), p. 49

Example 10—Development of bars in tension (tension-controlled section), p. 50

Example 11—Shear strength of slab at column support, p. 51

Example 1M—Flexural (moment) strength using equivalent rectangular concrete stress distribution (compression-controlled section), p. 52

Example 2M—Flexural (moment) strength using equivalent rectangular concrete stress distribution (tension-controlled section), p. 54

Example 3M—Design of a rectangular beam with tension reinforcement only, p. 56

Example 4M—Design of one-way solid slab, p. 58

Example 5M—Distribution of reinforcement for effective crack control, p. 61

Example 6M—Deflection of a simple-span nonprestressed rectangular beam, p. 63

Example 7M—Creep rupture stress check under sustained loads, p. 66

Example 8M—Design for shear (members subject to shear and flexure only), p. 68

Example 9M—Development of bars in tension (compression-controlled or transition zone section), p. 70

Example 10M—Development of bars in tension (tension-controlled section), p. 71

Example 11M—Shear strength of slab at column support, p. 73

CHAPTER 12—REFERENCES, p. 74

Authored documents, p. 74

APPENDIX A—SLABS-ON-GROUND, p. 83

A.1—Design of plain concrete slabs, p. 83

A.2—Design of slabs with shrinkage and temperature reinforcement, p. 83

CHAPTER 1—INTRODUCTION AND SCOPE**1.1—Introduction**

Conventional concrete structures are reinforced with nonprestressed and prestressed steel. The steel is initially protected against corrosion by the alkalinity of the concrete, usually resulting in durable and serviceable construction. For many structures subjected to aggressive environments, such as marine structures, bridges, and parking garages

exposed to deicing salts, combinations of moisture, temperature, and chlorides reduce the alkalinity of the concrete and result in the corrosion of reinforcing steel. The corrosion process ultimately causes concrete deterioration and loss of serviceability.

Composite materials made of fibers embedded in a polymeric resin, also known as fiber-reinforced polymer (FRP), are an alternative to steel reinforcement for concrete structures. Fiber-reinforced polymer reinforcing materials are made of continuous aramid fiber (AFRP), carbon fiber (CFRP), or glass fiber (GFRP) embedded in a resin matrix. Examples of FRP reinforcing bars are shown in Fig. 1.1. Because FRP materials are nonmagnetic and noncorrosive, the problems of electromagnetic interference and steel corrosion can be avoided with FRP reinforcement. Additionally, FRP materials exhibit several properties, such as high tensile strength, that make them suitable for use as structural reinforcement (ACI 440R; Benmokrane and Rahman 1998; Burgoyne 2001; Cosenza et al. 2001; Dolan et al. 1999; El-Badry 1996; Figueiras et al. 2001; Humar and Razaqpur 2000; Iyer and Sen 1991; Japan Society of Civil Engineers (JSCE) 1992, 1997a; Nanni 1993a; Nanni and Dolan 1993; Neale and Labossiere 1992; Saadatmanesh and Ehsani 1998; Taerwe 1995; Teng 2001; White 1992).

The mechanical behavior of FRP reinforcement differs from the behavior of conventional steel reinforcement. Accordingly, a change in the traditional design philosophy of concrete structures is needed for FRP reinforcement. Fiber-reinforced polymer materials are anisotropic and are characterized by high tensile strength only in the direction of the reinforcing fibers. This anisotropic behavior affects the shear strength and dowel action of FRP bars as well as the bond performance. Furthermore, FRP materials do not yield; rather, they are elastic until failure. Design procedures should account for a lack of ductility in structural concrete members reinforced with FRP bars.

This guide was first developed in 2001 as a guide for the design and construction of structural concrete with FRP bars. Other countries and regions, such as Japan (Japan Society of Civil Engineers 1997b), Canada (CAN/CSA-S6-06, CAN/CSA-S806-12), and Europe (fib 2007, 2010) have also established similar design-related documents. There is adequate analytical and experimental information on FRP-reinforced concrete, and significant field experience implementing this knowledge. Successful applications worldwide using FRP composite reinforcing bars during the past few decades have demonstrated that it can be used successfully and practically. Research and field implementation is ongoing and design recommendations continue to evolve. When using this technology, exercise judgment as to the appropriate application of FRP reinforcement and be aware of its limitations as discussed in this guide.

Note: Any reference to ACI 318 in this document without a year designation refers to ACI 318-11. All exceptions will have a specific year designation.



Fig. 1.1—Examples of FRP reinforcing bars.

1.2—Scope

This guide provides recommendations for the design and construction of FRP-reinforced concrete structures for nonprestressed FRP reinforcement; concrete structures prestressed with FRP tendons are covered in ACI 440.4R. The basis for this guide is knowledge gained from worldwide experimental research, analytical research work, and field applications of FRP reinforcement.

Design recommendations are based on the current knowledge and are intended to supplement existing codes and guidelines for conventionally reinforced concrete structures and to provide licensed design professionals and building officials with assistance in the design and construction of structural concrete reinforced with FRP bars.

ACI 440.3R provides a comprehensive list of test methods and material specifications to support design and construction guidelines. ACI 440.5 provides specification details for construction with FRP reinforcing bars. Material specifications for FRP bars are found in ACI 440.6.

The use of FRP reinforcement in combination with steel reinforcement for structural concrete is not addressed in this guide.

CHAPTER 2—NOTATION AND DEFINITIONS

2.1—Notation

a	=	depth of equivalent rectangular stress block, in. (mm)
A_f	=	area of fiber-reinforced polymer (FRP) reinforcement, in. ² (mm ²)
$A_{f,bar}$	=	area of one FRP bar, in. ² (mm ²)
$A_{f,min}$	=	minimum area of FRP reinforcement needed to prevent failure of flexural members upon cracking, in. ² (mm ²)
$A_{f,sh}$	=	area of shrinkage and temperature FRP reinforcement per linear ft (m), in. ² (mm ²)
A_{fv}	=	amount of FRP shear reinforcement within spacing s , in. ² (mm ²)
$A_{fv,min}$	=	minimum amount of FRP shear reinforcement within spacing s , in. ² (mm ²)
A_s	=	area of tension steel reinforcement, in. ² (mm ²)

b	= width of rectangular cross section, in. (mm)	f_y	= specified yield stress of nonprestressed steel reinforcement, psi (MPa)
b_o	= perimeter of critical section for slabs and footings, in. (mm)	h	= overall height of flexural member, in. (mm)
b_w	= width of the web, in. (mm)	I	= moment of inertia, in. ⁴ (mm ⁴)
c	= distance from extreme compression fiber to the neutral axis, in. (mm)	I_{cr}	= moment of inertia of transformed cracked section, in. ⁴ (mm ⁴)
c_b	= distance from extreme compression fiber to neutral axis at balanced strain condition, in. (mm)	I_e	= effective moment of inertia, in. ⁴ (mm ⁴)
c_c	= clear cover, in. (mm)	I_{e+}	= effective moment of inertia at location of maximum positive moment, in. ⁴ (mm ⁴)
C	= spacing or cover dimension, in. (mm)	I_{e1-}	= effective moment of inertia at location of maximum negative moment at near end of span, in. ⁴ (mm ⁴)
C_E	= environmental reduction factor for various fiber type and exposure conditions	I_{e2-}	= effective moment of inertia at location of maximum negative moment at far end of span, in. ⁴ (mm ⁴)
d	= distance from extreme compression fiber to centroid of tension reinforcement, in. (mm)	I_g	= gross moment of inertia, in. ⁴ (mm ⁴)
d_b	= diameter of reinforcing bar, in. (mm)	k	= ratio of depth of neutral axis to reinforcement depth
d_c	= thickness of concrete cover measured from extreme tension fiber to center of bar or wire location closest thereto, in. (mm)	k_b	= bond-dependent coefficient
$d_{c,side}$	= thickness of concrete cover measured from side face of member to center of longitudinal bar or wire location closest thereto, in. (mm)	K_1	= parameter accounting for boundary conditions
E_c	= modulus of elasticity of concrete, psi (MPa)	K_4	= coefficient used in computing development length of bent bar
E_f	= design or guaranteed modulus of elasticity of FRP defined as mean modulus of sample of test specimens ($E_f = E_{f,ave}$), psi (MPa)	ℓ	= span length of member, ft (m)
$E_{f,ave}$	= average modulus of elasticity of FRP, psi (MPa)	ℓ_a	= additional embedment length at support or at point of inflection, in. (mm)
E_s	= modulus of elasticity of steel, psi (MPa)	ℓ_{bhf}	= basic development length of FRP standard hook in tension, in. (mm)
f'_c	= specified compressive strength of concrete, psi (MPa)	ℓ_d	= development length, in. (mm)
$\sqrt{f'_c}$	= square root of specified compressive strength of concrete, psi (MPa)	ℓ_e	= embedded length of reinforcing bar, in. (mm)
f_f	= stress in FRP reinforcement in tension, psi (MPa)	ℓ_{thf}	= length of tail beyond hook in FRP bar, in. (mm)
f_{fb}	= strength of bent portion of FRP bar, psi (MPa)	L	= distance between joints in slab-on-grade, ft (m)
f_{fe}	= bar stress that can be developed for embedment length ℓ_e , psi (MPa)	M_a	= maximum service load moment in member, lb-in. (N-mm)
f_{fr}	= required bar stress, psi (MPa)	M_{cr}	= cracking moment, lb-in. (N-mm)
f_{fs}	= stress level induced in FRP at service loads, psi (MPa)	M_n	= nominal moment capacity, lb-in. (N-mm)
$f_{fs,sus}$	= stress level induced in FRP by sustained service loads, psi (MPa)	$M_{s,sus}$	= moment due to sustained service loads, lb-in. (N-mm)
f_{fu}	= design tensile strength of FRP, defined as the guaranteed tensile strength multiplied by the environmental reduction factor ($f_{fu} = C_E f_{fu}^*$), psi (MPa)	M_{serv}	= service level moment
f_{fu}^*	= guaranteed tensile strength of FRP bar, defined as mean tensile strength of sample of test specimens minus three times standard deviation ($f_{fu}^* = f_{fu,ave} - 3\sigma$), psi (MPa)	M_u	= factored moment at section, lb-in. (N-mm)
f_{fv}	= tensile strength of FRP for shear design, taken as smallest of design tensile strength f_{fu} , strength of bent portion of FRP stirrups f_{fb} , or stress corresponding to $0.004E_f$, psi (MPa)	n_f	= ratio of modulus of elasticity of FRP bars to modulus of elasticity of concrete
f_s	= service stress in steel reinforcement, psi (MPa)	r_b	= internal radius of bend in FRP reinforcement, in. (mm)
$f_{s,allow}$	= allowable service stress in steel reinforcement, psi (MPa)	s	= stirrup spacing or pitch of continuous spirals, in. (mm)
$f_{u,ave}$	= mean tensile strength of sample of test specimens, psi (MPa)	s_{max}	= maximum permissible center-to-center bar spacing for flexural crack control, in. (mm)
		T_g	= glass transition temperature, °F (°C)
		u	= average bond stress acting on the surface of FRP bar, psi (MPa)
		V_c	= nominal shear strength provided by concrete, lb (N)
		V_f	= shear resistance provided by FRP stirrups, lb (N)
		V_n	= nominal shear strength at section, lb (N)
		V_s	= shear resistance provided by steel stirrups, lb (N)
		V_u	= factored shear force at section, lb (N)
		w	= maximum allowable crack width, in. (mm)
		w_{slab}	= dead weight of slab, lb/ft ² (N/m ²)

y_t	= distance from centroidal axis of gross section, neglecting reinforcement, to tension face, in. (mm)
α	= top bar modification factor
α_L	= longitudinal coefficient of thermal expansion, $1/^\circ\text{F}$ ($1/^\circ\text{C}$)
α_T	= transverse coefficient of thermal expansion, $1/^\circ\text{F}$ ($1/^\circ\text{C}$)
α_1	= ratio of average stress of equivalent rectangular stress block to f'_c
β	= ratio of distance from neutral axis to extreme tension fiber to distance from neutral axis to center of tensile reinforcement
β_1	= factor taken as 0.85 for concrete strength f'_c up to and including 4000 psi (28 MPa). For strength above 4000 psi (28 MPa), this factor is reduced continuously at a rate of 0.05 per each 1000 psi (7 MPa) of strength in excess of 4000 psi (28 MPa), but is not taken less than 0.65
$\Delta_{(cp+sh)}$	= additional deflection due to creep and shrinkage under sustained loads, in. (mm)
$(\Delta_i)_{sus}$	= immediate deflection due to sustained loads, in. (mm)
$(\Delta/\ell)_{max}$	= limiting deflection-span ratio
ϵ_c	= strain in concrete
ϵ_{cu}	= ultimate strain in concrete
ϵ_f	= strain in FRP reinforcement
$\epsilon_{f,ave}$	= mean tensile strain at rupture of sample of test specimens
ϵ_{fs}	= strain level induced in FRP at service loads
ϵ_{fu}	= design rupture strain of FRP reinforcement, defined as the guaranteed tensile rupture strain multiplied by the environmental reduction factor ($\epsilon_{fu} = C_E \epsilon_{fu}^*$)
ϵ_{fu}^*	= guaranteed rupture strain of FRP reinforcement defined as the mean tensile strain at failure of sample of test specimens minus three times standard deviation ($\epsilon_{fu}^* = \epsilon_{f,ave} - 3\sigma$), in./in. (mm/mm)
ϕ	= strength reduction factor
γ	= parameter to account for the variation in stiffness along the length of the member
η	= ratio of distance from extreme compression fiber to centroid of tension reinforcement (d) to overall height of flexural member (h)
λ	= modification factor reflecting the reduced mechanical properties of lightweight concrete
λ_{Δ}	= multiplier for additional long-term deflection
μ	= coefficient of subgrade friction for calculation of shrinkage and temperature reinforcement
θ	= angle of inclination of stirrups or spirals
ρ'	= ratio of steel compression reinforcement; $\rho' = A_s'/bd$
ρ_b	= steel reinforcement ratio producing balanced strain conditions
ρ_f	= fiber-reinforced polymer reinforcement ratio
ρ_f'	= ratio of FRP compression reinforcement
$\rho_{f,ts}$	= reinforcement ratio for temperature and shrinkage FRP reinforcement

ρ_{fb}	= fiber-reinforced polymer reinforcement ratio producing balanced strain conditions
ρ_{fv}	= ratio of FRP shear reinforcement
ρ_{min}	= minimum reinforcement ratio for steel
σ	= standard deviation
ξ	= time-dependent factor for sustained load

2.2—Definitions

ACI provides a comprehensive list of definitions through an online resource, “ACI Concrete Terminology,” <http://www.concrete.org/tools/concreteterminology.aspx>. Definitions provided herein compliment that source.

alkalinity—the condition of having or containing hydroxyl (OH^-) ions; containing alkaline substances.

aramid fiber—highly oriented organic fiber derived from polyamide incorporating into an aromatic ring structure.

balanced fiber-reinforced polymer reinforcement ratio—an amount and distribution of reinforcement in a flexural member such that in strength design, the tensile fiber-reinforced polymer (FRP) reinforcement reaches its ultimate design strain simultaneously with the concrete in compression reaching its assumed ultimate strain of 0.003.

braiding—a process whereby two or more systems of yarns are intertwined in the bias direction to form an integrated structure; braided material differs from woven and knitted fabrics in the method of yarn introduction into the fabric and the manner by which the yarns are interlaced.

carbon fiber—fiber produced by heating organic precursor materials containing a substantial amount of carbon, such as rayon, polyacrylonitrile (PAN), or pitch in an inert environment.

cross-link—a chemical bond between polymer molecules; increased number of cross-links per polymer molecule increases strength and modulus at the expense of ductility.

deformability factor—ratio of energy absorption (area under the moment-curvature curve) at ultimate strength of the section to the energy absorption at service level.

degradation—deleterious change in the chemical structure, physical properties, or appearance of a FRP composite.

E-glass—a family of glass with a calcium alumina borosilicate composition and a maximum alkali content of 2.0 percent.

endurance limit—the number of cycles of deformation or load that causes a material, test specimen, or structural member to fail.

fiber-reinforced polymer (FRP) bar—composite material formed into a long, slender structural shape suitable for the internal reinforcement of concrete and consisting of primarily longitudinal unidirectional fibers bound and shaped by a rigid polymer resin material.

fiber volume fraction—the ratio of the volume of fibers to the volume of the composite.

fiber weight fraction—the ratio of the weight of fibers to the weight of the composite.

glass fiber—fiber drawn from an inorganic product of fusion that has cooled without crystallizing.

grid—a two-dimensional (planar) or three-dimensional (spatial) rigid array of interconnected FRP bars that form a contiguous lattice that can be used to reinforce concrete.

precursor—for carbon or graphite fiber, the rayon, PAN, or pitch fibers from which carbon and graphite fibers are derived.

pultrusion—continuous process for manufacturing composites that have a uniform cross-sectional shape; process consists of pulling a fiber-reinforcing material through a resin impregnation bath then through a shaping die where the resin is subsequently cured.

vinyl esters—class of thermosetting resins containing ester of acrylic, methacrylic acids, or both, many of which have been made from epoxy resin.

CHAPTER 3—BACKGROUND

3.1—Historical development

The development of fiber-reinforced polymer (FRP) reinforcement can be traced to the expanded use of composites after World War II in the 1940s. The aerospace industry had long recognized the advantages of the high strength and light weight of composite materials and, during the Cold War, advancements in the aerospace and defense industry caused an increase in their use. Furthermore, the rapidly expanding economy of the United States demanded inexpensive materials to meet consumer demands. Pultrusion offered a fast and economical method of forming constant profile parts, and pultruded composites were being used to make golf clubs and fishing poles. It was not until the 1960s, however, that these materials were seriously considered for use as reinforcement in concrete.

Expansion of the national highway systems in the 1950s increased the need to provide year-round maintenance. It became common to apply deicing salts on highway bridges and, as a result, reinforcing steel in these structures and those subject to marine salt experienced extensive corrosion, becoming a major concern and leading to high maintenance cost. Various solutions were investigated, including galvanized coatings, electro-static-spray fusion-bonded (powder resin) coatings, polymer-impregnated concrete, epoxy coatings, alloyed steel bars, and glass FRP reinforcing bars (ACI 440R). Of these options, epoxy-coated steel reinforcement appeared to be the best solution and was therefore implemented in aggressive corrosion environments. Fiber-reinforced polymer reinforcing bar was not considered a viable solution and not commercially available until the late 1970s.

Initially, GFRP bars were considered a viable alternative to steel as reinforcement for polymer concrete because their use eliminated the need to address the incompatibility of thermal expansion characteristics between polymer concrete and steel. The 1980s market demanded nonmetallic reinforcement for specific advanced technology. The largest demand for electrically nonconductive reinforcement was in facilities for MRI medical equipment. FRP reinforcement became the standard in this type of construction. Other uses developed as the advantages of FRP reinforcement became better known and desired, specifically in seawall construc-

tion, substation reactor bases, airport runways, and electronics laboratories (Brown and Bartholomew 1996).

Concern for the deterioration of bridges due to chloride-ion-induced corrosion dates back to the 1970s, and its effects on aging bridges in the United States has become apparent (Boyle and Karbhari 1994). Additionally, detection of corrosion in the commonly used epoxy-coated reinforcing bars increased interest in alternative methods of avoiding corrosion. Once again, FRP reinforcement began to be considered as a general solution to address problems of corrosion in bridge decks and other structures (Benmokrane et al. 1996).

3.2—History of use

Up to the mid-1990s, the Japanese had the most FRP reinforcement applications, with more than 100 demonstration or commercial projects. Fiber-reinforced polymer design provisions were included in the design and construction recommendations of the Japanese Society of Civil Engineering (1997b). In the 2000s, China became the largest user of composite reinforcement for new construction in applications that span from bridge decks to underground works (Ye et al. 2003).

The use of FRP reinforcement in Europe began in Germany with the construction of a prestressed FRP highway bridge in 1986 (Meier 1992). Since the construction of this bridge, programs have been implemented to increase the research and use of FRP reinforcement in Europe (Taerwe 1997).

Canadian civil engineers have developed provisions for FRP reinforcement in the Canadian Highway Bridge Design Code (CAN/CSA-S6-06) and have constructed a number of FRP-reinforced concrete structures. The Headingley Bridge in Manitoba included both CFRP and GFRP reinforcement (Rizkalla 1997). The Floodway Bridge over the Red River in Winnipeg, MB, Canada, was completed in 2006. The bridge comprises 16 spans, each approximately 50 x 143 ft (15.3 x 43.5 m). All concrete elements above the girders are reinforced with GFRP bars. The project consumed 310,000 lb (140,000 kg) of GFRP reinforcing bar, making it the largest nonmetallic-reinforced concrete bridge in the world. Moreover, several bridges have been built in Quebec using GFRP bars in the decks, such as the Wotton Bridge in Wotton, the Magog Bridge on Highway 55 North, the Cookshire-Eaton Bridge on Route 108, and the Val-Alain Bridge on Highway 20 East (El-Salakawy and Benmokrane 2003; El-Salakawy et al. 2003, 2005; Benmokrane et al. 2004, 2007). Some of these bridges have been in service for more than 10 years without any signs of deterioration of the GFRP reinforcement (Mufti et al. 2007, 2011). Consequently, there is a remarkable increase in the use of GFRP bars in Canada where more than 200 bridge structures have been successfully constructed. Straight and bent FRP bars were used for the deck slab, for the concrete barriers and girders of the bridges, or both (Drouin et al. 2011). In addition, GFRP bars have been used in Canada in other concrete structures such as parking garages (Benmokrane et al. 2012), highway concrete pavement (Benmokrane et al. 2007), water tanks (Benmokrane and Mohamed 2014), and incinerators (Beaulieu-Michaud et al. 2013). In the United States, typical uses



Fig. 3.2a—FRP-reinforced deck constructed in Lima, OH (Pierce Street Bridge), in 1999.



Fig. 3.2b—GFRP bars used in the redecking of Dayton, OH, Salem Avenue Bridge in 1999.

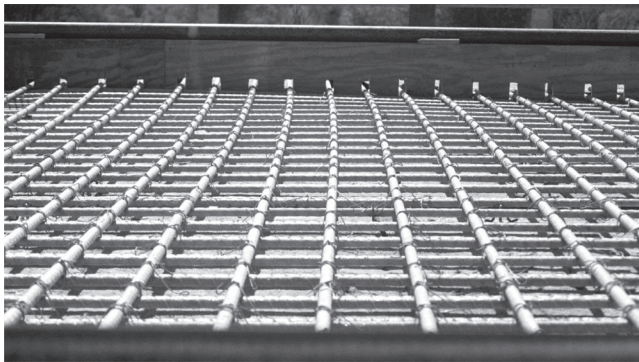


Fig. 3.2c—Transverse view of GFRP bars in Sierrita de la Cruz Creek Bridge deck near Amarillo, TX, in 2000.

of FRP reinforcement have been previously reported (ACI 440R). Figures 3.2a, 3.2b, and 3.2c show applications in bridge deck construction. The use of GFRP bars in MRI hospital room additions is becoming commonplace. Other applications, such as waterfront construction, top mat reinforcing for bridge decks, various precast applications, and ornamental and architectural concrete, are also becoming more frequent. Some of the largest projects include the Gonda Building at the Mayo Clinic in Rochester, MN; the



Fig. 3.2d—Emma Park Bridge deck panel with GFRP reinforcing bars, top and bottom mat.

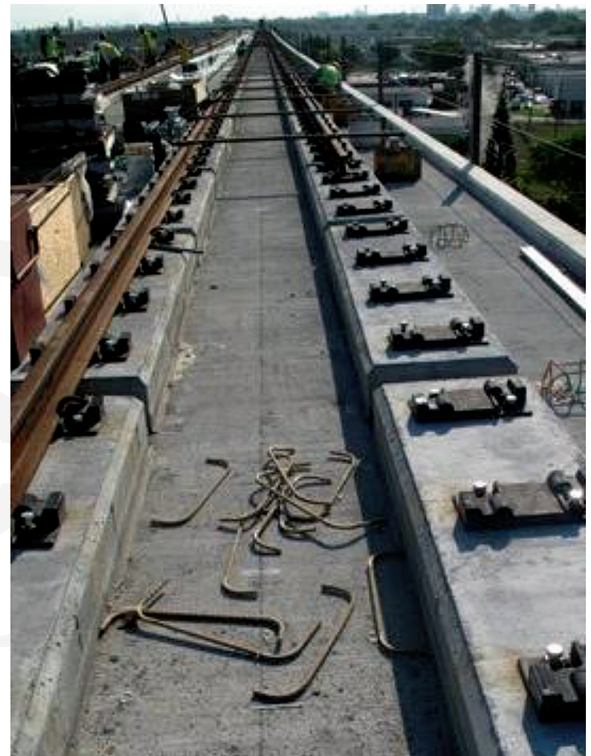


Fig. 3.2e—GFRP bars used in rail plinths.

National Institute of Health in Bethesda, MD, for MRI applications; the bridge on RM 1061 at Sierrita de la Cruz Creek in Potter County, TX, and the bridge at 53rd Avenue in Bettendorf, IA, for deck reinforcement applications (Nanni 2001). Glass FRP bars are making great strides to support accelerated bridge construction with application in precast concrete deck panels. One example is the Emma Park Bridge in Utah constructed in 2009. Glass FRP bars were used in the top and bottom mat, as shown in Fig. 3.2d. In 2011 in Miami, FL, 2.4 miles (3.9 km) of GFRP bar were used in the rail plinths (Fig. 3.2e) for AirportLink, which connects the existing Earlington Heights Station to the new Miami Intermodal Center (MIC). Glass FRP bars were selected, as they provided electrical insulation in the rail bed. Designed by the Florida Department of Transportation, the MIC is a major transportation hub that serves as a central transfer point to different modes of transportation, including Metrorail,



Fig. 3.2f—Construction of seawall with GFRP bars.



Fig. 3.2g—I-635 Bridge over State Ave. (Kansas City, KS).

Metrobus, Tri-Rail, Amtrak, intercity buses, tour buses, taxi cabs, rental cars, and the Automated People Mover (APM) connection to the Miami International Airport (Gremel 2012).

Seawalls constructed with GFRP reinforcing bar are being used in aggressive salt environments to provide long-term service. An example is the seawall that protects the Honoapiilani Highway, Maui, HI. First constructed in 2001 with steel reinforcing bar, the seawall required replacement in 2012, as shown in Fig. 3.2f.

Glass FRP reinforcing bar is also found on larger and high-volume traffic bridges. In 2013, the I-635 bridge deck over State Avenue in Kansas City, KS was replaced with cast-in-place GFRP reinforcing bar. Figure 3.2g shows GFRP reinforcing bar in the top and bottom mat of the deck panels used in the 32 x 232 ft (9.8 x 70.7 m) bridge. Construction bids for this project were the same for installed cost of epoxy-coated as well as GFRP reinforcement.

Tunnel construction, where GFRP reinforcement is used in the portion of the concrete wall to be excavated by the tunnel-boring machine, has become common in many major metropolitan areas of the world.

3.3—Material characteristics

The material characteristics of fiber-reinforced polymer (FRP) reinforcement should be considered when determining whether FRP reinforcement is suitable or necessary in a particular structure. The material characteristics are

Table 3.3—Considerations for the use of fiber-reinforced polymer (FRP) reinforcing bars

Why should FRP bars be considered?	
a)	Impervious to chloride ion and chemical attack
b)	Tensile strength is greater than steel
c)	Light weight – one-fourth to one-fifth the weight of steel reinforcing bar
d)	Transparent to magnetic fields, radio frequencies (glass FRP only)
e)	Thermally and electrically nonconductive (glass FRP only)
f)	Less concrete cover is possible
g)	Admixtures to reduce corrosion are not needed
h)	High fatigue endurance
i)	Easily “consumed” by excavation equipment when used in temporary structures
j)	In corrosive environments, service life much greater than that of steel
k)	Better field handling damage tolerance than epoxy coated steel and no touch-ups required
Differences between FRP and steel	
a)	FRP is linear elastic to failure whereas steel yields
b)	FRP is anisotropic whereas steel is isotropic
c)	Due to lower modulus of FRP bars, design for serviceability often controls
d)	FRP bars have a lower creep-rupture threshold than steel
e)	Coefficient of thermal expansion different in longitudinal and radial directions
f)	Endurance time in fire and elevated temperature applications less than that of steel
g)	Should degradation of FRP bars occur, the degradation mechanism is benign to the surrounding concrete unlike steel that expands and causes failure of the member
Where should FRP bars be considered?	
a)	Any concrete member susceptible to corrosion by chloride ions or chemicals
b)	Any concrete member requiring nonferrous reinforcement due to electromagnetic considerations
c)	As a cost-effective alternative to epoxy-coated and galvanized
d)	As a first cost savings over stainless steel bar
e)	Where machinery will “consume” the reinforced member, mainly in tunneling and mining
f)	Applications requiring thermal nonconductivity
g)	In mass concrete exposed to marine chlorides near chloride exposure in hybrid applications with steel

described in detail in Chapter 5. Table 3.3 provides some guidance on appropriate conditions for the use of FRP bars.

The corrosion resistance of FRP reinforcement is a significant benefit for structures in highly corrosive environments such as seawalls and other marine structures, bridge decks and superstructures exposed to deicing salts, and pavements treated with deicing salts. In structures supporting magnetic resonance imaging (MRI) units or other equipment sensitive to electromagnetic fields, the nonmagnetic properties of FRP reinforcement are of principal importance. Fiber-reinforced polymer reinforcement has a high tensile strength, significant elongation, and exhibits linear stress-strain behavior to failure. The use of FRP reinforcement should be limited to structures that will significantly benefit from other properties, such as the noncorrosive or nonconductive behavior of its materials. Due to lack of experience in its use, FRP reinforcement is not recommended for moment frames or zones where moment redistribution is required.

Research on circular and rectangular columns reinforced with glass FRP (GFRP) or carbon FRP (CFRP) bars and stirrups (De Luca et al. 2010; Tobbi et al. 2012; Pantelides et

al. 2013; Affi et al. 2013) indicates that FRP circular hoops and spirals were found to be efficient in confining concrete and that the GFRP and CFRP bars can develop up to 0.4 percent and 0.7 percent compressive strain, confirming that the FRP bars were effective in resisting compression until after crushing of the concrete (Affi et al. 2013). However, the average load carried by the longitudinal FRP bars in the GFRP- and CFRP-reinforced columns ranged between only 5 percent and 12 percent of the maximum load. Due to the combined effect, the relatively lower elastic modulus of FRP compared with steel and the lower elastic modulus of FRP bars in compression as compared to tension, the maximum contribution of compression FRP reinforcement calculated at ultimate concrete strain (typically at $\epsilon_{cu} = 0.003$) is expected to be small. Therefore, the contribution of FRP reinforcement should be neglected when used as reinforcement in columns, in compression members, or as compression reinforcement in flexural members. It is acceptable for FRP tension reinforcement to experience compression due to moment reversals or changes in load pattern.

There are advantages and disadvantages regarding sustainability when comparing FRP reinforcement to steel reinforcement. Because of the high temperatures required for production, steel reinforcement has a higher carbon footprint than FRP reinforcement (Pearson et al. 2011). Recycling FRP reinforcement, however, is not as easy or commonplace as recycling steel reinforcement. Because FRP does not corrode, life cycle costs associated with FRP reinforced structures are likely to be lower than those for steel-reinforced structures where steel corrosion is a concern (Pearson et al. 2011). Katz (2004) compared the environmental impact of FRP-reinforced pavements to steel-reinforced pavements and determined that the FRP reinforcement had a significantly smaller environmental impact than steel-reinforced pavement over the pavement lifetime.

CHAPTER 4—MATERIAL CHARACTERISTICS

This chapter presents physical and mechanical properties of fiber-reinforced polymer (FRP) reinforcing bars to provide a fundamental understanding of the behavior of these bars and the properties that affect their use in concrete structures. Furthermore, the effects of factors, such as loading history and duration, temperature, and moisture, on the properties of FRP bars are discussed.

Fiber-reinforced polymer bars are anisotropic in nature and can be manufactured using a variety of techniques such as pultrusion, braiding, and weaving (Bank 1993; Bakis 1993). Factors such as fiber volume, fiber type, resin type, fiber orientation, dimensional effects, and quality control during manufacturing all play a major role in defining the characteristics of an FRP bar. The material characteristics described in this chapter may not apply to all commercially available products. Therefore, the manufacturer's material data should be consulted for specific product properties. In addition, several consensus-based test methods for FRP reinforcement for use in structural concrete are presented (ACI 440.3R; ASTM D7205; ASTM D7337; ASTM D7617; ASTM D7705; Japan Society of Civil Engineers 1997b).

Table 4.1.1—Typical densities of reinforcing bars, lb/ft³ (g/cm³)

Steel	GFRP	CFRP	AFRP
493.00 (7.90)	77.8 to 131.00 (1.25 to 2.10)	93.3 to 100.00 (1.50 to 1.60)	77.80 to 88.10 (1.25 to 1.40)

Table 4.1.2—Typical coefficients of thermal expansion for reinforcing bars*

Direction	CTE, $\times 10^{-6}/^{\circ}\text{F}$ ($\times 10^{-6}/^{\circ}\text{C}$)				
	Steel	GFRP	CFRP	AFRP	Concrete [†]
Longitudinal, α_L	6.5 (11.7)	3.3 to 5.6 (6.0 to 10.0)	-4.0 to 0.0 (-9.0 to 0.0)	-3.3 to -1.1 (-6 to -2)	4 to 6 (7.2 to 10.8)
Transverse, α_T	6.5 (11.7)	11.7 to 12.8 (21.0 to 23.0)	41 to 58 (74.0 to 104.0)	33.3 to 44.4 (60.0 to 80.0)	4 to 6 (7.2 to 10.8)

*Typical values for fiber volume fraction ranging from 0.5 to 0.7.

[†]Mindess et al. (2003).

4.1—Physical properties

4.1.1 Density—Fiber-reinforced polymer bars have a density ranging from 77.8 to 131.3 lb/ft³ (1.25 to 2.1 g/cm³), one-sixth to one-fourth that of steel (Table 4.1.1). Reduced weight lowers transportation costs and eases handling of the bars on the project site.

4.1.2 Coefficients of thermal expansion—The coefficients of thermal expansion of FRP bars vary in the longitudinal and transverse directions, depending on the types of fiber, resin, and volume fraction of fiber. The longitudinal coefficient of thermal expansion is dominated by the properties of the fibers whereas the transverse coefficient is dominated by the resin (Bank 1993). Table 4.1.2 lists the longitudinal and transverse coefficients of thermal expansion for typical FRP and steel bars. Note that a negative coefficient of thermal expansion indicates that the material contracts with increased temperature and expands with decreased temperature. Fiber-reinforced polymers have a thermal expansion in the transverse direction much higher than in the longitudinal direction and also higher than the thermal expansion of hardened concrete (Masmoudi et al. 2005). The difference between the transverse coefficient of thermal expansion of FRP bars and concrete may cause splitting cracks within the concrete under temperature increase and, ultimately, failure of the concrete cover if the confining action of concrete is insufficient (Gentry and Husain 1999; Bellakehal et al. 2013; Zaidi et al. 2013). Experimental results show that the transverse coefficient of thermal expansion of glass FRP (GFRP) bars is $12 \times 10^{-6}/^{\circ}\text{F}$ ($22 \times 10^{-6}/^{\circ}\text{C}$) on average, and the ratio between the transverse and longitudinal coefficients of thermal expansion of these FRP bars is equal to 4. A ratio of concrete cover thickness to bar diameter, c/d_b , greater than 1.6 is sufficient to avoid cracking of concrete under high temperature up to 175°F (80°C) (Masmoudi et al. 2005; Zaidi and Masmoudi 2008; Zaidi et al. 2013). Experimental results, however, showed no significant reduction in bond strength for temperatures up to 140°F (60°C) (Masmoudi et al. 2011). For reference, concrete has a coefficient of thermal expansion that varies from 4×10^{-6} to $6 \times 10^{-6}/^{\circ}\text{F}$ (7.2×10^{-6}

Table 4.2.1—Typical tensile properties of reinforcing bars*

	Steel	GFRP	CFRP	AFRP
Nominal yield stress, ksi (MPa)	40 to 75 (276 to 517)	NA	NA	NA
Tensile strength, ksi (MPa)	70 to 100 (483 to 1600)	70 to 230 (483 to 690)	87 to 535 (600 to 3690)	250 to 368 (1720 to 2540)
Elastic modulus, $\times 10^3$ ksi (GPa)	29.0 (200.0)	5.1 to 7.4 (35.0 to 51.0)	15.9 to 84.0 (120.0 to 580.0)	6.0 to 18.2 (41.0 to 125.0)
Yield strain, percent	0.14 to 0.25	NA	NA	NA
Rupture strain, percent	6.0 to 12.0	1.2 to 3.1	0.5 to 1.7	1.9 to 4.4

*Typical values for fiber volume fraction ranging from 0.5 to 0.7.

to $10.8 \times 10^{-6}/^\circ\text{C}$) and is usually assumed to be isotropic (Mindess et al. 2003).

4.2—Mechanical properties and behavior

4.2.1 Tensile behavior—When loaded in tension, FRP bars exhibit no plastic behavior (yielding) before rupture. The tensile behavior of FRP bars consisting of one type of fiber material is characterized by a linearly elastic stress-strain relationship until failure. The tensile properties of some commonly used FRP bars are summarized in Table 4.2.1.

The tensile strength and stiffness of an FRP bar are dependent on several factors. Because the resin has a much lower strength than the fibers, the ratio of the volume of fiber to the overall volume of the FRP (fiber-volume fraction) significantly affects the tensile properties of an FRP bar. Strength and stiffness variations will occur in bars with various fiber-volume fractions, even in bars with the same diameter, appearance, and constituents. The rate of curing, the manufacturing process, and the manufacturing quality control also affect the mechanical characteristics of the bar (Wu 1990).

Unlike steel, the unit tensile strength of an FRP bar can vary with diameter. For example, GFRP bars from three different manufacturers show tensile strength reductions of up to 40 percent as the diameter increases proportionally from 0.375 to 0.875 in. (9.5 to 22.2 mm) (Faza and GangaRao 1993b). However, similar cross section changes do not appear to affect the strength of twisted carbon FRP (CFRP) strands (Santoh 1993). The sensitivity of aramid FRP (AFRP) bars to cross section size has been shown to vary from one commercial product to another. For example, in braided AFRP bars, there is a less than 2 percent strength reduction as bars increase in diameter from 0.28 to 0.58 in. (7.3 to 14.7 mm) (Tamura 1993). The strength reduction in a unidirectionally pultruded AFRP bar with added aramid fiber surface wraps is approximately 7 percent for diameters increasing from 0.12 to 0.32 in. (3 to 8 mm) (Noritake et al. 1993). The FRP bar manufacturer should be contacted for particular strength values of differently sized FRP bars.

Determining FRP bar strength by testing is challenging because stress concentrations in and around anchorage points on the test specimen can lead to premature failure. An adequate testing grip should allow failure to occur in the middle of the test specimen. Test methods for determining the tensile strength and stiffness of FRP bars are available in ASTM D7205.

The tensile properties of a particular FRP bar should be obtained from the bar manufacturer. Usually, a normal (Gaussian) distribution is assumed to represent the strength of a population of bar specimens (Kocaoz et al. 2005). Manufacturers should report a guaranteed tensile strength f_{fu}^* ($f_{fu}^* = f_{u,ave} - 3\sigma$), and similarly report a guaranteed rupture strain, ϵ_{fu}^* ($\epsilon_{fu}^* = \epsilon_{u,ave} - 3\sigma$), and a specified tensile modulus E_f ($E_f = E_{f,ave}$). These guaranteed values of strength and strain provide a 99.87 percent probability that the indicated values are exceeded by similar FRP bars, provided that at least 25 specimens are tested (Dally and Riley 1991; Mutsuyoshi et al. 1990). If fewer specimens are tested or a different distribution is used, texts and manuals on statistical analysis should be consulted to determine the confidence level of the distribution parameters. In any case, the manufacturer should provide a description of the method used to obtain the reported tensile properties.

An FRP bar cannot be bent once it has been manufactured (an exception to this would be an FRP bar with a thermoplastic resin that could be reshaped with the addition of heat and pressure). Fiber-reinforced polymer bars, however, can be fabricated with bends. In FRP bars produced with bends, a strength reduction of 40 to 50 percent, compared with the tensile strength of a straight bar, can occur in the bend portion due to fiber bending and stress concentrations (Nanni et al. 1998b).

4.2.2 Compressive behavior—While design of FRP bars to resist compressive stresses is not recommended, the following section is presented to fully describe the behavior of FRP bars. In the technical literature, there is no direct measurement of time-dependent creep of FRP bar coupons subject to compression. Experimental evidence obtained from FRP-pultruded shapes indicates that the ratio of creep strain to initial strain is low for stress level up to 26 percent of the ultimate compressive strength (25 ksi [170 MPa] in this research) (McClure and Mohammadi 1995). Accordingly, creep should not cause geometrical integrity problems at the stress levels typical of FRP bars in compression.

Tests on FRP bars with a length-diameter ratio from 1:1 to 2:1 have shown that the compressive strength is lower than the tensile strength (Wu 1990). The mode of failure for FRP bars subjected to longitudinal compression can include transverse tensile failure, fiber microbuckling, or shear failure. The mode of failure depends on the type of fiber, the fiber-volume fraction, and the type of resin. Compressive strengths of 55, 78, and 20 percent of the tensile strength

have been reported for GFRP, CFRP, and AFRP, respectively (Mallick 1988; Wu 1990). In general, compressive strengths are higher for bars with higher tensile strengths, except in the case of AFRP, where the fibers exhibit nonlinear behavior in compression at a relatively low level of stress.

The compressive modulus of elasticity of FRP reinforcing bars appears to be smaller than its tensile modulus of elasticity. Test reports on samples containing 55 to 60 percent volume fraction of continuous E-glass fibers in a matrix of vinyl ester or isophthalic polyester resin indicate a compressive modulus of elasticity of 5000 to 7000 ksi (35 to 48 GPa) (Wu 1990). According to reports, the compressive modulus of elasticity is approximately 80 percent for GFRP, 85 percent for CFRP, and 100 percent for AFRP of the tensile modulus of elasticity for the same product (Mallick 1988; Ehsani 1993). The most widely accepted explanation for the slightly lower values of modulus of elasticity in compression is the premature failure in the test resulting from end brooming and internal fiber microbuckling under compressive loading.

Standard test methods are not yet established to characterize the compressive behavior of FRP bars. If the compressive properties of a particular FRP bar are needed, they should be obtained from the bar manufacturer. The manufacturer should provide a description of the test method used to obtain the reported compression properties.

4.2.3 Shear behavior—Most FRP bar composites are relatively weak in interlaminar shear where layers of unreinforced resin lie between layers of fibers. Because there is usually no reinforcement across layers, the interlaminar shear strength is governed by the relatively weak polymer matrix. Orientation of the fibers in an off-axis direction across the layers of fiber will increase the shear resistance, depending on the degree of offset. For FRP bars, this can be accomplished by braiding or winding fibers transverse to the main fibers. Off-axis fibers can also be placed in the pultrusion process by introducing a continuous strand mat in the roving/mat creel. If the shear properties of a particular FRP bar are needed, these should be obtained from the bar manufacturer. The manufacturer should provide a description of the test method used to obtain the reported shear values.

4.2.4 Bond behavior—Bond performance of an FRP bar is dependent on the design, manufacturing process, mechanical properties of the bar itself, and the environmental conditions (Al-Dulaijan et al. 1996; Nanni et al. 1997; Bakis et al. 1998; Bank et al. 1998; Freimanis et al. 1998). When anchoring a steel reinforcing bar in concrete, the bond force can be transferred by adhesion resistance of the interface, also known as chemical bond; frictional resistance of the interface against slip; and mechanical interlock due to irregularity of the interface.

In FRP bars, it is postulated that bond force is transferred through the resin to the reinforcement fibers, and a bond-shear failure in the resin is also possible. When a bonded deformed bar is subjected to increasing tension, the adhesion between the bar and the surrounding concrete breaks down, and deformations on the surface of the bar cause inclined contact forces between the bar and the surrounding concrete.

The stress at the surface of the bar resulting from the force component in the direction of the bar can be considered the bond stress between the bar and the concrete.

The bond properties of FRP bars have been extensively investigated by numerous researchers through different types of tests, such as pullout tests, splice tests, and cantilever beams, to determine an empirical equation for embedment length (Faza and GangaRao 1990; Ehsani et al. 1996a,b; Benmokrane 1997; Shield et al. 1999; Mosley 2002; Wambeke and Shield 2006; Tighiouart et al. 1999).

4.3—Time-dependent behavior

4.3.1 Creep rupture—Fiber-reinforced polymer reinforcing bars subjected to a constant tension over time can suddenly fail after a time period called the endurance time. This phenomenon is known as creep rupture or static fatigue. Creep rupture is not an issue with steel bars in reinforced concrete except in extremely high temperatures, such as those encountered in a fire. As the ratio of the sustained tensile stress to the short-term strength of the FRP bar increases, endurance time decreases. The creep rupture endurance time can also irreversibly decrease under sufficiently adverse environmental conditions such as high temperature, ultraviolet radiation exposure, high alkalinity, wet and dry cycles, or freezing-and-thawing cycles. Literature on the effects of such environments exists, although the extraction of generalized design criteria is hindered by a lack of standard creep test methods and reporting as well as the diversity of constituents and processes used to make proprietary FRP products. In addition, little data are currently available for endurance times beyond 100 hours. These factors have resulted in design criteria judged to be conservative until more research has been done on this subject. Several representative examples of endurance times for bar and bar-like materials follow. No creep strain data are available in these cases.

In general, carbon fibers are the least susceptible to creep rupture, whereas aramid fibers are moderately susceptible, and glass fibers are the most susceptible. A comprehensive series of creep rupture tests was conducted on 0.25 in. (6 mm) diameter smooth FRP bars reinforced with glass, aramid, and carbon fibers (Yamaguchi et al. 1997). The bars were tested at different load levels at room temperature in laboratory conditions using split conical anchors. Results indicated that a linear relationship exists between creep rupture strength and the logarithm of time for times up to nearly 100 hours. The ratios of stress level at creep rupture to the initial strength of the GFRP, AFRP, and CFRP bars after 500,000 hours (more than 50 years) were linearly extrapolated to be 0.29, 0.47, and 0.93, respectively.

In another investigation, endurance times were determined for braided AFRP bars and twisted CFRP bars, both using epoxy resin as the matrix material (Ando et al. 1997). These commercial bars were tested at room temperature in laboratory conditions and were anchored with an expansive cementitious grout inside of friction-type grips. Bar diameters ranged from 0.26 to 0.6 in. (5 to 15 mm), but were not found to affect the results. The ratios of stress level at creep rupture to the initial strength after 50 years calculated using

a linear relationship extrapolated from data available to 100 hours was found to be 0.79 for CFRP and 0.66 for AFRP.

An investigation of creep rupture in GFRP bars in room-temperature laboratory conditions was reported by [Seki et al. \(1997\)](#). The molded E-glass/vinyl ester bars had a small (0.0068 in.² [4.4 mm²]) rectangular cross section and integral GFRP tabs. The percentage of initial tensile strength retained followed a linear relationship with logarithmic time, reaching a value of 55 percent at an extrapolated 50-year endurance time.

Creep rupture data characteristics of a 0.5 in. (12.5 mm) diameter commercial CFRP twisted strand in an indoor environment is available ([Tokyo Rope 2000](#)). The rupture strength at a projected 100-year endurance time is reported to be 85 percent of the initial strength.

An investigation of creep deformation (not rupture) in one commercial AFRP and two commercial CFRP bars tested to 3000 hours has been reported ([Saadatmanesh and Tannous 1999a,b](#)). The bars were tested in laboratory air and in room-temperature solutions with a pH equal to 3 and 12. The bars had diameters between 0.313 to 0.375 in. (8 to 10 mm), and the applied stress was fixed at 40 percent of initial strength. The results indicated a slight trend toward higher creep strain in the larger-diameter bars and in the bars immersed in the acidic solution. Bars tested in air had the lowest creep strains of the three environments. Considering all environments and materials, the range of strains recorded after 3000 hours was 0.002 to 0.037 percent. Creep strains were slightly higher in the AFRP bar than in the CFRP bars.

For experimental characterization of creep rupture, refer to the test method proposed by [Japan Society of Civil Engineers \(1997b\)](#). Creep characteristics of FRP bars can also be determined from pullout test methods cited in [ACI 440.3R](#). Recommendations on sustained stress limits imposed to avoid creep rupture are provided in [7.4](#).

4.3.2 Fatigue—A substantial amount of data for fatigue behavior and life prediction of stand-alone FRP materials exists ([National Research Council 1991](#); [Wicaksono and Chai 2013](#)). During most of this time period, the focus of research investigations was on materials suitable for aerospace applications. Some general observations on the fatigue behavior of FRP materials can be made, even though the bulk of the data is obtained from FRP specimens intended for aerospace applications rather than construction. Unless stated otherwise, the cases that follow are based on flat, unidirectional coupons with approximately 60 percent fiber-volume fraction and subjected to tension-tension sinusoidal cyclic loading at a frequency low enough not to cause self-heating, ambient laboratory environments, a stress ratio (ratio of minimum applied stress to maximum applied stress) of 0.1, and a direction parallel to the principal fiber alignment.

Test conditions that raise the temperature and moisture content of FRP materials generally degrade the ambient environment fatigue behavior.

Of all types of current FRP composites for infrastructure applications, CFRP is generally thought to be the least prone to fatigue failure. On a plot of stress versus the logarithm

of the number of cycles at failure (S-N curve), the average downward slope of CFRP data is usually approximately 5 to 8 percent of initial static strength per decade of logarithmic life. At 1 million cycles, the fatigue strength is generally between 50 and 70 percent of initial static strength and is relatively unaffected by realistic moisture and temperature exposures of concrete structures unless the resin or fiber/resin interface is substantially degraded by the environment. Some specific reports of data to 10 million cycles indicated a continued downward trend of 5 to 8 percent per decade in the S-N curve ([Curtis 1989](#)).

Individual glass fibers, such as E-glass and S-glass, are generally not prone to fatigue failure. Individual glass fibers, however, have demonstrated delayed rupture caused by the stress corrosion induced by the growth of surface flaws in the presence of even minute quantities of moisture in ambient laboratory environment tests ([Mandell and Meier 1983](#)). When many glass fibers are embedded into a matrix to form an FRP composite, a cyclic tensile fatigue effect of approximately 10 percent loss in the initial static capacity per decade of logarithmic lifetime has been observed ([Mandell 1982](#)). This fatigue effect is thought to be due to fiber-fiber interactions and is not dependent on the stress corrosion mechanism described for individual fibers. No clear fatigue limit can usually be defined. Environmental factors play an important role in the fatigue behavior of glass fibers due to their susceptibility to moisture, alkaline, and acidic solutions.

Aramid fibers, for which substantial durability data are available, appear to behave similarly to carbon and glass fibers in fatigue. The tension-tension fatigue behavior of an impregnated aramid fiber bar is excellent. Strength degradation per decade of logarithmic lifetime is approximately 5 to 6 percent ([Roylance and Roylance 1981](#)). While no distinct endurance limit is known for AFRP, 2 million cycle fatigue strengths of commercial AFRP bars for concrete applications have been reported in the range of 54 to 73 percent of initial bar strengths ([Odagiri et al. 1997](#)). Based on these findings, [Odagiri et al. \(1997\)](#) suggested that the maximum stress be set at 54 to 73 percent of the initial tensile strength. Because the slope of the applied stress versus logarithmic creep-rupture time of AFRP is similar to the slope of the stress versus logarithmic cyclic lifetime data, the individual fibers appear to fail by a strain-limited creep-rupture process. This failure condition in commercial AFRP bars was noted to be accelerated by exposure to moisture and elevated temperature ([Roylance and Roylance 1981](#); [Rostasy 1997](#)).

Although the influence of moisture on the fatigue behavior of unidirectional FRP materials is generally thought to be detrimental if the resin or fiber/matrix interface is degraded, research findings are inconclusive because the performance depends on fiber and matrix types, preconditioning methods, solution content, and the environmental condition during fatigue ([Hayes et al. 1998](#); [Rahman et al. 1997](#)). In addition, factors such as gripping and presence of concrete surrounding the bar during the fatigue test need to be considered.

Fatigue strength of CFRP bars encased in concrete has been observed to decrease when the environmental temperature increases from 68 to 104°F (20 to 40°C) ([Adimi et al.](#)

1998). In this same investigation, the endurance limit was found to be inversely proportional to the loading frequency. It was also found that higher cyclic loading frequencies in the 0.5 to 8 Hz range corresponded to higher bar temperatures due to sliding friction. Thus, an endurance limit at 1 Hz could be more than 10 times higher than that at 5 Hz. In the cited investigation, a stress ratio (minimum stress divided by maximum stress) of 0.1 and a maximum stress of 50 percent of initial strength resulted in runouts of greater than 400,000 cycles when the loading frequency was 0.5 Hz. These runout specimens had no loss of residual tensile strength.

With CFRP bars, the endurance limit also depends on the mean stress and the ratio of maximum-to-minimum cyclic stress. Higher mean stress or a lower stress ratio (minimum divided by maximum) will cause a reduction in the endurance limit (Rahman and Kingsley 1996; Saadatmanesh and Tannous 1999a).

Although GFRP is weaker than steel in shear, fatigue tests on specimens with unbonded GFRP dowel bars have shown fatigue behavior similar to that of steel dowel bars for cyclic transverse shear loading of up to 10 million cycles. The test results and the stiffness calculations have shown that an equivalent performance can be achieved between FRP and steel bars subjected to transverse shear by changing some of the parameters, such as diameter, spacing, or both (Porter et al. 1993; Hughes and Porter 1996).

The addition of ribs, wraps, and other types of deformations improve the bond behavior of FRP bars. Such deformations, however, have been shown to induce local stress concentrations that significantly affect the performance of a GFRP bar under fatigue loading situations (Katz 1998). Local stress concentrations degrade fatigue performance by imposing multi-axial stresses that serve to increase matrix-dominated damage mechanisms normally suppressed in fiber-dominated composite materials. Additional fiber-dominated damage mechanisms can be also activated near deformations, depending on the construction of the bar.

The effect of fatigue on the bond of deformed GFRP bars embedded in concrete has been investigated in detail using specialized bond tests (Sippel and Mayer 1996; Nanni et al. 1998a; Katz 2000). Different GFRP materials, environments, and test methods were followed in each cited case, and the results indicated that bond strength can increase, decrease, or remain the same following cyclic loading. Bond fatigue behavior has not been sufficiently investigated to date, and conservative design criteria based on specific materials and experimental conditions are recommended.

Design limitations on fatigue stress ranges for FRP bars ultimately depend on the manufacturing process of the FRP bar, environmental conditions, and the type of fatigue load being applied. Given the ongoing development in the manufacturing process of FRP bars, conservative design criteria should be used for all commercially available FRP bars. Design criteria are given in 7.4.2.

With regard to the fatigue characteristics of FRP bars, the designer is referred to the provisional standard test methods cited in ACI 440.3R. The designer should always consult with the bar manufacturer for fatigue response properties.

4.4—Effects of high temperatures and fire

The fire resistance of FRP-reinforced concrete flexural elements can, given due consideration to possible differences in their response to heating, be determined in a similar way as that of steel-reinforced concrete slabs (ACI 216.1). The effects of elevated temperature exposure on the shear and axial compressive capacity of FRP-reinforced concrete elements are not well known, and additional research is warranted in these areas.

The type of reinforcement, aggregate type, and concrete cover thickness will all influence the fire performance of FRP-reinforced members. The type of reinforcement is important because all FRP materials will experience significantly different reductions in mechanical and bond properties at elevated temperatures (Bisby et al. 2005). The aggregate type and concrete cover are important because these two parameters significantly influence heat transfer to the reinforcement and, hence, the temperatures experienced during fire exposure both in the bars along the exposed zone and in the anchorage zone (Kodur and Bisby 2005; Nigro et al. 2011b).

4.4.1 Heat transfer—Research has shown (Kodur and Bisby 2005; Nigro et al. 2011b) that the heat transfer behavior of fire-exposed FRP-reinforced concrete slabs and beams is similar to those reinforced with steel bars.

4.4.2 Material degradation—Because FRP materials are generally more sensitive than steel reinforcing bars to elevated temperatures, the reinforcement type influences the fire resistance of FRP-reinforced concrete elements; these may have lower fire resistances compared to steel-reinforced elements of equivalent ambient temperature capacity (Bisby and Kodur 2007). Because FRP reinforcement is embedded within concrete, the reinforcement does not contribute significantly to fire severity or toxicity; however, the fire resistance of FRP-reinforced concrete members could be less than that of steel-reinforced members due to reduction of FRP mechanical properties, the loss of bond from a softening of the resin from which the bars are fabricated, or both.

4.4.3 Serviceability limit state—The properties of the polymer at the surface of the bar are essential in maintaining bond between FRP and concrete. At a temperature close to its glass transition temperature T_g , the mechanical properties of the polymer begin to reduce and the polymer is less able to transfer stresses from the concrete to the fibers, resulting in considerable reductions in bond strength (Katz et al. 1999; Nigro et al. 2012). The value of T_g depends on the type of resin, but is typically in the range of 200 to 250°F (93 to 120°C) for the resins used in most FRP bars for concrete. The fibers, which generally for glass and carbon fibers exhibit better thermal properties than the resin with a melting point of 1600°F (880°C) for glass fibers and 2900°F (1600°C) for carbon, can continue to support considerable load in the longitudinal direction; however, the tensile strength and stiffness of the overall FRP composite are reduced due to a reduction in force transfer between fibers through bond to the resin (Chowdhury et al. 2011). Reduction of stiffness is generally expected later than reduction in strength. The onset glass transition temperature, obtained by dynamic

mechanical analysis (DMA) testing, should generally not be exceeded to assure preservation of the mechanical and bond properties of the FRP reinforcement.

4.4.4 Ultimate limit state—Should an anchorage length of FRP remain outside the area exposed to high temperature during fire, loss of bond in the heated zone is less critical, as the fibers themselves are less sensitive to elevated temperature. Hence, well-anchored FRP bars can retain considerable strength and stiffness at temperatures well above T_g . For example, **Robert and Benmokrane (2010)** demonstrated that well-anchored GFRP bars with a T_g of 250°F (120°C) retained as much as 50 percent of their tensile strength at temperatures exceeding 570°F (300°C); **Maluk et al. (2011)** demonstrated that well-anchored CFRP bars with a T_g of 250°F (121°C) retained as much as 65 percent of their tensile strength at temperatures exceeding 625°F (330°C).

4.4.5 Structural fire resistance design—The applicable load and resistance factors, as well as the deflection and crack width serviceability criteria used during the design process, will also affect fire performance. Differences in the design philosophy between design guides and codes for steel-reinforced concrete (which is typically controlled by strength), when compared to those for FRP-reinforced concrete (which is often controlled by serviceability criteria), mean that when subjected to a fire, the flexural capacity of FRP-reinforced members may inherently have a much greater reserve strength. This issue is discussed in detail by **Bisby and Kodur (2007)**.

Given these aforementioned issues, rational design of FRP-reinforced concrete members for fire safety should be performed with a clear understanding of the appropriate structural fire endurance criteria applicable to the buildings in which they are proposed. The designer should account for temperature-induced reductions in the bond between FRP bars and concrete; note that bond strength reductions are not typically considered important for fire-safety design with conventional deformed steel reinforcing bars. The general approach to fire endurance testing given by **ASTM E119** is recommended. When conducting fire tests using ASTM E119 for FRP-reinforced concrete members, the critical temperature approach should not be taken for the FRP reinforcement unless rational consideration of holistic member performance in fire has been performed and has led to the definition of the critical temperature. In most cases, the concrete element should be tested in a loaded condition and the fire endurance should be determined based on strength and deflection requirements rather than on the temperature in the FRP. Relevant integrity and insulation fire resistance criteria still apply (**ACI 216.1**).

Several full-scale tests performed in accordance with ASTM E119, **CAN/ULC S101-M89**, DIN EN 1363 (**Deutsches Institut für Normung e.V. 2012**), and **ISO 834-1** provisions have been performed on GFRP- and CFRP-reinforced beams and slabs (**Nigro et al. 2011a, 2013**). These tests have led to structural fire resistance ratings for FRP-reinforced concrete elements in excess of 3 hours for cases where the FRP bars were well anchored into cool regions of the concrete. For example, **Nigro et al. (2013)** showed

that simply-supported concrete slabs reinforced with well-anchored GFRP bars (with T_g of 210°F [100°C] and a clear concrete cover of 1 in. [25.4 mm]) were able to carry 60 percent of their design ultimate strength for more than 3 hours of exposure to the ISO 834 standard fire. The temperature of the bars exceeded 930°F (500°C); however, the bars continued to carry load due to the presence of effective anchoring details.

CHAPTER 5—DURABILITY

Fiber-reinforced polymer (FRP) bars are susceptible to varying amounts of strength and stiffness changes in the presence of environments before, during, and after construction. These environments can include water, ultraviolet exposure, elevated temperature, alkaline or acidic solutions, and saline solutions. Strength and stiffness may increase, decrease, or remain the same, depending on the particular material and exposure conditions. Tensile and bond properties of FRP bars are the primary parameters of interest for reinforced concrete construction.

5.1—Accelerated durability testing

The environmental condition that has attracted the most interest by investigators concerned with FRP bars is the highly alkaline pore water found in outdoor concrete structures (**Gerritse 1992; Takewaka and Khin 1996; Rostasy 1997; Yamaguchi et al. 1997**). Methods for systematically accelerating the strength degradation of bare, unstressed, glass filaments in concrete using temperature have been successful (**Litherland et al. 1981**) and have also often been applied to glass FRP (GFRP) materials to predict long-term performance in alkaline solutions. Test methods for evaluating the durability of FRP bars in alkaline solutions are presented in **ASTM D7705**. There is no substantiation to date, however, that accelerated methods for bare glass (where only one chemical reaction controls degradation) apply to GFRP composites (where multiple reactions and degradation mechanisms may be activated at once or sequentially). Also, the effect of applied stress during exposure should be factored as well. Due to insufficient data on combined weathering and applied stress, the discussions of weathering, creep, and fatigue are kept separate in this guide. Therefore, while short-term experiments using aggressive environments enable quick comparisons of materials, extrapolation of the results to field conditions and expected lifetimes is not possible in the absence of real-time data (**Barkatt et al. 1998; Clarke and Sheard 1998**). In most cases available to date, bare bars were subjected to the aggressive environment under no load. The relationships between data on bare bars and data on bars embedded in concrete are affected by additional variables, such as the degree of protection offered to the bars by the concrete (**Clarke and Sheard 1998; Scheibe and Rostasy 1998; Sen et al. 1998a,b**). Test times are typically in the 10- to 30-month range.

5.2—Durability of FRP bars

Due to the large amount of literature on the subject (**Benmokrane and Rahman 1998**) and the limited space

herein, some generalizations should be made at the expense of presenting particular quantitative results. With these cautions in mind, representative experimental results for a range of FRP bar materials and test conditions are reviewed in the balance of this section. Conservatism is advised in applying these results in design until additional long-term durability data are available.

5.2.1 Alkaline solutions—Aqueous solutions with high values of pH varying from 11.5 to 13.0 are known to degrade the tensile strength and stiffness of GFRP bars (Porter and Barnes 1998). Particular results, however, vary significantly according to differences in test methods that, in addition to pH, include composition of the chemical solution, temperature, and presence of load. Higher temperatures and longer exposure times exacerbate the problem. Most data have been generated using temperatures as low as slightly subfreezing and as high as a few degrees below the T_g of the resin. The degree to which the resin protects the glass fibers from the diffusion of deleterious hydroxyl (OH^-) ions figures prominently in the alkali resistance of GFRP bars (Bank and Puterman 1997; Coomarasamy and Goodman 1997; GangaRao and Vijay 1997b; Porter et al. 1997; Bakis et al. 1998; Tannous and Saadatmanesh 1999; Uomoto 2000). Most researchers believe that vinyl ester resins have superior resistance to moisture ingress compared with other commodity resins. The type of glass fiber also appears to be an important factor in the alkali resistance of GFRP bars (Devalapura et al. 1996). Research examining the durability of different glass-fiber-based products, including North American GFRP reinforcing bars, have been performed by several researchers (Robert and Benmokrane 2013; Belarbi and Wang 2012; Kamal and Boulfiza 2011; Robert et al. 2009; Chen et al. 2007). Tensile strength reductions in GFRP bars ranging from 0 to 75 percent of initial values have been reported in the cited literature. Tensile stiffness reductions in stressed and unstressed GFRP bars range between 0 and 20 percent in many cases. Tensile strength and stiffness of aramid FRP (AFRP) rods in elevated-temperature alkaline solutions, either with or without tensile stress applied, have been reported to decrease between 10 and 50 percent and 0 and 20 percent of initial values, respectively (Takewaka and Khin 1996; Rostasy 1997; Sen et al. 1998b). In the case of unstressed carbon FRP (CFRP), strength and stiffness have been reported to each decrease between 0 and 20 percent (Takewaka and Khin 1996).

5.2.2 Ultraviolet radiation and moisture—Exposure of FRP bars to ultraviolet rays and moisture before their placement in concrete could adversely affect their tensile strength due to degradation of the polymer constituents, including aramid fibers and all resins. Proper construction practices and resin additives can mitigate this type of weathering problem significantly. It is highly recommended that, before placement in concrete, FRP bars are protected from direct exposure to sunlight and moisture. Some results from combined ultraviolet and moisture exposure tests with and without applied stress applied to the bars have shown tensile strength reductions of 0 to 20 percent of initial values in CFRP, 0 to 30 percent in AFRP, and 0 to 40 percent in GFRP (Sasaki et

al. 1997; Uomoto 2000). An extensive study of GFRP, AFRP, and CFRP bars kept outdoors in a rack by the ocean showed no significant change of tensile strength or modulus of any of the bars (Tomosawa and Nakatsuji 1996, 1997).

5.2.3 Saline solutions—It has been shown (Rahman et al. 1996) that the addition of various types of salts to the solution in which FRP bars are immersed does not necessarily make a significant difference in the strength and stiffness of many FRP bars when compared with those in a solution without salt. Most studies, however, do not separate the effects of water and salt added to water. One study found a 0 to 20 percent reduction of initial tensile strength in GFRP bars subjected to a saline solution at room temperature and cyclic freezing-and-thawing temperatures (Vijay and GangaRao 1999); another found a 15 percent reduction in the strength of AFRP bars in a marine environment (Sen et al. 1998b).

5.3—Durability of bond between FRP and concrete

Studies of the durability of bond between FRP and concrete have been mostly concerned with the moist, alkaline environment found in concrete. The bond of FRP reinforcement relies on the transfer of shear and transverse forces at the interface between bar and concrete, and between individual fibers within the bar. These resin-dominated mechanisms are in contrast to the fiber-dominated mechanisms that control properties such as longitudinal strength and stiffness of FRP bars. Environments that degrade the polymer resin or fiber/resin interface are therefore also likely to degrade the bond strength of an FRP bar.

Numerous bond test methods (pullout tests, tension tests, and beam-end tests) have been proposed for FRP bars, although the direct pullout test has been the most popular due to its simplicity and low cost despite its inability to represent the concrete stress state in most of the practical situations (Nanni et al. 1995; Tepfers 2002). Pullout specimens with CFRP and GFRP bars have been subjected to natural environmental exposures and have not indicated significant decreases in bond strength over periods of time between 1 and 2 years (Clarke and Sheard 1998; Sen et al. 1998a). Positive and negative trends in pullout strength with respect to shorter periods of time have been obtained with GFRP bars subjected to wet elevated-temperature environments in concrete, with or without artificially added alkalinity (Al-Dulaijan et al. 1996; Bakis et al. 1998; Bank et al. 1998; Porter and Barnes 1998). Similar observations on such pullout tests using specimens subjected to accelerated environmental exposure carry over to AFRP and CFRP bars (Conrad et al. 1998). Longitudinal cracking in the concrete cover can seriously degrade the bond capability of FRP bars, and sufficient measures should be taken to prevent such cracking in laboratory tests and field applications (Sen et al. 1998a). The ability of chemical agents to pass through the concrete to the FRP bar is another important factor thought to affect bond strength (Porter and Barnes 1998).

CHAPTER 6—GENERAL DESIGN CONSIDERATIONS

The general design recommendations for flexural concrete elements reinforced with FRP bars are presented in this chapter. Recommendations are based on principles of equilibrium and compatibility, and the constitutive laws of the materials. Also, the brittle behavior of both FRP reinforcement and concrete allows for consideration to be given to either compression-controlled or tension-controlled modes of flexural failure. Detrimental effects of high temperature and fire on FRP-reinforced structures are discussed in 4.4.

6.1—Design philosophy

Although strength and working stress design approaches were considered, the strength design approach of reinforced concrete members reinforced with FRP bars was preferred to ensure consistency with other ACI documents. Design recommendations are based on limit state design principles. In many instances, serviceability criteria or fatigue and creep rupture endurance limits could control the design of concrete members reinforced for flexure with FRP bars, especially aramid FRP (AFRP) and glass FRP (GFRP) that exhibit low stiffness.

The load factors given in ACI 318 are used to determine the required strength of a concrete member reinforced with FRP.

6.2—Design material properties

Material properties provided by the manufacturer, such as the guaranteed tensile strength, should be considered as initial properties that do not include the effects of long-term exposure to the environment. Because long-term exposure to various types of environments can reduce the tensile strength and creep rupture and fatigue endurance of FRP bars, the material properties used in design equations should be reduced based on the type and level of environmental exposure.

Equations (6.2a) and (6.2b) give the tensile properties that should be used in all design equations. The design tensile strength should be determined by

$$f_{fu} = C_E f_{fu}^* \quad (6.2a)$$

The design rupture strain should be determined as

$$\varepsilon_{fu} = C_E \varepsilon_{fu}^* \quad (6.2b)$$

The design modulus of elasticity will be the same as the value reported by the manufacturer as the mean elastic modulus (guaranteed value) of a sample of test specimens ($E_f = E_{f,ave}$).

The environmental reduction factors given in Table 6.2 are conservative estimates, depending on the durability of each fiber type, and are based on the consensus of ACI Committee 440. Temperature effects are included in the C_E values. Fiber-reinforced polymer bars, however, should not be used in environments with a service temperature higher than the T_g of the resin used for their manufacturing. It is expected

Table 6.2—Environmental reduction factor for various fibers and exposure conditions

Exposure condition	Fiber type	Environmental reduction factor C_E
Concrete not exposed to earth and weather	Carbon	1.0
	Glass	0.8
	Aramid	0.9
Concrete exposed to earth and weather	Carbon	0.9
	Glass	0.7
	Aramid	0.8

that with continued research, these values will become more reflective of actual effects of environment. The methodology regarding the use of these factors, however, is not expected to change.

6.2.1 Tensile strength of FRP bars at bends—The design tensile strength of FRP bars at a bend can be determined as

$$f_{fb} = \left(0.05 \cdot \frac{r_b}{d_b} + 0.3 \right) f_{fu} \leq f_{fu} \quad (6.2.1)$$

Equation (6.2.1) is adapted from design recommendations by the **Japan Society of Civil Engineers (1997b)**. Limited research on FRP hooks (**Ehsani et al. 1995**) indicates that the tensile force developed by the bent portion of a GFRP bar is mainly influenced by the ratio of the bend radius to the bar diameter, r_b/d_b ; the tail length; and, to a lesser extent, the concrete strength.

For an alternative determination of the reduction in tensile strength due to bending, manufacturers of bent bars may provide test results based on test methodologies cited in **ACI 440.3R**.

CHAPTER 7—FLEXURE

The design of FRP-reinforced concrete members for flexure is analogous to the design of steel-reinforced concrete members. Experimental data on concrete members reinforced with FRP bars show that flexural capacity can be calculated based on assumptions similar to those made for members reinforced with steel bars (**Faza and GangaRao 1993a; Nanni 1993b; GangaRao and Vijay 1997a**). The design of members reinforced with FRP bars should take into account the uniaxial stress-strain relationship of FRP materials.

7.1—General considerations

This chapter specifically references rectangular sections with a single layer of one type of tensile FRP reinforcement, as the experimental work has almost exclusively considered members with this cross-sectional shape and reinforcement layout. The concepts described herein, however, can also be applied to the analysis and design of members with different geometry and multiple types, multiple layers, or both, of FRP reinforcement. Although there is no evidence that the flexural theory, as developed herein, does not apply equally well to nonrectangular sections, the behavior of nonrectangular sections has yet to be confirmed by experimental results.

7.1.1 Flexural design philosophy—Steel-reinforced concrete sections are commonly designed to ensure tension-controlled behavior exhibited by yielding of steel before the crushing of concrete. The yielding of the steel provides ductility and a warning of failure of the member. The nonductile behavior of FRP reinforcement necessitates a reconsideration of this approach.

If FRP reinforcement ruptures, failure of the member is sudden and catastrophic (Nanni 1993b; Jaeger et al. 1997; GangaRao and Vijay 1997a; Theriault and Benmokrane 1998); however, there would be limited warning of impending failure in the form of extensive cracking and large deflection due to the significant elastic elongation that FRP reinforcement experiences before rupture. In any case, the member would not exhibit ductility as is commonly observed for tension-controlled concrete beams reinforced with steel reinforcing bars, in which the bars exhibit plastic deformation prior to concrete crushing.

Compression-controlled behavior is marginally more desirable for flexural members reinforced with FRP bars (Nanni 1993b). By experiencing concrete crushing prior to tensile rupture of the FRP reinforcement, a flexural member does exhibit some inelastic behavior before failure.

In conclusion, both compression- and tension-controlled sections are acceptable in the design of flexural members reinforced with FRP bars, provided that strength and serviceability criteria are satisfied. To compensate for the lack of ductility, the member should possess a higher reserve of strength. The margin of safety suggested by this guide against failure is therefore higher than that used in traditional steel-reinforced concrete design.

The use of high-strength concrete allows for better use of the high-strength properties of FRP bars and can increase the stiffness of the cracked section, but the brittleness of high-strength concrete, as compared with normal-strength concrete, can reduce the overall deformability of the flexural member (GangaRao and Vijay 1997a).

Figure 7.1.1 shows a comparison of the theoretical moment-curvature behavior of beam cross sections designed for the same strength ϕM_n following the principles of ultimate strength design described in this chapter, including the recommended strength reduction factors according to this guide for FRP and ACI 318 for steel. Three cases are presented in addition to the steel-reinforced cross section: two sections reinforced with glass FRP (GFRP) bars, and one reinforced with carbon FRP (CFRP) bars. For the tension-controlled GFRP-reinforced section, the concrete dimensions are larger than for the other beams to attain the same design capacity.

7.1.2 Assumptions—Computations of the strength of cross sections should be performed based on the following assumptions:

a) Strain in the concrete and the FRP reinforcement is proportional to the distance from the neutral axis (a plane section before loading remains plane after loading).

b) The maximum usable compressive strain in the concrete is assumed to be 0.003.

c) The tensile strength of concrete is ignored.

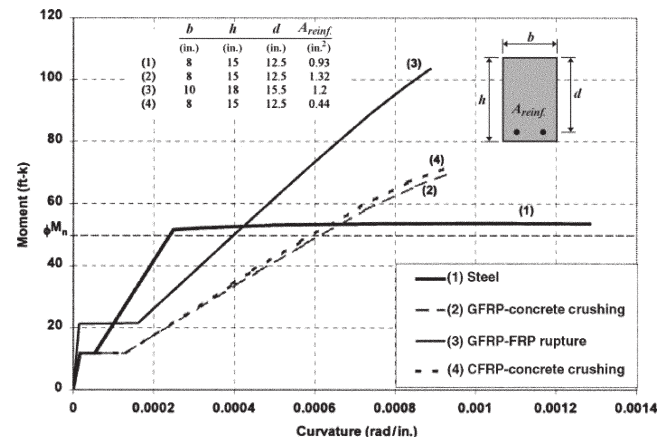


Fig. 7.1.1—Theoretical moment-curvature relationships for reinforced concrete sections using steel and FRP bars (ϕ factors of 0.9, 0.65, 0.55, and 0.65 for tension-controlled steel, compression-controlled GFRP, tension-controlled GFRP, and compression-controlled CFRP, respectively).

d) The tensile behavior of the FRP reinforcement is linearly elastic until failure.

e) A perfect bond exists between concrete and FRP reinforcement.

7.2—Flexural strength

The strength design philosophy states that the design flexural strength at a section of a member should exceed the factored moment (Eq. (7.2)). Design flexural strength refers to the nominal flexural strength of the member multiplied by a strength reduction factor (ϕ , discussed in 7.2.3). The factored moment refers to the moments calculated by the use of factored loads as prescribed in ACI 318 (for example, $1.2D + 1.6L + \dots$)

$$\phi M_n \geq M_u \quad (7.2)$$

The nominal flexural strength of an FRP-reinforced concrete member can be determined based on strain compatibility, internal force equilibrium, and the controlling strength limit state (concrete crushing or FRP rupture). Figure 7.2 illustrates the stress, strain, and internal forces for the three possible cases of a rectangular section reinforced with FRP bars.

7.2.1 Strength limit states—The flexural capacity of an FRP-reinforced flexural member is dependent on whether it is controlled by concrete crushing or FRP rupture. The controlling limit state can be determined by comparing the FRP reinforcement ratio to the balanced reinforcement ratio, which is a ratio where concrete crushing and FRP rupture occur simultaneously. Because FRP does not yield, the balanced ratio of FRP reinforcement is computed using its design tensile strength. The FRP reinforcement ratio can be computed from Eq. (7.2.1a), and the balanced FRP reinforcement ratio can be computed from Eq. (7.2.1b)

$$\rho_f = \frac{A_f}{bd} \quad (7.2.1a)$$

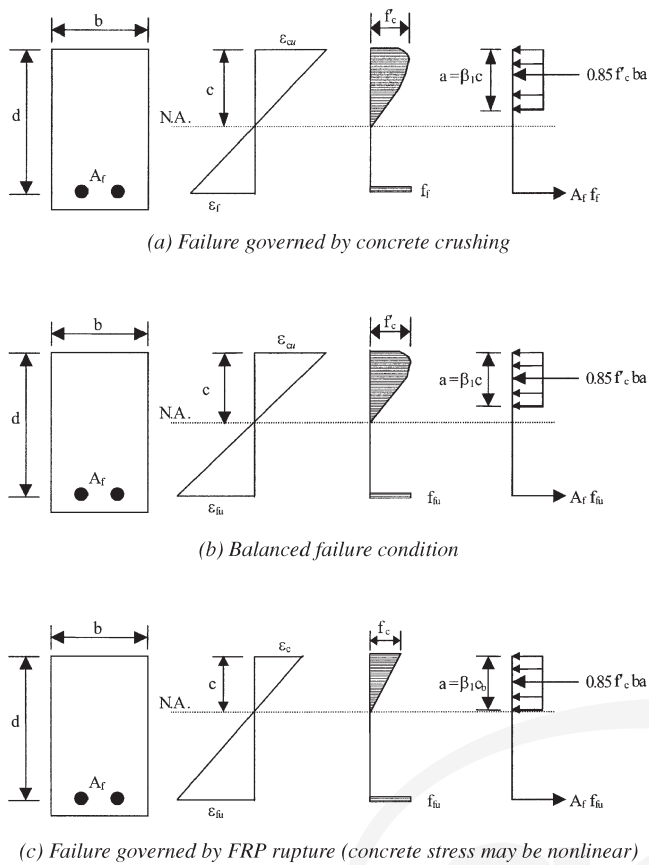


Fig. 7.2—Strain and stress distribution at ultimate conditions.

$$\rho_{fb} = 0.85\beta_1 \frac{f'_c}{f_{fu}} \frac{E_f \epsilon_{cu}}{E_f \epsilon_{cu} + f_{fu}} \quad (7.2.1b)$$

If the reinforcement ratio is less than the balanced ratio ($\rho_f < \rho_{fb}$), the FRP rupture limit state controls. Otherwise, ($\rho_f > \rho_{fb}$) the concrete crushing limit state controls.

Table 7.2.1 reports some typical values for the balanced reinforcement ratio, showing that the balanced ratio for FRP reinforcement ρ_{fb} is much lower than the balanced ratio for steel reinforcement ρ_b . The balanced ratio for FRP reinforcement can be even lower than the minimum reinforcement ratio for steel ($\rho_{min} = 0.0035$ for Grade 60 steel and $f'_c = 5000$ psi [35 MPa]).

7.2.2 Nominal flexural strength—When $\rho_f > \rho_{fb}$, the controlling limit state is crushing of the concrete, and the stress distribution in the concrete can be approximated with the ACI rectangular stress block. Based on the equilibrium of forces and strain compatibility (shown in Fig. 7.2), the following can be derived

$$M_n = A_f f_f \left(d - \frac{a}{2} \right) \quad (7.2.2a)$$

$$a = \frac{A_f f_f}{0.85 f'_c b} \quad (7.2.2b)$$

$$f_f = E_f \epsilon_{cu} \frac{\beta_1 d - a}{a} \quad (7.2.2c)$$

Table 7.2.1—Typical values for balanced reinforcement ratio for a rectangular section with $f'_c = 5000$ psi (34.5 MPa)

Bar type	Yield strength f_y or tensile strength f_{tu} , ksi (MPa)	Modulus of elasticity, ksi (GPa)	ρ_b or ρ_{fb}
Steel	60 (414)	29,000 (200)	0.0335
GFRP	80 (552)	6000 (41.4)	0.0078
AFRP	170 (1172)	12,000 (82.7)	0.0035
CFRP	300 (2070)	22,000 (152)	0.0020

Substituting a from Eq. (7.2.2b) into Eq. (7.2.2c) and solving for f_f gives

$$f_f = \left(\sqrt{\frac{(E_f \epsilon_{cu})^2}{4} + \frac{0.85\beta_1 f'_c}{\rho_f} E_f \epsilon_{cu}} - 0.5 E_f \epsilon_{cu} \right) \leq f_{fu} \quad (7.2.2d)$$

The nominal flexural strength can be determined from Eq. (7.2.2a), (7.2.2b), and (7.2.2d). The FRP reinforcement is linearly elastic at the concrete crushing limit state, so the stress level in the FRP can be found from Eq. (7.2.2c) because it is less than f_{fu} .

Alternatively, the nominal flexural strength at a section can be expressed in terms of the FRP reinforcement ratio, as given in Eq. (7.2.2e) to replace Eq. (8.2.2a).

$$M_n = \rho_f f_f \left(1 - 0.59 \frac{\rho_f f_f}{f'_c} \right) b d^2 \quad (7.2.2e)$$

When $\rho_f < \rho_{fb}$, the controlling limit state is rupture of the FRP reinforcement, and the nominal flexural strength at a section can be computed as shown in Eq. (7.2.2f)

$$M_n = A_f f_{fu} \left(d - \frac{\beta_1 c}{2} \right) \quad (7.2.2f)$$

Although the stress in the reinforcement is known, the analysis incorporates two unknowns: the concrete compressive strain at ultimate when the FRP ruptures in tension (ϵ_c) and the depth to the neutral axis c . The analysis involving these unknowns becomes complex and is not easily solved by closed-form solution. The ACI equivalent rectangular stress block parameters are also not applicable because the maximum concrete strain may not be attained ($\epsilon_c < \epsilon_{cu}$). In this case, equivalent rectangular stress block parameters (α_1 and β_1) that approximate the centroid of the stress distribution in the concrete at the particular strain level reached would need to be used. The factor α_1 is the ratio of the average concrete stress to the concrete strength. Factor β_1 is the ratio of the depth of the equivalent rectangular stress block to the depth of the neutral axis.

For a given section, the product of $\beta_1 c$ in Eq. (7.2.2f) varies depending on material properties and FRP reinforcement ratio. For a section controlled by the limit state of FRP rupture, the maximum value for this product is equal to $\beta_1 c_b$

and is achieved when the maximum concrete strain (0.003) is attained. Therefore, a simplified and conservative lower bound calculation of the nominal flexural strength of the member can be based on Eq. (7.2.2g) and (7.2.2h) as follows

$$M_n = A_f f_{fu} \left(d - \frac{\beta_1 c_b}{2} \right) \quad (7.2.2g)$$

$$c_b = \left(\frac{\epsilon_{cu}}{\epsilon_{cu} + \epsilon_{fu}} \right) d \quad (7.2.2h)$$

7.2.3 Strength reduction factor for flexure—Because FRP members do not exhibit ductile behavior, a conservative strength reduction factor should be adopted to provide a higher reserve of strength in the member. The Japanese recommendations for design of flexural members using FRP suggest a strength reduction factor equal to 0.77 (Japan Society of Civil Engineers 1997b). Other researchers (Benmokrane et al. 1996) suggest a value of 0.75 based on probabilistic concepts.

Based on ACI 318, the ϕ factor for design of a compression-controlled section is 0.65, with a target reliability index between 3.5 and 4.0 (Szerszen and Nowak 2003). A reliability analysis on FRP-reinforced beams in flexure using Load Combination 2 from ACI 318 for live-to-dead load ratios between 1 and 3 indicated reliability indexes between 3.5 and 4.0 when the ϕ factor was set to 0.65 for a compression-controlled section, and 0.55 for a tension-controlled section using Eq. (7.2.2g) (Shield et al. 2011). A nonlinear sectional analysis of curvatures at failure showed that the curvatures of typical FRP-reinforced beams at failure varied between $0.016/d$ and $0.018/d$ for tension-controlled failures, and between $0.011/d$ and $0.02/d$ for compression-controlled failures (Shield et al. 2011).

ACI 318 considers the section tension-controlled whenever the curvature is greater than $0.008/d$ (corresponding to a strain in the steel of 0.005). This indicates that due to the low modulus of elasticity of the reinforcement, FRP-reinforced beams will have large deflections at ultimate, and that FRP-reinforced beams with controlling limit states of FRP reinforcing bar rupture will have larger deflections at ultimate than those that are controlled by concrete crushing. Even though the curvature values of FRP-reinforced beams are larger than those of equivalent steel-reinforced beams, the committee recommends a ϕ factor of 0.55 for tension-controlled section design to maintain a minimum reliability index of 3.5.

While a concrete crushing limit state can be predicted based on calculations, the member as constructed may not fail accordingly. For example, if the concrete strength is higher than specified, the section capacity may be controlled by FRP rupture. For this reason, and to establish a transition between the two values of ϕ , a compression-controlled FRP reinforced concrete section is defined as a section in which $\rho_f \geq 1.4\rho_{fb}$, and a tension-controlled FRP reinforced concrete section is defined as one in which $\rho_f \leq \rho_{fb}$. A section with ρ_{fb}

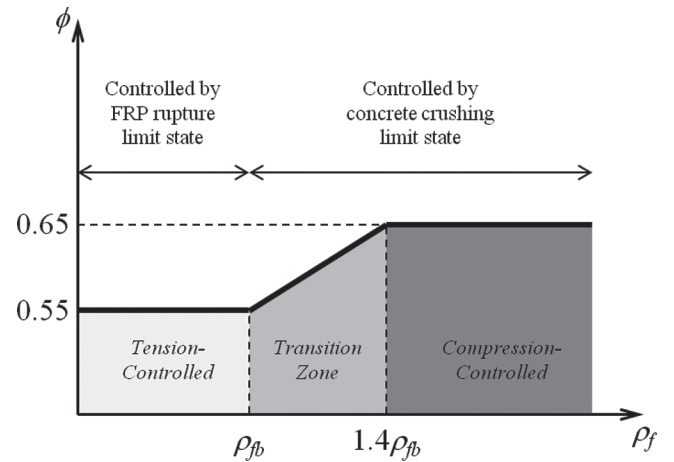


Fig. 7.2.3—Strength reduction factor as function of reinforcement ratio.

$< \rho_f < 1.4\rho_{fb}$ will theoretically be controlled by the concrete crushing limit state, but a reduced value of ϕ should be used, relative to a compression-controlled section.

The strength reduction factor for flexure can be computed by Eq. (7.2.3). This equation is represented graphically by Fig. 7.2.3, and gives a factor of 0.65 for compression-controlled sections, 0.55 for tension-controlled sections, and provides a linear transition between the two.

$$\phi = \begin{cases} 0.55 & \text{for } \rho_f \leq \rho_{fb} \\ 0.3 + 0.25 \frac{\rho_f}{\rho_{fb}} & \text{for } \rho_{fb} < \rho_f < 1.4\rho_{fb} \\ 0.65 & \text{for } \rho_f \geq 1.4\rho_{fb} \end{cases} \quad (7.2.3)$$

7.2.4 Minimum FRP reinforcement—If a section is tension controlled ($\rho_f \leq \rho_{fb}$), a minimum amount of reinforcement should be provided to prevent failure upon concrete cracking, $\phi M_n \geq M_{cr}$, where M_{cr} is the cracking moment. The provisions in ACI 318 for minimum reinforcement are based on this concept and, with modifications, are applicable to FRP-reinforced members. The modifications result from a different strength reduction factor—0.55 for tension-controlled sections instead of 0.9. The minimum reinforcement area for FRP-reinforced members is obtained by multiplying the existing ACI 318 equation for steel reinforcement by 1.64 ($1.64 = 0.90/0.55$). This results in Eq. (7.2.4)

$$A_{f,min} = \frac{4.9\sqrt{f'_c}}{f_{fu}} b_w d \geq \frac{330}{f_{fu}} b_w d \quad (7.2.4)$$

For SI units

$$A_{f,min} = \frac{0.41\sqrt{f'_c}}{f_{fu}} b_w d \geq \frac{2.3}{f_{fu}} b_w d$$

If a section is not tension controlled ($\rho_f > \rho_{fb}$), the minimum amount of reinforcement to prevent failure upon cracking is

automatically achieved. Therefore, Eq. (7.2.4) is required as a check only if $\rho_f \leq \rho_{fb}$. The requirements of Eq. (7.2.4) need not be applied if at every section the area of tensile reinforcement provided is at least one-third greater than that required by analysis.

7.2.5 Special considerations

7.2.5.1 Multiple layers of reinforcement and combinations of different FRP types—In a tension-controlled section, all steel tension reinforcement is assumed to yield at ultimate when using the strength design method to calculate the nominal flexural strength of members with steel reinforcement arranged in multiple layers. Therefore, the tension force is assumed to act at the centroid of the reinforcement with a magnitude equal to the area of tension reinforcement times the yield strength of steel. Because FRP materials have no plastic region, the stress in each reinforcement layer will vary depending on its distance from the neutral axis. In these cases, strain in the outermost layer should be used to determine if the section is compression- or tension-controlled. The analysis of the flexural capacity should be based on a strain-compatibility approach. Similarly, if different types of FRP bars are used to reinforce the same member, the variation in the stress level in each bar type should be considered when calculating the flexural capacity.

7.2.5.2 Moment redistribution—Plastic hinges do not form in members reinforced with FRP bars due to their linear-elastic behavior up to rupture. Consequently, moment redistribution in continuous beams or other statically indeterminate structures should not be considered for FRP-reinforced concrete.

7.2.5.3 Compression reinforcement—FRP reinforcement has a significantly lower compressive strength than tensile strength, and is subject to significant variation (Kobayashi and Fujisaki 1995; Japan Society of Concrete Engineers 1997b). Therefore, the strength of any FRP bar in compression should be ignored in design calculations (Almusallam et al. 1997).

Placing FRP bars in the compression zone of flexural members, however, cannot be avoided in some cases. Examples include the supports of continuous beams or where bars secure the stirrups in place. In these cases, confinement should be considered for the FRP bars in compression regions to prevent their instability and to minimize the effect of the relatively high transverse expansion of some types of FRP bars. The transverse FRP reinforcement in the form of ties should have a spacing smaller than the least cross-sectional dimension or 16 longitudinal bar diameters or 48 tie bar diameters.

7.3—Serviceability

Fiber-reinforced polymer reinforced concrete members have a relatively small stiffness after cracking, when compared to steel-reinforced concrete members with the same reinforcement ratio. Consequently, permissible deflections under service loads can control the design. In general, designing FRP-reinforced cross sections for flexural strength may not satisfy serviceability criteria for deflection and crack

control (Nanni 1993a; GangaRao and Vijay 1997a; Theriault and Benmokrane 1998; Bischoff 2005).

Serviceability can be defined as satisfactory performance under service load conditions. This, in turn, can be described in terms of two criteria:

1) Cracking—Excessive crack width is undesirable for aesthetic and other reasons (for example, to prevent water leakage) that can damage or deteriorate the structural concrete.

2) Deflection—Deflections should be within acceptable limits imposed by the use of the structure (for example, supporting attached nonstructural elements without damage).

The serviceability provisions given in ACI 318, Section 9.5 for deflection and Section 10.6 for crack control, need to be modified for FRP-reinforced members to account for the increased flexibility when using lower stiffness reinforcement. The substitution of FRP for steel on an equal area basis, for example, would typically result in larger deflections and wider crack widths (Gao et al. 1998a; Tighiouart et al. 1998).

7.3.1 Cracking—Fiber-reinforced polymer bars are corrosion-resistant; therefore, larger crack widths as compared to steel-reinforced concrete can be tolerated when corrosion of reinforcement is the primary reason for crack control. Other considerations with regard to acceptable crack width limits include aesthetics, creep rupture, and shear effects.

Two design methodologies exist for proportioning reinforcement to control flexural cracking: 1) a direct procedure in which crack widths are calculated; and 2) an indirect procedure in which maximum bar spacing limits are specified. Direct crack control refers to the calculation of a probable crack width and its comparison with an allowable crack width. This approach is followed by the Japan Society of Civil Engineers (1997b), which only considers aesthetics in setting a maximum allowable crack width of 0.020 in. (0.50 mm) and by CAN/CSA S6-06, which explicitly permits proportioning of the FRP reinforcement in such a way that the crack width does not exceed 0.020 in. (0.50 mm) for members subjected to aggressive environments, and 0.028 in. (0.70 mm) for other members. The ACI 318 crack control provisions do not address FRP reinforcement. For comparison purposes, the crack control provisions for steel reinforcement in ACI 318 correspond to a maximum crack width that varies approximately between 0.018 and 0.022 in. (0.46 and 0.56 mm).

Because of concerns about the adequacy of the empirically tuned model proposed by Gergely and Lutz (1968) for predicting crack widths in flexural members with large bar covers, ACI 318-99 replaced the traditional z -factor approach for crack control with an indirect procedure that controls flexural crack widths through a maximum reinforcing bar spacing. The dependence on exposure conditions was also eliminated. Rather than specifying a maximum allowable crack width, the objective now is to determine the maximum bar spacing necessary to achieve the required serviceability limit state of cracking based on the FRP reinforcement properties and the corresponding FRP bar stress (or strain) at service load levels. The current procedure also acknowledges the dominant effect that clear cover has on flexural cracking.

The maximum reinforcement spacing provisions of ACI 318 are derived from the crack width formulation developed by Frosch (1999), which is based on a physical model rather than being empirically derived.

To be consistent with ACI 318, flexural crack control in FRP-reinforced concrete beams and one-way slabs can be accomplished by specifying a maximum FRP bar spacing equal to

$$s_{max} = 1.15 \frac{E_f w}{f_{fs} k_b} - 2.5c_c \leq 0.92 \frac{E_f w}{f_{fs} k_b} \quad (7.3.1a)$$

The proposed flexural crack control procedure is said to be indirect because the maximum FRP bar spacing stipulated by Eq. (7.3.1a) would indirectly comply with a target maximum allowable crack width. The rationale behind this indirect flexural crack control approach is described by Ospina and Bakis (2007).

For the selected FRP stress level and target crack width limit, the evaluation of the maximum bar spacing per Eq. (7.3.1a) shall be based on a d_c value that complies with Eq. (7.3.1b). If a larger d_c value is required for specific durability requirements or any other reason and the maximum crack width limit cannot be relaxed, it is then necessary to reduce the stress level in the FRP reinforcement. This can be accomplished, for example, by increasing the amount of flexural reinforcement.

$$d_c \leq \frac{E_f w}{2f_{fs} \beta k_b} \quad (7.3.1b)$$

Selection of the limiting crack width to be used in Eq. (7.3.1a) and (7.3.1b) depends on the intended use of the structure. The procedure allows for controlling different levels of flexural cracking, spanning from very narrow cracks in structures in aggressive environments or where water tightness is required, to situations where wider cracks may be acceptable due to the superior corrosion resistance of FRP reinforcement. In general, crack widths in FRP-reinforced members will be larger than those in steel-reinforced members. In situations where crack widths are limited by aesthetic reasons, limiting crack widths in the range of 0.016 to 0.028 in. (0.4 to 0.7 mm) are generally acceptable.

The FRP stress at service, f_{fs} , can be evaluated by performing a cracked-elastic section analysis. Recommendations for the bar stress at service load in ACI 318 ($f_s = 0.67f_y$) are only applicable to steel-reinforced concrete when strength governs design and the steel reinforcement yields at failure. The same approach is not possible for FRP-reinforced concrete, as design is most often governed by serviceability limits related to deflection and crack width control or by fatigue and creep rupture effects.

The k_b term is a coefficient that accounts for the degree of bond between the FRP bar and the surrounding concrete. For FRP bars having bond behavior similar to uncoated steel bars, the bond coefficient k_b is assumed equal to 1.0. For

FRP bars having bond behavior inferior to steel, k_b is larger than 1.0, and for FRP bars having bond behavior superior to steel, k_b is smaller than 1.0. A test method for the determination of k_b has been approved by the Canadian Standards Association in CAN/CSA S806-12. For an analysis of crack width data performed by Bakis et al. (2006) on a variety of concrete cross-sections and FRP bar manufacturers, fiber types, resin formulations, and surface treatments, average k_b values ranged from 0.60 to 1.72, with a mean of 1.10. Data for rough sand-coated FRP bar surface treatments trended toward the lower end of this range. The consensus of the committee, for the case where k_b is not known from experimental data, is that a conservative value of 1.4 should be assumed. Smooth bars and grids are specifically excluded from this recommendation. Further analysis is needed before a committee consensus can be reached on k_b for such reinforcement.

Bakis and Boothby (2004) found that crack widths in GFRP-reinforced concrete beams under sustained loads increased beyond initial values by approximately 40 percent in an indoor environment and by approximately 60 percent in an outdoor environment over a period of 3 years. Further research is needed to examine the impact of long-term effects on these flexural crack control design provisions.

7.3.2 Deflections—In general, ACI 318 provisions for deflection control are concerned with deflections that occur at service levels under immediate and sustained static loads, and do not apply to dynamic loads such as earthquakes, transient winds, or vibration of machinery. Two methods are given in ACI 318 for control of deflections of one-way flexural members:

- 1) The indirect method of mandating the minimum thickness of the member (Table 9.5(a) in ACI 318).
- 2) The direct method of limiting computed deflections (Table 9.5(b) in ACI 318).

Because of the variable stiffness, brittle-elastic nature, and particular bond features of FRP reinforcement, deflections of FRP-reinforced concrete members are more sensitive to the variables affecting deflection than steel-reinforced members of identical size and reinforcement layout. Deflections in members with FRP reinforcement also tend to be greater in magnitude because of the lower stiffness associated with commercially available FRP reinforcement. This guide therefore recommends the use of a direct method of deflection control, as outlined as follows in 7.3.2.2 and 7.3.2.3. Recommended minimum thicknesses for FRP-reinforced members are provided in 7.3.2.1 for convenience in establishing initial member proportions for design only. Member dimensions may need to be revised based on the limits of calculated deflections.

7.3.2.1 Recommended minimum thicknesses for design—Recommended minimum thicknesses for design of one-way slabs and beams are provided in Table 7.3.2.1. The table is intended only to provide guidance for initial design. Use of these recommended minimum thicknesses does not guarantee that all deflection considerations will be satisfied for a particular project.

Values in Table 7.3.2.1 are based on a generic maximum span-to-depth ratio limitation (Ospina et al. 2001) corre-

Table 7.3.2.1—Recommended minimum thickness of nonprestressed beams or one-way slabs

Member	Minimum thickness h			
	Simply supported	One end continuous	Both ends continuous	Cantilever
Solid one-way slabs	$\ell/13$	$\ell/17$	$\ell/22$	$\ell/5.5$
Beams	$\ell/10$	$\ell/12$	$\ell/16$	$\ell/4$

sponding to the limiting curvature associated with a target deflection-span ratio (Eq. (7.3.2.1)). The procedure, which is described in detail by [Ospina and Gross \(2005\)](#), can be applied to flexural members at service loads with any type of linear-elastic reinforcement.

$$\frac{\ell}{h} \leq \frac{48\eta}{5K_1} \left(\frac{1-k}{\epsilon_{fs}} \right) \left(\frac{\Delta}{\ell} \right)_{max} \quad (7.3.2.1)$$

where $\eta = d/h$; k is as defined in Eq. (7.3.2.2b); and $(\Delta/\ell)_{max}$ is the limiting service load deflection-span ratio. K_1 is a parameter that accounts for boundary conditions. It may be taken as 1.0, 0.8, 0.6, and 2.4 for uniformly loaded simply supported, one end continuous, both ends continuous, and cantilevered spans, respectively. The term ϵ_{fs} is the strain in the FRP reinforcement under service loads, evaluated at midspan except for cantilevered spans. For cantilevers, ϵ_{fs} shall be evaluated at the support.

Equation (7.3.2.1) assumes no tensile contribution from concrete between cracks, also referred to as tension stiffening. To consider the effects of tension stiffening in developing Table 7.3.2.1, the values resulting from Eq. (7.3.2.1) were modified by the ratio of effective and fully cracked moments of inertia computed using Eq. (7.3.2.2c) and (7.3.2.2a), respectively. Tabulated values are based on an assumed service deflection limit of $\ell/240$ under total service load, and assumed reinforcement ratios of $2.0\rho_{fb}$ and $3.0\rho_{fb}$ for slabs and beams, respectively.

7.3.2.2 Effective moment of inertia—An uncracked section has a moment of inertia equal to the gross moment of inertia, I_g . Cracking occurs when the maximum service load moment M_a exceeds the cracking moment M_{cr} , and this causes a reduction in member stiffness. The moment of inertia of the cracked section, I_{cr} , for a singly-reinforced rectangular member is calculated for a cracked transformed section using an elastic analysis given by Eq. (7.3.2.2a) and (7.3.2.2b).

$$I_{cr} = \frac{bd^3}{3} k^3 + n_f A_f d^2 (1-k)^2 \quad (7.3.2.2a)$$

$$k = \sqrt{2\rho_f n_f + (\rho_f n_f)^2} - \rho_f n_f \quad (7.3.2.2b)$$

The overall flexural stiffness $E_c I$ of a cracked member varies between $E_c I_g$ and $E_c I_{cr}$, depending on the magnitude of the applied service moment and the extent of cracking along the member. [Branson \(1965\)](#) introduced the concept of an effective moment of inertia, I_e , to allow for a gradual transi-

tion from I_g to I_{cr} . This approach accounts for two different phenomena: the effect of concrete tension stiffening and the variation of EI along the member. Branson's (1965) equation for the effective moment of inertia, I_e , was adopted by [ACI 318-71](#).

As demonstrated by [Bischoff \(2005\)](#), Branson's equation overestimates member stiffness when the I_g/I_{cr} of the member is greater than approximately 3 or 4. This corresponds to most FRP-reinforced concrete beams that typically have an I_g/I_{cr} between 5 and 25. It is for this reason that past research on deflection of FRP-reinforced concrete beams ([Nawy and Neuwerth 1977](#); [Benmokrane et al. 1996](#); [Yost et al. 2003](#)) has shown that Branson's equation underestimates deflection, particularly for members with a high I_g/I_{cr} .

Several authors have proposed effective moment of inertia expressions for FRP-reinforced concrete. [Benmokrane et al. \(1996\)](#) first incorporated an empirical correction factor in Branson's equation that was needed to reduce tension stiffening and gave reasonable estimates of computed deflection. Other modifications to Branson's equation involving various correction factors have been proposed in the literature ([Gao et al. 1998a](#); [Toutanji and Saafi 2000](#); [Yost et al. 2003](#)). This modified-Branson approach was adopted by past editions of ACI 440.1R. Others have proposed a variety of methods that rely on different assumptions regarding tension stiffening and variations in stiffness along the length of the member ([Faza and GangaRao 1992](#); [Razaqpur et al. 2000](#); [Rasheed et al. 2004](#); [Bischoff 2005](#)). These models have displayed varying degrees of accuracy when compared to experimental databases ([Mota et al. 2006](#); [Bischoff et al. 2009](#)).

[Bischoff \(2005\)](#) proposed an alternative section-based expression for the effective moment of inertia, I_e , that works equally well for both steel- and FRP-reinforced concrete members without the need for empirical correction factors. Branson's original expression represents a weighted average of the uncracked and cracked member stiffness ($E_c I$), whereas [Bischoff's](#) proposed approach represents a weighted average of flexibility ($1/E_c I$). The approach using a weighted average of flexibility better represents the deflection response of members with discrete cracks along their length ([Bischoff and Scanlon 2007](#)).

The section-based expression proposed by [Bischoff \(2005\)](#) is modified as follows to include an additional factor γ to account for the variation in stiffness along the length of the member.

$$I_e = \frac{I_{cr}}{1 - \gamma \left(\frac{M_{cr}}{M_a} \right)^2 \left[1 - \frac{I_{cr}}{I_g} \right]} \leq I_g \quad \text{where } M_a \geq M_{cr} \quad (7.3.2.2c)$$

This approach provides reasonable estimates of deflection for FRP-reinforced concrete beams and one-way slabs ([Bischoff et al. 2009](#)). The factor γ is dependent on load and boundary conditions and accounts for the length of the uncracked regions of the member and for the change in stiffness in the cracked regions. In place of a more comprehensive analysis as suggested in [Bischoff and Gross \(2011\)](#),

the factor can be taken as $\gamma = 1.72 - 0.72(M_{cr}/M_a)$, which is the result from integrating the curvature over the length of a simply-supported beam with a uniformly distributed load.

Unless stiffness values are obtained by more comprehensive analysis, immediate deflections should be computed with the effective moment of inertia given by Eq. (7.3.2.2c) using the maximum service load moment M_a in the member. Deflection of continuous members can be estimated using a weighted average of I_e computed at the critical positive and negative moment sections, as recommended by ACI 318 and ACI 435R. For spans with both ends continuous, the effective moment of inertia may be approximated as $I_e = 0.70I_{e+} + 0.15(I_{e1-} + I_{e2-})$. For spans with one end continuous, I_e may be approximated based on the location of maximum moment along the span (DeSimone 2009).

The cracking moment M_{cr} is as specified in ACI 318 and should be computed using

$$M_{cr} = \frac{7.5\lambda\sqrt{f'_c}I_g}{y_t} \quad (7.3.2.2d)$$

For SI units

$$M_{cr} = \frac{0.62\lambda\sqrt{f'_c}I_g}{y_t}$$

When $M_a \geq M_{cr}$, the effects of cracking should be considered using Eq. (7.3.2.2c). Recommended minimum thickness values in Table 7.3.2.1 assume this condition. When calculations result in $M_a < M_{cr}$ but the difference between the two values is small, inherent variability in the tensile strength of concrete and the restraint of shrinkage due to the reinforcement may still cause the section to crack. In such cases, deflections will be significantly underestimated by the use of gross section properties. The designer should exercise judgment and consider the project-specific impacts of underestimating deflections in determining whether Eq. (7.3.2.2c) should be employed with a M_{cr}/M_a less than unity to give a more conservative estimate of deflection.

7.3.2.3 Calculation of deflection (direct method)—When deflections are estimated by computation according to the provisions of this section, the designer should compare computed deflections to acceptable limits set as part of the design criteria for the project. In many cases, these deflection criteria are set by local building codes.

The short-term deflections (instantaneous deflection under service loads) of an FRP one-way flexural member can be calculated using the effective moment of inertia of the FRP-reinforced beam and the usual structural analysis techniques.

The magnitude of long-term deflection can be several times the short-term deflection, and both short-term and long-term deflections under service loads should be considered in the design. The long-term increase in deflection is a function of member geometry (reinforcement area and member size), load characteristics (age of concrete at the time of loading, and magnitude and duration of sustained load), and mate-

rial characteristics (elastic moduli of the concrete and FRP reinforcement, creep and shrinkage of concrete, formation of new cracks, and widening of existing cracks).

Data on time-dependent deflections of FRP-reinforced members due to creep and shrinkage indicate that the time-versus-deflection curves of FRP- and steel-reinforced members have the same basic shape, indicating that the same fundamental approach for estimating the long-term deflection can be used (Brown 1997).

According to ACI 318, the long-term deflection due to creep and shrinkage $\Delta_{(cp+sh)}$ can be computed according to the following equations

$$\Delta_{(cp+sh)} = \lambda_{\Delta}(\Delta_t)_{sus} \quad (7.3.2.3a)$$

$$\lambda_{\Delta} = \frac{\xi}{1 + 50\rho'_f} \quad (7.3.2.3b)$$

The parameter λ_{Δ} in Eq. (7.3.2.3b) reduces to ξ because compression reinforcement is not considered for FRP reinforced members ($\rho'_f = 0$). Values of ξ are reported in ACI 318.

These equations can be used for FRP reinforcement with modifications to account for the differences in the axial stiffness of the reinforcement for FRP-reinforced concrete members as compared with steel-reinforced concrete members. With either FRP or steel reinforcement, concrete creep leads to an effective reduction in the flexural stiffness E_cI . For simplicity, this reduction can be considered as the superposition of two contradictory effects. The first effect is the decrease in effective elastic modulus as a direct result of the concrete creep. The second effect, which can be approximated using an elastic cross section analysis with the reduced elastic modulus for concrete, is an increase in neutral axis depth. This increased neutral axis depth leads to an effective increase in the moment of inertia of the cracked section. The increase in neutral axis depth can be shown to be proportionally more significant for FRP-reinforced members than for steel-reinforced members because of the lower axial stiffness of the reinforcement in typical FRP-reinforced concrete members. As a result, the time-dependent deflection increase for FRP-reinforced concrete can be expected to be proportionally less than for steel-reinforced concrete.

Brown (1997) observed that the time-dependent deflection of FRP-reinforced beams with no compression reinforcement over a sustained loading period of 6 months was 60 to 90 percent of the initial deflection. The measured additional time-dependent deflection was only 50 to 75 percent of the deflection suggested by Eq. (7.3.2.3a) and (7.3.2.3b). Similar results have been reported in other studies (Vijay et al. 1998; Arockiasamy et al. 1998) for both glass FRP (GFRP) and carbon FRP (CFRP).

Based on the aforementioned results, a modification factor of 0.6 is recommended to be applied to Eq. (7.3.2.3a). For typical applications, the long-term deflection of FRP-reinforced members can therefore be determined from Eq. (7.3.2.3c)

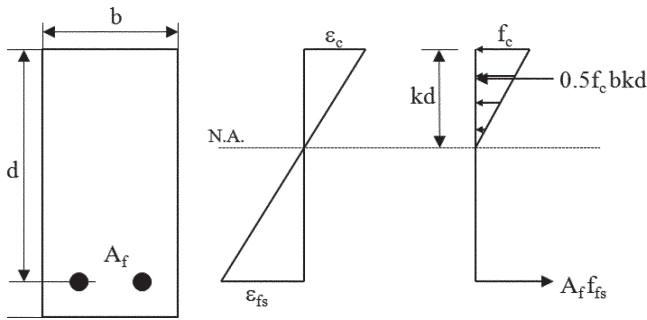


Fig. 7.4—Elastic stress and strain distribution.

$$\Delta_{(cp+sh)} = 0.6\xi(\Delta_i)_{sus} \quad (7.3.2.3c)$$

Gross et al. (2003) found that for beams that are not cracked prior to application of the sustained load, Eq. (7.3.2.3c) may significantly underestimate the time-dependent deflection multiplier. This situation may be found in members where most or all of the service load is sustained load. Gross et al. (2003) attributed this underestimation to the fact that additional flexural cracks were observed to form in the beams over time under the sustained loading. Further experimental work is necessary to validate Eq. (7.3.2.3c) for applications with high levels of sustained load.

7.4—Creep rupture and fatigue

To avoid creep rupture of the FRP reinforcement under sustained stresses or failure due to cyclic stresses and fatigue of the FRP reinforcement, the stress levels in the FRP reinforcement under these stress conditions should be limited. Because these stress levels will be within the elastic range of the member, the stresses can be computed through an elastic analysis, as depicted in Fig. 7.4.

7.4.1 Creep rupture stress limits—To avoid failure of an FRP-reinforced member due to creep rupture of the FRP, stress limits should be imposed on the FRP reinforcement. The stress level in the FRP reinforcement can be computed using Eq. (7.4.1), with $M_{s,sus}$ equal to the unfactored moment due to all sustained loads (dead loads and the sustained portion of the live load)

$$f_{fs,sus} = M_{s,sus} \frac{n_f d (1-k)}{I_{cr}} \quad (7.4.1)$$

The cracked moment of inertia, I_{cr} , and the ratio of the effective depth to the depth of the elastic neutral axis, k , are computed using Eq. (7.3.2.2a) and (7.3.2.2b).

Values for safe sustained stress levels are given in Table 7.4.1. These values are based on the creep rupture stress limits previously stated in 4.3.1, with an imposed safety factor of 1/0.60.

7.4.2 Fatigue stress limits—If the structure is subjected to fatigue regimes, the FRP stress should be limited to the values stated in Table 7.4.1. The FRP stress can be calculated using Eq. (7.4.1), by replacing $M_{s,sus}$ with the moment due to

Table 7.4.1—Creep rupture stress limits in FRP reinforcement

Fiber type	GFRP	AFRP	CFRP
Creep rupture stress limit $f_{fs,sus}$	$0.20f_{fu}$	$0.30f_{fu}$	$0.55f_{fu}$

all sustained loads plus the maximum moment induced in a fatigue loading cycle.

CHAPTER 8—SHEAR

The design of fiber-reinforced polymer (FRP)-reinforced concrete is similar to that of steel-reinforced concrete members. The different mechanical properties of FRP bars, however, affect shear strength and should be considered. This chapter addresses the shear resistance of FRP-reinforced beams and one-way slabs, the use of FRP stirrups, and the punching shear capacity of FRP-reinforced two-way slabs.

8.1—General considerations

Several issues should be considered for the shear design of FRP-reinforced members. Fiber-reinforced polymer has:

- 1) A relatively low modulus of elasticity;
- 2) A low transverse shear resistance;
- 3) A high tensile strength and no yield point.

Also, the tensile strength of the bent portion of an FRP bar is significantly lower than that of the straight portion.

8.1.1 Shear design philosophy—The design of FRP shear reinforcement is based on the strength design method. The strength reduction factor of 0.75 given by ACI 318 for reducing nominal shear capacity of steel-reinforced concrete members should also be used for FRP reinforcement. The design shear strength ϕV_n must be larger than the factored shear force V_u at the section considered. Computation of the maximum shear force V_u at beam supports can be attained following ACI 318 provisions.

8.2—Shear strength of FRP-reinforced members

According to ACI 318, the nominal shear strength of a reinforced concrete cross section, V_n , is the sum of the shear resistance provided by concrete, V_c , and the steel shear reinforcement, V_s .

Compared with a steel-reinforced section with equal areas of longitudinal reinforcement, a cross section using FRP flexural reinforcement after cracking has a smaller depth to the neutral axis because of the lower axial stiffness (product of reinforcement area and modulus of elasticity). The compression region of the cross section is reduced, and the crack widths are wider. As a result, the shear resistance provided by both aggregate interlock and compressed concrete is smaller. Research on the shear capacity of flexural members without shear reinforcement has indicated that the concrete shear strength is influenced by the stiffness of the tensile (flexural) reinforcement (Nagasaka et al. 1993; Zhao et al. 1995; Japan Society of Concrete Engineers 1997b; Sonobe et al. 1997; Michaluk et al. 1998; Tureyen and Frosch 2002, 2003).

The contribution of longitudinal FRP reinforcement in terms of dowel action has not been determined. Because of the lower strength and stiffness of FRP bars in the transverse direction, however, it is assumed that their dowel action

contribution is less than that of an equivalent steel area. Further research is needed to quantify this effect.

The concrete shear capacity V_c of flexural members using FRP as main reinforcement can be evaluated according to Eq. (8.2a)

$$V_c = 5\sqrt{f'_c}b_w(kd) \quad (8.2a)$$

For SI units

$$V_c = \frac{2}{5}\sqrt{f'_c}b_w(kd)$$

The parameter k may be evaluated using Eq. (8.3.2.2b).

Equation (8.2a) accounts for the axial stiffness of the FRP reinforcement through the neutral axis depth kd , which is a function of the reinforcement ratio ρ_f and the modular ratio n_f . This equation has been shown to provide a reasonable factor of safety for FRP-reinforced specimens across the range of reinforcement ratios and concrete strengths tested to date (Tureyen and Frosch 2003). Research on lightweight concrete members reinforced with GFRP bars is limited (Pantelides et al. 2012a,b). Based on these experiments, a reduction factor $\lambda = 0.80$ in conjunction with Eq. (8.2a) has been proposed for predicting the shear capacity of sand-lightweight concrete reinforced with GFRP bars (Liu and Pantelides 2013); alternatively, the Modified Compression Field Theory could be used to predict the shear capacity (Liu and Pantelides 2012).

Equation (8.2a) may be rewritten as Eq. (8.2b). This form of the equation indicates that Eq. (8.2a) is simply the ACI 318 shear equation for steel reinforcement V_c modified by the factor $([5/2]k)$, which accounts for the axial stiffness of the FRP reinforcement.

$$V_c = \left(\frac{5}{2}k\right)2\sqrt{f'_c}b_w d \quad (8.2b)$$

The ACI 318 method used to calculate the shear contribution of steel stirrups is applicable when using FRP as shear reinforcement. The shear resistance provided by FRP stirrups perpendicular to the axis of the member, V_f , can be written as

$$V_f = \frac{A_{fv}f_{fv}d}{s} \quad (8.2c)$$

The stress level in the FRP shear reinforcement should be limited to control shear crack widths and maintain shear integrity of the concrete and to avoid failure at the bent portion of the FRP stirrup (Eq. (6.2.1)). Equation (8.2d) gives the stress level in the FRP shear reinforcement at ultimate for use in design

$$f_{fv} = 0.004E_f \leq f_{fb} \quad (8.2d)$$

When using shear reinforcement perpendicular to the axis of the member, the required spacing and area of shear reinforcement can be computed from Eq. (8.2e)

$$\frac{A_{fv}}{s} = \frac{(V_u - \phi V_c)}{\phi f_{fv} d} \quad (8.2e)$$

When inclined FRP stirrups are used as shear reinforcement, Eq. (8.2f) is used to calculate the contribution of the FRP stirrups

$$V_f = \frac{A_{fv}f_{fv}d}{s}(\sin\theta + \cos\theta) \quad (8.2f)$$

When continuous FRP rectangular spirals are used as shear reinforcement (in this case, s is the pitch and θ is the angle of inclination of the spiral), Eq. (8.2g) gives the contribution of the FRP spirals

$$V_f = \frac{A_{fv}f_{fv}d}{s}(\sin\theta) \quad (8.2g)$$

Shear failure modes of members with FRP as shear reinforcement can be classified into two types (Nagasaka et al. 1993): shear-tension failure mode (controlled by the rupture of FRP shear reinforcement) and shear-compression failure mode (controlled by the crushing of the concrete web). The first mode is more brittle, and the latter results in larger deflections. Experimental results have shown that the modes of failure depend on the shear reinforcement index $\rho_{fv}E_f$, where ρ_{fv} is the ratio of FRP shear reinforcement A_{fv}/b_ws . As the value of $\rho_{fv}E_f$ increases, the shear capacity in shear tension increases, and the mode of failure changes from shear tension to shear compression.

8.2.1 Limits on tensile strain of shear reinforcement—The design assumption that concrete and reinforcement capacities are added is accurate when shear cracks are adequately controlled. Therefore, the tensile strain in FRP shear reinforcement should be limited to ensure that the ACI design approach is applicable.

CAN/CSA-S6-06 limits the tensile strain in FRP shear reinforcement to 0.002 in./in. (mm/mm). It is recognized that this strain value (corresponding to the yield strain of Grade 60 steel) may be very conservative. Experimental evidence indicated that higher strain values were always attained (Wang 1998; Zhao et al. 1995; Okamoto et al. 1994). The Eurocrete Project provisions limit the value of the shear strain in FRP reinforcement to 0.0025 in./in. (mm/mm) (Dowden and Dolan 1997). In no case should effective strain in FRP shear reinforcement exceed 0.004, nor should the design strength exceed the strength of the bent portion of the stirrup, f_{fb} . Ahmed et al. (2010a,b) reported that using 0.004 yields more accurate yet conservative predictions of the shear strength of concrete members reinforced with GFRP stirrups. The value of 0.004 is justified as the

strain that prevents degradation of aggregate interlock and corresponding concrete shear (Priestley et al. 1996). CAN/CSA-S6S1-10 adopted the 0.004 limit in the shear design of concrete members reinforced with FRP stirrups.

8.2.2 Minimum amount of shear reinforcement—ACI 318 requires a minimum amount of shear reinforcement when V_u exceeds $\phi V_c/2$. This requirement is to prevent or restrain shear failure in members where the sudden formation of cracks can lead to excessive distress (Joint ACI-ASCE Committee 426 1973). To prevent brittle shear failure, adequate reserve strength should be provided to ensure a factor of safety similar to ACI 318 provisions for steel reinforcement. Equation (8.2.2) gives the recommended minimum amount of FRP shear reinforcement

$$A_{f_v, \min} = \frac{50b_w s}{f_{f_v}} \quad (8.2.2)$$

For SI units

$$A_{f_v, \min} = 0.35 \frac{b_w s}{f_{f_v}}$$

with b_w and s in in. (mm), and f_{f_v} in psi (MPa).

The minimum amount of reinforcement given by Eq. (8.2.2) is independent of the concrete strength. If steel stirrups are used, the minimum amount of reinforcement provides a shear strength that varies from $1.50V_c$ when f'_c is 2500 psi (17 MPa) to $1.25V_c$ when f'_c is 10,000 psi (69 MPa). Equation (8.2.2), which was derived for steel-reinforced members, is more conservative when used with FRP-reinforced members. For example, when applied to a flexural member having GFRP as longitudinal reinforcement, the shear strength provided by Eq. (8.2.2) could exceed $3V_c$. The ratio of the shear strength provided by Eq. (8.2.2) to V_c will decrease as the stiffness of longitudinal reinforcement increases or as the strength of concrete increases.

8.2.3 Shear failure due to crushing of the web—Studies by Nagasaka et al. (1993) indicate that for FRP-reinforced sections, the transition from rupture to crushing limit states occurs at an average value of $0.3f'_c b_w d$ for V_c , but can be as low as $0.18f'_c b_w d$. When V_c is smaller than $0.18f'_c b_w d$, shear-tension can be expected, whereas when V_c exceeds $0.3f'_c b_w d$, crushing is expected. The correlation between rupture and the crushing limit states is not fully understood, and it is more conservative and recommended to use the ACI 318 limit of $8\sqrt{f'_c} b_w d$ rather than $0.3f'_c b_w d$. In fact, the ACI limitation is aimed at controlling excess shear crack widths and is, thus, below values corresponding to crushing of the web.

8.3—Detailing of shear stirrups

The maximum spacing of vertical steel stirrups given in ACI 318 as the smaller of $d/2$ or 24 in. (600 mm) is used for vertical FRP shear reinforcement. This limit ensures that each shear crack is intercepted by at least one stirrup.

Tests by Ehsani et al. (1995) indicated that for specimens with r_b/d_b of zero, the reinforcing bars failed in shear at very

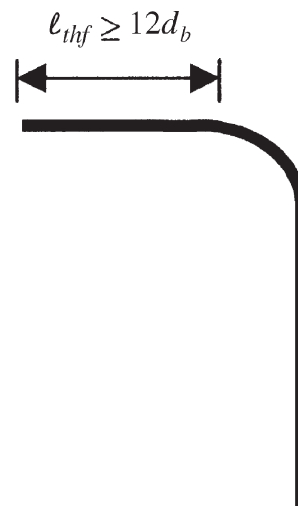


Fig. 8.3—Required tail length for FRP stirrups.

low load levels at the bends. Therefore, although manufacturing of FRP bars with sharp bends is possible, such details should be avoided. A minimum r_b/d_b ratio of 3 is recommended. In addition, FRP stirrups should be closed with 90-degree hooks.

ACI 318 provisions for bond of hooked steel bars cannot be applied directly to FRP reinforcing bars because of their different mechanical properties. The tensile force in a vertical stirrup leg is transferred to the concrete through the tail beyond the hook, as shown in Fig. 8.3. Ehsani et al. (1995) found that for a tail length ℓ_{thf} beyond $12d_b$, there is no significant slippage and no influence on the tensile strength of the stirrup leg. Therefore, a minimum tail length of $12d_b$ should be used.

8.4—Shear strength of FRP-reinforced two-way concrete slabs

Experimental evidence (Ahmad et al. 1993; Bank and Xi 1995; Bantia et al. 1995; Matthys and Taerwe 2000; El-Ghandour et al. 2003; Ospina et al. 2003) shows that the axial stiffness of the FRP reinforcement, as well as the concrete strength f'_c , significantly affect the transverse shear response of interior FRP-reinforced two-way slab-column connections. Test results of isolated FRP-reinforced two-way slab specimens subjected to uniform gravity loading indicate that an increase in the top FRP mat stiffness increases punching shear capacity and decreases the ultimate slab deflection. Punching shear failure in slabs reinforced with FRP bars is sudden and brittle. Conversely, punching test results (Bank and Xi 1995; Ospina et al. 2003) show that two-way slabs reinforced with FRP grids rather than bars do not exhibit a sharp load drop at punching failure. Instead, they continue to absorb energy in a stable fashion following initial failure. Hassan et al. (2013a) reported that increasing the reinforcement ratio resulted in higher punching-shear capacity, lower reinforcement and concrete strains, and lower deflections. In addition, the use of high-strength concrete increased the punching-shear capacity, significantly reduced concrete strains, increased strains in the GFRP reinforcing

bars, and reduced deflection due to the high tensile strength and modulus of elasticity.

A statistical evaluation of test results reveal that the one-way shear design model proposed by **Tureyen and Frosch (2003)**, which accounts for reinforcement stiffness, can be modified (**Ospina 2005**) to account for the shear transfer in two-way concrete slabs. The modification leads to Eq. (8.4a), which can be used to calculate the concentric punching shear capacity of FRP-reinforced two-way concrete slabs that are either supported by interior columns or subjected to concentrated loads that are either square or circular in shape

$$V_c = 10\sqrt{f'_c}b_o(kd) \quad (8.4a)$$

For SI units

$$V_c = \frac{4}{5}\sqrt{f'_c}b_o(kd)$$

The parameter k may be evaluated using Eq. (7.3.2.2b).

In the evaluation of Eq. (8.4a), b_o should be computed at $d/2$ away from the column face. In addition, the shape of the critical surface should be the same as that of the column.

Equation (8.4a) can be rewritten as Eq. (8.4b). This equation is simply the basic **ACI 318** concentric punching shear equation for steel-reinforced slabs V_c modified by the factor $([5/2]k)$ that accounts for the axial stiffness of the FRP reinforcement.

$$V_c = \left(\frac{5}{2}k\right)4\sqrt{f'_c}b_o d \quad (8.4b)$$

Equation (8.4a) provides a reasonable factor of safety for FRP-reinforced concrete two-way slabs across the range of reinforcement ratios and concrete strengths tested. Experimental results and design recommendations on shear strength of FRP-reinforced two-way slabs can be found in the literature (**CAN/CSA S806-12 2012**; **Lee et al. 2009**; **Dulude et al. 2013**; **Hassan et al. 2013b**). Further research is needed to examine the punching capacity of FRP-reinforced two-way slabs supported by edge and corner columns, as well as the effects of column rectangularity and unbalanced moment transfer on the punching capacity of FRP-reinforced concrete two-way slabs supported on interior columns.

CHAPTER 9—SHRINKAGE AND TEMPERATURE REINFORCEMENT

Shrinkage and temperature reinforcement is intended to limit crack width. The stiffness and strength of reinforcing bars control this behavior. Shrinkage cracks perpendicular to the member span are restricted by flexural reinforcement; therefore, shrinkage and temperature reinforcement are only required in the direction perpendicular to the span. ACI 318 requires a minimum steel reinforcement ratio of 0.0020 when using Grade 40 or 50 deformed steel bars, and 0.0018 when using Grade 60 deformed bars or welded reinforce-

ment (deformed or smooth). ACI 318 also requires that the spacing of shrinkage and temperature reinforcement not exceed five times the member thickness or 18 in. (500 mm).

9.1—Minimum FRP reinforcement ratio

No experimental data are available for the minimum FRP reinforcement ratio for shrinkage and temperature. ACI 318, Section 7.12.2, states that for slabs with steel reinforcement having a yield stress exceeding 60 ksi (414 MPa) measured at a yield strain of 0.0035, the ratio of reinforcement to gross area of concrete should be at least $0.0018 \times 60/f_y$, where f_y is in ksi, but not less than 0.0014. The stiffness and the strength of shrinkage and temperature FRP reinforcement can be incorporated in this formula. Therefore, when deformed FRP shrinkage and temperature reinforcement is used, the amount of reinforcement should be determined by using Eq. (9.1)

$$\rho_{f,ts} = 0.0018 \times \frac{60,000}{f_{fu}} \frac{E_s}{E_f} \quad (9.1)$$

For SI units

$$\rho_{f,ts} = 0.0018 \times \frac{414}{f_{fu}} \frac{E_s}{E_f}$$

Due to limited experience, it is recommended that the ratio of temperature and shrinkage reinforcement given by Eq. (9.1) be taken not less than 0.0014, the minimum value specified by ACI 318 for steel shrinkage and temperature reinforcement. The licensed design professional may consider an upper limit for the ratio of temperature and shrinkage reinforcement equal to 0.0036, or compute the ratio based on calculated strain levels corresponding to the nominal flexural capacity rather than the strains calculated using Eq. (9.1). Spacing of shrinkage and temperature FRP reinforcement should not exceed three times the slab thickness or 12 in. (300 mm), whichever is less. The use of FRP for temperature and shrinkage reinforcement for slabs-on-ground is presented in Appendix A.

CHAPTER 10—DEVELOPMENT AND SPLICES OF REINFORCEMENT

In a reinforced concrete flexural member, the tension force carried by the reinforcement balances the compression force in the concrete. The tension force is transferred to the reinforcement through the bond between the reinforcement and the surrounding concrete. Bond stresses exist whenever the force in the tensile reinforcement changes. Bond between fiber-reinforced polymer (FRP) reinforcement and concrete is developed through a mechanism similar to that of steel reinforcement and depends on FRP type, elastic modulus, surface deformation, and the shape of the FRP bar (**Al-Zahrani et al. 1996**; **Uppuluri et al. 1996**; **Gao et al. 1998b**).

10.1—Development of stress in straight bar

Figure 10.1 shows the equilibrium condition of an FRP bar of length l_e embedded in concrete. The force in the bar

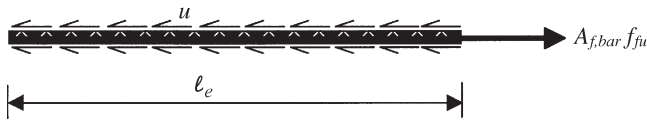


Fig. 10.1—Transfer of force through bond.

is resisted by an average bond stress u acting on the surface of the bar. Equilibrium of forces can be written as follows

$$\ell_e \pi d_b u = A_{f,bar} f_{fu} \quad (10.1a)$$

where f_f is the stress developed in the bar at the end of the embedment length. In contrast to steel bars, the full strength of an FRP bar need not be developed, especially when flexural capacity is controlled by concrete crushing and the required stress in the bar at failure is less than its guaranteed ultimate strength. Additionally, changing the limit state from bar fracture or concrete crushing to bond failure does not significantly change the ductility associated with the failure.

The development length equation for steel reinforcing bars found in ACI 318 is based on the work done by Orangun et al. (1977). The development length equation was based on 62 unconfined splice tests and 54 confined splice tests that failed by splitting concrete. Orangun et al. (1977) developed an equation relating the average bond stress normalized by the square root of the concrete compressive strength to the normalized cover to the center of the bar C/d_b and the normalized splice length d_b/ℓ_e using linear regression. This equation served as the foundation for the development length equation for steel reinforcing bars found in ACI 318.

A similar methodology was followed by Wambeke and Shield (2006) in which a consolidated database of 269 beam bond tests was created. The database was limited to beam-end tests, notch-beam tests, and splice tests. The majority of the bars represented in the database were composed of glass FRP (GFRP). In Wambeke and Shield's database (2006), there were 82 beam tests that resulted in splitting failures based on the work of Ehsani et al. (1996a), Daniali (1992), Shield et al. (1997, 1999), and Tighiouart et al. (1999). The tests included both spiral wrap and helical lug patterned bars with and without confining reinforcement. A linear regression of the normalized average bond stress versus the normalized cover and embedment (splice) length resulted in the following relationship after rounding the coefficients

$$\frac{u}{\sqrt{f'_c}} = 4.0 + 3.0 \frac{C}{d_b} + 100 \frac{d_b}{\ell_e} \quad (10.1b)$$

For SI units

$$\frac{u}{0.083\sqrt{f'_c}} = 4.0 + 0.3 \frac{C}{d_b} + 100 \frac{d_b}{\ell_e}$$

where C is the lesser of the cover to the center of the bar ($d_{c,side}$ or $d_{c,side}$) or one-half of the center-on-center spacing of the bars being developed. The bar surface (spiral wrap versus

helical lug) did not appear to affect the results, nor surprisingly did the presence of confining reinforcement (Wambeke and Shield 2006). Darwin et al. (1996) found that confining steel used in beams that had steel reinforcing bars with a high relative rib area had more of a beneficial increase in the bond force over the same-size steel bars with moderate rib area. The counter-argument is proposed herein. The GFRP bars have a very low relative rib area and, therefore, the presence of confinement may not increase the average bond stress. Additional research into the effect of confining reinforcement on bond of GFRP bars, however, is warranted.

Equations (10.1a) and (10.1b) can be solved for the achievable bar stress given the existing embedment length and cover. A random subset of the full database developed by Wambeke and Shield (2006) was used to determine a factor of safety for use with these equations. The resulting probability of a test-predicted ratio less than 1.0 was 22 percent. This database included both splitting and pullout failures with embedment lengths of at least $19d_b$. Additionally, a limit of 3.5 was put on the C/d_b term so that the same equation could be used to predict developable bar stresses for either splitting or pullout bond failure mode. When the normalized cover was over 3.5 and the embedment length was greater than $19d_b$, the failure mode was always pullout. The resulting expression for developable bar stress is

$$f_{fe} = \frac{\sqrt{f'_c}}{\alpha} \left(13.6 \frac{\ell_e}{d_b} + \frac{C}{d_b} \frac{\ell_e}{d_b} + 340 \right) \leq f_{fu} \quad (10.1c)$$

For SI units

$$f_{fe} = \frac{0.083\sqrt{f'_c}}{\alpha} \left(13.6 \frac{\ell_e}{d_b} + \frac{C}{d_b} \frac{\ell_e}{d_b} + 340 \right) \leq f_{fu}$$

in which the term C/d_b should not be taken larger than 3.5, and α is a factor to account for bar location (discussed in 10.1.1). The mean of the test-predicted ratio of bar stresses using this equation was 1.14, with a coefficient of variation of 15.8 percent. The appropriateness of this equation for embedment lengths greater than $100d_b$ is questionable, as the dataset used to develop it did not include any bond failures with embedment lengths greater than $100d_b$. Embedment lengths shorter than $20d_b$ are not recommended. Additional work needs to be performed to determine the effect of the chosen factor of safety for bond on the flexural reliability of the section.

When applying Eq. (10.1c) for design purposes, it should be assumed that the maximum achievable bar stress varies linearly from 0 to the value produced by Eq. (10.1c) along the first $20d_b$ of the bar embedment. After this point, Eq. (10.1c) can be used to determine the achievable bar stress along the bar. A check should be made to determine if adequate moment capacity can be achieved at the end of the available embedment length. If not, then the embedment length should be increased, the number of bars increased so that a lower stress in each bar is required at ultimate, or the

nominal moment capacity should be recalculated to include the possibility of bond failure, as described in 10.1.3. Note that increasing the number of bars may decrease the stress developed in any one bar, as the term C/d_b may decrease as the bar spacing decreases.

10.1.1 Bar location modification factor—The default bar location modification factor is 1.0. While placing concrete, air, water, and fine particles migrate upward through the concrete. This can cause a significant drop in bond strength under the horizontal reinforcement. The term “top reinforcement” usually refers to horizontal reinforcement with more than 12 in. (305 mm) of concrete below it at the time of embedment. The database assembled by **Wambeke and Shield (2006)** included 15 tests using top bars with embedment lengths greater than $16d_b$ that resulted in bond failure (**Ehsani et al. 1996a; Mosley 2002**). Based on these data, for bars with more than 12 in. (300 mm) of concrete cast below, α in Eq. (10.1c) should be taken as 1.5.

10.1.2 Material modification factor—A limited amount of bond data exists in the Wambeke and Shield (2006) database for aramid FRP (AFRP) bars (Mosley 2002). Based on these few tests, however, the development length of AFRP bars appears to be similar to that of GFRP bars. Therefore, the development length equations provided are also reasonable for AFRP bars without the addition of a material modification factor. No data exist in the database for carbon FRP (CFRP) bars; it is anticipated that the much larger stiffness of the CFRP bars will likely decrease the required development lengths and, correspondingly, its material modification factor. At this time, a material factor equal to 1.0 is recommended for CFRP bars.

10.1.3 Nominal moment strength of bond critical sections—Bond critical sections are defined as sections where the maximum achievable stress in the FRP bar is limited by Eq. (10.1c). For this case, the nominal moment capacity should be recalculated using a modification of the method described in 7.2. When bond limits the stress that can be developed in the bar, the two possible limit states are concrete crushing and bond failure. The capacity for a concrete crushing limit state can be calculated using Eq. (7.2.2e). This equation is applicable if the bar stress that can be developed (f_{fe} as determined from Eq. (10.1c)) is greater than or equal to the bar stress determined by Eq. (7.2.2d). When $\rho_f \leq \rho_{fb}$ or $\rho_f > \rho_{fb}$ and the bar stress required in Eq. (7.2.2d) cannot be developed, the capacity for the limit state of bond failure can be determined using Eq. (7.2.2g) with f_{fe} from Eq. (10.1c) substituted for f_{fu} , and f_{fe}/E_f substituted for ϵ_{fu} in Eq. (7.2.2h). A strength reduction factor of 0.55 is recommended for flexure when the limit state is bond failure.

10.2—Development length of bent bar

Limited experimental data are available on the bond behavior of hooked FRP reinforcing bars. **ACI 318** provisions for development length of hooked steel bars are not applicable to FRP bars due to the differences in material characteristics.

Ehsani et al. (1996b) tested 36 specimens with hooked GFRP bars. Based on the results of the study, the expression

for the development length of a 90-degree hooked bar ℓ_{bhf} was proposed as follows

$$\ell_{bhf} = K_4 \frac{d_b}{\sqrt{f'_c}} \quad (10.2a)$$

The K_4 factor for the calculation of the development length in this equation is 1820 (150 for SI units) for bars with f_{fu} less than 75,000 psi (517 MPa). This factor should be multiplied by $f_{fu}/75,000$ ($f_{fu}/517$) for bars having a tensile strength between 75,000 and 150,000 psi (517 and 1034 MPa).

When the side cover (normal to the plane of hook) is more than 2-1/2 in. (64 mm) and the cover extension beyond hook is not less than 2 in. (50 mm), another multiplier of 0.7 can be applied (Ehsani et al. 1996b). These modification factors are similar to those in ACI 318, Section 12.5.3, for steel hooked bars. To account for the lack of experimental data, the use of Eq. (10.2b) in calculating the development length of hooked bars is recommended

$$\ell_{bhf} = \begin{cases} 2000 \frac{d_b}{\sqrt{f'_c}} & \text{for } f_{fu} \leq 75,000 \text{ psi} \\ \frac{f_{fu}}{37.5} \frac{d_b}{\sqrt{f'_c}} & \text{for } 75,000 < f_{fu} < 150,000 \text{ psi} \\ 4000 \frac{d_b}{\sqrt{f'_c}} & \text{for } f_{fu} \geq 150,000 \text{ psi} \end{cases} \quad (10.2b)$$

For SI units

$$\ell_{bhf} = \begin{cases} 165 \frac{d_b}{\sqrt{f'_c}} & \text{for } f_{fu} \leq 520 \text{ MPa} \\ \frac{f_{fu}}{3.1} \frac{d_b}{\sqrt{f'_c}} & \text{for } 520 < f_{fu} < 1040 \text{ MPa} \\ 330 \frac{d_b}{\sqrt{f'_c}} & \text{for } f_{fu} \geq 1040 \text{ MPa} \end{cases}$$

with ℓ_{bhf} and d_b in in. (mm) and f_{fu} and f'_c in psi (MPa), in mm.

The value calculated using Eq. (10.2b) should not be less than $12d_b$ or 9 in. (230 mm). These values are based on test results reported by **Ehsani et al. (1995)**, in which the tensile force and slippage of a hooked bar stabilized near $12d_b$. The tail length of a hooked bar, ℓ_{thf} (Fig. 8.3), should not be less than $12d_b$. Longer tail lengths were found to have an insignificant influence on the ultimate tensile force and slippage of the hook. To avoid shear failure at the bend, the radius of the bend should not be less than $3d_b$ (Ehsani et al. 1995).

10.3—Development of positive moment reinforcement

In general, the requirements of 12.10 and 12.11 of ACI 318 should be met when using FRP reinforcement with the following changes: for straight bars, the stress to be developed f_{fr} should be the minimum of f_{fu} , the stress given by Eq. (7.2.2d), and the stress given by Eq. (11.1c). The development length for straight bars is defined as the bond length required to develop f_{fr} and is given by

$$\ell_d = \frac{\alpha \frac{f_{fr}}{\sqrt{f'_c}} - 340}{13.6 + \frac{C}{d_b}} d_b \quad (10.3a)$$

For SI units

$$\ell_d = \frac{\alpha \frac{f_{fr}}{0.083\sqrt{f'_c}} - 340}{13.6 + \frac{C}{d_b}} d_b$$

where C is the lesser of the cover to the center of the bar (d_c or $d_{c,side}$) or one-half of the center-on-center spacing of the bars being developed. Because of the reduced resistance factor compared with steel, the provision for development of positive reinforcement at points of inflection and simple supports given in ACI 318, Section 12.11.3, should be altered to

$$\ell_d \leq \frac{\phi M_n}{V_u} + \ell_a \quad (10.3b)$$

where M_n is the nominal moment strength assuming all reinforcement at the section to be stressed to the required bar stress f_{fr} ; V_u is the factored shear force at the section; and ℓ_a , at a support, is the embedment length beyond center of the support, or ℓ_a , at a point of inflection, is the larger of the effective depth of the member or $12d_b$. The value of $\phi M_n/V_u$ may be increased by 30 percent when the ends of the reinforcement are confined by a compressive reaction. This restriction on the development length need not be met if it can be shown by refined analysis that the design moment capacity is greater than the factored moment everywhere along the development length.

10.4—Tension lap splice

ACI 318, Section 12.15, distinguishes between two types of tension lap splices, depending on the fraction of the bars spliced in a given length and on the reinforcement stress in the splice. For steel reinforcement, the splice length for a Class A splice is $1.0\ell_d$, and for a Class B splice is $1.3\ell_d$. This classification for FRP applications is inappropriate, as often the full tensile strength of the bar need not be developed; hence, the assumption that all splices are Class B splices is conservative. Limited data are available for the minimum development length of FRP tension lap splices (Benmokrane 1997; Mosley 2002). Consequently, a value of $1.3\ell_d$ is recommended for all splices.

CHAPTER 11—DESIGN EXAMPLES

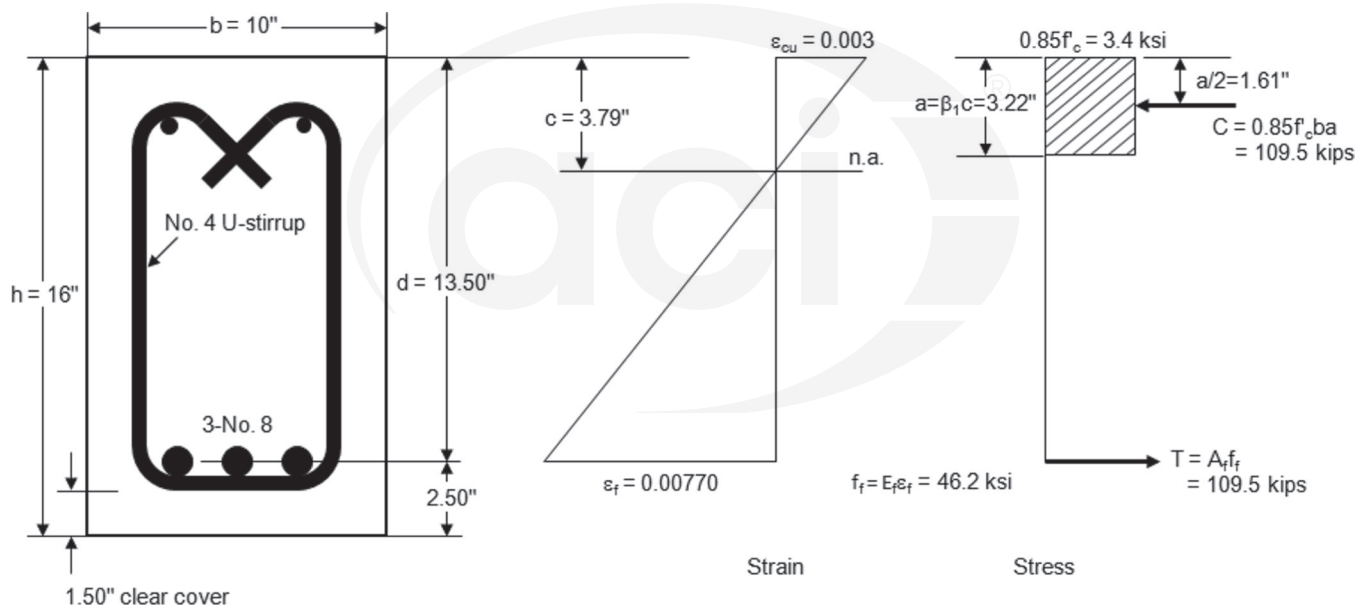
A series of design examples is provided to illustrate the design concepts and procedures presented earlier in this design guide. The examples have been developed to be similar to examples presented in the Portland Cement Association (PCA) publication, *Notes on ACI 318-08 Building Code Requirements for Structural Concrete* (Portland Cement Association 2008). In a few cases, the problem statements are identical. In most cases, minor modifications have been made to the original PCA (2008) *Notes* problem statements to make them more suitable for use as examples for FRP-reinforced concrete. It is anticipated that additional examples will be added, as new provisions are developed for future editions of this design guide. Examples are presented first in customary inch-pound units, and then in SI units.

Material properties are given for the concrete and reinforcement in the problem statement for each example. Material properties are generally reflective of glass FRP (GFRP) reinforcement because this is the most commonly used FRP reinforcing material for internal reinforcement today. As noted in 4.2.1, the guaranteed ultimate tensile strength (f_{fu}^*) of the reinforcement typically varies with bar size for a given manufacturer, with smaller reinforcement having higher strengths. For simplicity, this variation is neglected in the examples presented herein, and the tensile strength is taken as a single value regardless of bar diameter.

Example 1—Flexural (moment) strength using equivalent rectangular concrete stress distribution (compression-controlled section)

This example is similar to Example 6.1 of PCA Notes on ACI 318-08.

For the beam section shown, calculate moment strength based on static equilibrium using the equivalent rectangular concrete stress distribution as shown in Fig. 7.2 of this guide. Assume $f'_c = 4000$ psi, $f_{fu}^* = 80,000$ psi, and $E_f = 6000$ ksi. Assume interior exposure conditions and neglect compression reinforcement.


Calculations and discussion

No. 8 bar properties:

$$d_b = 1.00 \text{ in.}$$

$$A_{f,bar} = 0.79 \text{ in.}^2$$

Design material properties:

$$C_E = 0.8$$

$$f_{fu} = C_E f_{fu}^* = (0.8)(80) = 64 \text{ ksi}$$

1. Determine the strength reduction factor.

$$d = 16 - 1.5 - 0.5 - (1.00/2) = 13.50 \text{ in.}$$

$$A_f = (3)(0.79 \text{ in.}^2) = 2.37 \text{ in.}^2$$

$$\rho_f = \frac{A_f}{bd} = \frac{2.37}{(10)(13.50)} = 0.01756$$

Reference

440.6-08, Table 7.1

440.1R, Table 6.2

440.1R, Eq. (6.2a)

440.1R, Eq. (7.2.1a)

$$\rho_{fb} = 0.85\beta_1 \frac{f'_c}{f_{fu}} \frac{E_f \epsilon_{cu}}{E_f \epsilon_{cu} + f_{fu}} \quad 440.1R, \text{ Eq. (7.2.1b)}$$

$$E_f \epsilon_{cu} = (6000)(0.003) = 18.00 \text{ ksi}$$

$$\rho_{fb} = 0.85(0.85) \frac{(4)}{(64)} \frac{(18.00)}{(18.00 + 64)} = 0.00991$$

$$\frac{\rho_f}{\rho_{fb}} = \frac{0.01756}{0.00991} = 1.77$$

Because $\rho_f \geq 1.4\rho_{fb}$, the section is compression-controlled.
 $\phi = 0.65$

440.1R, Eq. (7.2.3)

2. Determine stress in tensile reinforcement at ultimate conditions.

$$f_f = \sqrt{\frac{(E_f \epsilon_{cu})^2}{4} + \frac{0.85\beta_1 f'_c}{\rho_f} E_f \epsilon_{cu} - 0.5 E_f \epsilon_{cu}} \leq f_{fu} \quad 440.1R, \text{ Eq. (7.2.2d)}$$

$$f_f = \sqrt{\frac{(18.00)^2}{4} + \frac{0.85(0.85)(4)}{(0.01756)}(18.00) - 0.5(18.00)} \leq 64$$

$$f_f = 46.2 \text{ ksi}$$

3. Determine nominal flexural strength M_n and design flexural strength ϕM_n .

$$a = \frac{A_f f_f}{0.85 f'_c b} = \frac{(2.37)(46.2)}{0.85(4)(10)} = 3.22 \text{ in.} \quad 440.1R, \text{ Eq. (7.2.2b)}$$

$$M_n = A_f f_f \left(d - \frac{a}{2} \right) = (2.37)(46.2) \left(13.50 - \frac{3.22}{2} \right) = 1302 \text{ in.-kip} = 108.5 \text{ ft-kip} \quad 440.1R, \text{ Eq. (7.2.2a)}$$

Alternatively, compute M_n directly:

$$M_n = \rho_f f_f \left(1 - 0.59 \frac{\rho_f f_f}{f'_c} \right) b d^2 \quad 440.1R, \text{ Eq. (7.2.2e)}$$

$$= (0.01756)(46.2) \left(1 - 0.59 \frac{(0.01756)(46.2)}{4} \right) (10)(13.50)^2 = 1302 \text{ in.-kip} = 108.5 \text{ ft-kip}$$

$$\phi M_n = (0.65)(108.5) = 70.5 \text{ ft kip}$$

4. Minimum reinforcement.

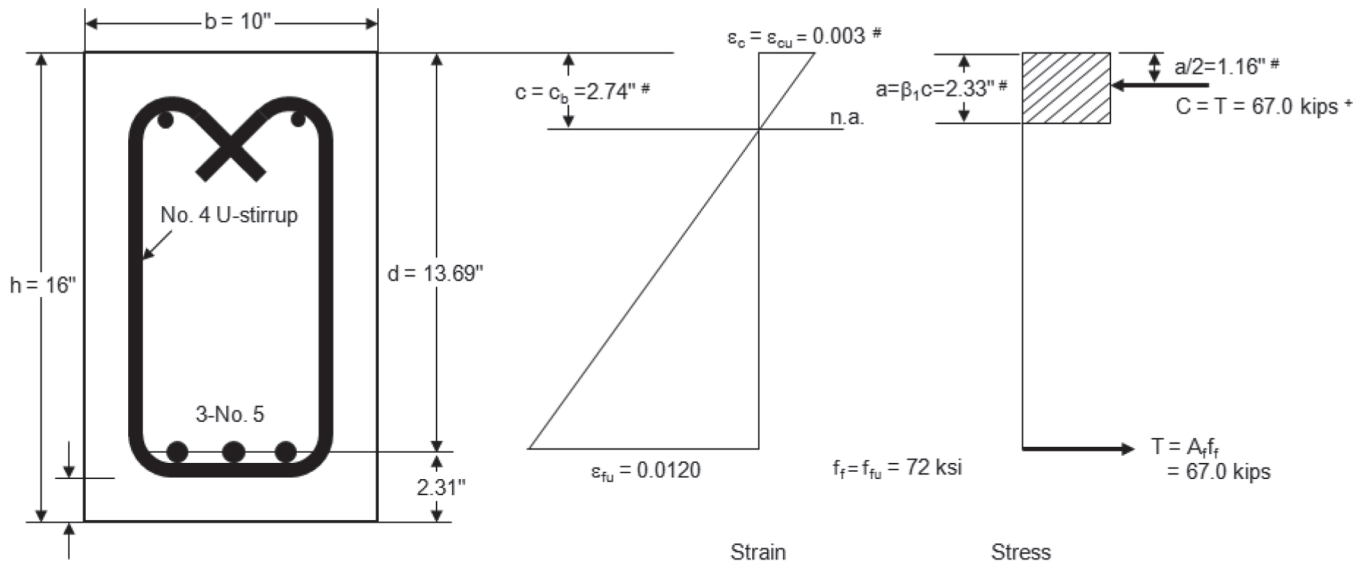
The minimum reinforcement provisions do not apply because the section is not tension-controlled. 440.1R, Sec. 7.2.4

Note: While the general procedure and principles used in this example are applicable for an FRP-reinforced beam of any cross-sectional shape, the specific equations used in this example are restricted to singly-reinforced rectangular cross sections (or flanged sections that exhibit rectangular section behavior) with reinforcement in a single layer.

Example 2—Flexural (moment) strength using equivalent rectangular concrete stress distribution (tension-controlled section)

This example is similar to Example 6.1 of PCA Notes on ACI 318-08.

For the beam section shown, calculate moment strength based on static equilibrium using the equivalent rectangular concrete stress distribution as shown in Fig. 7.2 of this guide. Assume $f'_c = 4000$ psi, $f_{fu}^* = 90,000$ psi, and $E_f = 6000$ ksi. Assume interior exposure conditions and neglect compression reinforcement.



1.5" clear cover

Conservatively assumed for design simplification. True values for c , a , and ϵ_c will be smaller, since actual NA will be higher.
 * Compression force must equal tension force. C cannot be calculated as $0.85f'_c b a$, since the correct value of a is not known.

Calculations and discussion

No. 5 bar properties:

$d_b = 0.625$ in.
 $A_{f,bar} = 0.31$ in.²

Design material properties:

$C_E = 0.8$
 $f_{fu} = C_E f_{fu}^* = (0.8)(90) = 72$ ksi

1. Determine the strength reduction factor.

$d = 16 - 1.5 - 0.5 - (0.625/2) = 13.69$ in.
 $A_f = (3)(0.31 \text{ in.}^2) = 0.93 \text{ in.}^2$

$\rho_f = \frac{A_f}{bd} = \frac{0.93}{(10)(13.69)} = 0.00679$

$\rho_{fb} = 0.85\beta_1 \frac{f'_c}{f_{fu}} \frac{E_f \epsilon_{cu}}{E_f \epsilon_{cu} + f_{fu}}$

$E_f \epsilon_{cu} = (6000)(0.003) = 18.00$ ksi

$\rho_{fb} = 0.85(0.85) \frac{(4)}{(72)} \frac{(18.00)}{(18.00 + 72)} = 0.00803$

$\frac{\rho_f}{\rho_{fb}} = \frac{0.00679}{0.00803} = 0.85$

Because $\rho_f \leq \rho_{fb}$, the section is tension-controlled and $\phi = 0.55$.

2. Determine stress in tensile reinforcement at ultimate conditions.

Because section is tension-controlled, $f_f = f_{fu} = 72$ ksi

3. Determine nominal flexural strength M_n and design flexural strength ϕM_n .

Reference

440.6-08, Table 7.1

440.1R, Table 6.2
 440.1R, Eq. (6.2a)

440.1R, Eq. (7.2.1a)

440.1R, Eq. (7.2.1b)

440.1R, Eq. (7.2.3)

$$c_b = \left(\frac{\epsilon_{cu}}{\epsilon_{cu} + \epsilon_{fu}} \right) d = \left(\frac{0.003}{0.003 + \frac{72}{6000}} \right) (13.69) = 2.74 \text{ in.} \quad 440.1R, \text{ Eq. (7.2.2h)}$$

$$M_n = A_f f_{fu} \left(d - \frac{\beta_1 c_b}{2} \right) = (0.93)(72) \left(13.69 - \frac{(0.85)(2.74)}{2} \right) = 839 \text{ in.-kip} = 69.9 \text{ ft-kip} \quad 440.1R, \text{ Eq. (7.2.2g)}$$

$$\phi M_n = (0.55)(69.9) = 38.4 \text{ ft-kip}$$

4. Minimum reinforcement

The minimum reinforcement provisions apply since the section is tension-controlled. 440.1R, Sec. 7.2.4

$$A_{f,min} = \frac{4.9\sqrt{f'_c}}{f_{fu}} b_w d \geq \frac{330}{f_{fu}} b_w d \quad 440.1R, \text{ Eq. (7.2.4)}$$

$$A_{f,min} = \frac{4.9\sqrt{4000}}{(72)(1000)} (10)(13.69) \geq \frac{330}{(72)(1000)} (10)(13.69)$$

$$= 0.59 \geq 0.63$$

$$A_{f,min} = 0.63 \text{ in.}^2$$

$$A_f(\text{provided}) = 0.93 \text{ in.}^2 > A_{f,min} = 0.63 \text{ in.}^2 \quad \text{OK}$$

Note: Whereas the general procedure and principles used in this example are applicable for an FRP-reinforced beam of any cross-sectional shape, the specific equations used in this example are restricted to singly-reinforced rectangular cross sections (or flanged sections that exhibit rectangular section behavior) with reinforcement in a single layer.

The procedure used in this example, described in 7.2.2, is approximate and conservative. A more detailed analysis of a tension-controlled cross section would require the computation of the neutral axis location based on the principles of strain compatibility and a numerical constitutive model for the concrete (for example, parabolic and Hognestad). This type of analysis can be computationally intensive and is generally not suitable for hand calculations. For problems such as the one shown in this example, differences in results (computed flexural strength) are likely to be negligible. A strain compatibility analysis is suggested for cases where there are multiple layers of reinforcement or when different FRP bar types are mixed (7.2.5.1).

Example 3—Design of a rectangular beam with tension reinforcement only

This example is similar to Example 7.1 of PCA Notes on ACI 318-08.

Design a rectangular beam of width $b = 12$ in. to have adequate flexural strength. The beam must resist service load moments $M_D = 56$ ft-kip and $M_L = 35$ ft-kip. Assume interior exposure conditions.

$$f'_c = 4000 \text{ psi}$$

$$f_{fu}^* = 80,000 \text{ psi}$$

$$E_f = 6500 \text{ ksi}$$

Calculations and discussion

Design material properties:

$$C_E = 0.8$$

$$f_{fu} = C_E f_{fu}^* = (0.8)(80) = 64 \text{ ksi}$$

Reference

440.1R, Table 6.2

440.1R, Eq. (6.2a)

1. A common starting point for design of a reinforced concrete member of unknown dimensions is the assumption of a reinforcement ratio.

As a starting point, assume $\rho_f = 1.5\rho_{fb}$.

$$\rho_{fb} = 0.85\beta_1 \frac{f'_c}{f_{fu}} \frac{E_f \epsilon_{cu}}{E_f \epsilon_{cu} + f_{fu}} \quad 440.1R, \text{ Eq. (7.2.1b)}$$

$$E_f \epsilon_{cu} = (6500)(0.003) = 19.50 \text{ ksi}$$

$$\rho_{fb} = 0.85(0.85) \frac{(4)}{(64)} \frac{(19.50)}{(19.50 + 64)} = 0.01055$$

$$\rho_f = 1.5\rho_{fb} = 1.5(0.01055) = 0.01583$$

Because $\rho_f \geq 1.4\rho_{fb}$, the section is compression-controlled.
 $\phi = 0.65$

440.1R, Eq. (7.2.3)

2. Compute bd^2 required.

First, determine the required design moment strength:

$$\phi M_{n, reqd} = M_u = 1.2M_D + 1.6M_L = 1.2(56) + 1.6(35) = 123.2 \text{ ft-kip}$$

318-11, Eq. (9-2)

Calculate the stress in the tensile reinforcement (f_f) at ultimate conditions for the assumed value of ρ_f .

$$f_f = \sqrt{\frac{(E_f \epsilon_{cu})^2}{4} + \frac{0.85\beta_1 f'_c}{\rho_f} E_f \epsilon_{cu} - 0.5E_f \epsilon_{cu}} \leq f_{fu} \quad 440.1R, \text{ Eq. (7.2.2d)}$$

$$f_f = \sqrt{\frac{(19.50)^2}{4} + \frac{0.85(0.85)(4)}{(0.01583)}(19.50) - 0.5(19.50)} \leq 64$$

$$f_f = 50.7 \text{ ksi}$$

Use the moment capacity equation to determine required dimensions for the cross section.

$$M_u = \phi M_n = \phi \rho_f f_f \left(1 - 0.59 \frac{\rho_f f_f}{f'_c}\right) b d^2 \quad 440.1R, \text{ Eq. (7.2.2e)}$$

$$(123.2)(12) = (0.65)(0.01583)(50.7) \left(1 - 0.59 \frac{(0.01583)(50.7)}{(4)}\right) b d^2$$

$$b d^2 = 3214 \text{ in.}^3$$

3. Size member so that $(bd^2)_{provided} \geq (bd^2)_{required}$.

$$\text{Recall } b = 12 \text{ in., so } d = \sqrt{\frac{3214}{12}} = 16.36 \text{ in.}$$

4. Now, determine the required reinforcement, select bars, and determine depth.

$$A_{f, reqd} = \rho_f b d = (0.01583)(12)(16.36) = 3.11 \text{ in.}^2$$

Select four No. 8 bars ($A_f = 3.16 \text{ in.}^2$)

Note: Examining alternative designs using other bar sizes may require changing the assumed value of f_{fu} to a value appropriate for the selected bar size.

No. 8 bar diameter: $d_b = 1.00 \text{ in.}$

440.6-08, Table 7.1

For interior exposure, clear cover is 1.5 in.

440.5-08, Table 3.1

Assuming No. 4 stirrups:

$$h = (16.36) + (1.5) + (0.5) + \frac{(1.00)}{2} = 18.86 \text{ in.}$$

Round up to be conservative. So, select a 12 x 20 in. beam.

5. Determine capacity of cross section.

$$d = 20 - \left[(1.5) + (0.5) + \frac{(1.00)}{2} \right] = 17.50 \text{ in.}$$

$$\rho_f = \frac{A_f}{bd} = \frac{3.16}{(12)(17.50)} = 0.01505 \quad 440.1R, \text{ Eq. (7.2.1a)}$$

$$\frac{\rho_f}{\rho_{fb}} = \frac{0.01505}{0.01055} = 1.43$$

Because $\rho_f \geq 1.4\rho_{fb}$, $\phi = 0.65$. 440.1R, Eq. (7.2.3)

$$f_f = \sqrt{\frac{(E_f \epsilon_{cu})^2}{4} + \frac{0.85\beta_1 f'_c}{\rho_f} E_f \epsilon_{cu}} - 0.5 E_f \epsilon_{cu} \leq f_{fu} \quad 440.1R, \text{ Eq. (7.2.2d)}$$

$$f_f = \sqrt{\frac{(19.50)^2}{4} + \frac{0.85(0.85)(4)}{(0.01505)} (19.50) - 0.5(19.50)} \leq 64$$

$$f_f = 52.2 \text{ ksi}$$

$$M_n = \rho_f f_f \left(1 - 0.59 \frac{\rho_f f_f}{f'_c} \right) b d^2 \quad 440.1R, \text{ Eq. (7.2.2e)}$$

$$= (0.01505)(52.2) \left(1 - 0.59 \frac{(0.01505)(52.2)}{4} \right) (12)(17.50)^2 = 2553 \text{ in.-kip} = 212.7 \text{ ft-kip}$$

$$\phi M_n = (0.65)(212.7) = 138.3 \text{ ft-kip} > M_u = 123.2 \text{ ft-kip} \quad \text{OK}$$

Note: Many designs for FRP-reinforced concrete are governed by serviceability requirements related to crack control, deflections, and creep rupture, rather than by flexural strength requirements. Calculations related to these serviceability requirements are covered in other example problems in this chapter.

Example 4—Design of one-way solid slab

This example is similar to Example 7.2 of PCA Notes on ACI 318-08.

Determine the required thickness and reinforcement for a one-way slab continuous over three or more equal spans. Center-to-center span $\ell = 19$ ft and clear span $\ell_n = 18$ ft. Assume interior exposure conditions.

$$f'_c = 4000 \text{ psi}$$

$$f_{fu}^* = 95,000 \text{ psi}$$

$$E_f = 6000 \text{ ksi}$$

Service loads: $w_D =$ slab self-weight (no superimposed dead load), $w_L = 50 \text{ lb/ft}^2$

Calculations and discussion

Design material properties:

$$C_E = 0.8$$

$$f_{fu} = C_E f_{fu}^* = (0.8)(95) = 76 \text{ ksi}$$

1. Determine required slab thickness.

Based on minimum thickness table, consider estimated depth.

End span will control thickness:

$$h \approx \frac{\ell}{17} = \frac{(19)(12)}{17} = 13.4 \text{ in.} \quad 440.1R, \text{ Table 7.3.2.1}$$

Table 7.3.2.1 is only intended to provide guidance for initial design, therefore, assume $h = 12$ in.

2. Compute the design moments using approximate moment analysis permitted by ACI 318-11,

Sec. 8.3.3. Design will be based on the end span because it will yield the highest moments.

Assume the end of the end span is integral with the support.

$$12 \text{ in. slab weighs } [(12)/(12)](150) = 150 \text{ lb/ft}^2$$

$$\text{Factored load } q_u = 1.2(150) + 1.6(50) = 260 \text{ lb/ft}^2$$

$$318-11, \text{ Eq. (9-2)}$$

Reference

440.1R, Table 6.2

440.1R, Eq. (6.2a)

Positive moment at discontinuous end integral with support:

$$+M_u = \frac{q_u \ell_n^2}{14} = \frac{(0.260)(18)^2}{14} = 6.02 \text{ ft-kip/ft} \quad 318-11, \text{ Sec. 8.3.3}$$

Negative moment at exterior face of first interior support:

$$-M_u = \frac{q_u \ell_n^2}{10} = \frac{(0.260)(18)^2}{10} = 8.42 \text{ ft-kip/ft} \quad 318-11, \text{ Sec. 8.3.3}$$

3. Determine required reinforcement and select bars.

Assume section is tension-controlled. For this case, $f_f = f_{fu} = 76$ ksi and $\phi = 0.55$.

For interior exposure, clear cover is 0.75 in.

440.5-08, Table 3.1

Assume No. 5 bars for flexural reinforcement.

No. 5 bar diameter: $d_b = 0.625$ in.

440.6-08, Table 7.1

$$d = 12 - \left[(0.75) + \frac{(0.625)}{2} \right] = 10.94 \text{ in.}$$

$$c_b = \left(\frac{\epsilon_{cu}}{\epsilon_{cu} + \epsilon_{fu}} \right) d = \left(\frac{0.003}{0.003 + \frac{76}{6000}} \right) (10.94) = 2.09 \text{ in.} \quad 440.1R, \text{ Eq. (7.2.2h)}$$

Use moment strength equation to solve for area of reinforcement.

Consider $-M$ because it governs.

$$M_u = \phi M_{n, reqd} = \phi A_{f, reqd} f_{fu} \left(d - \frac{\beta_1 c_b}{2} \right) \quad 440.1R, \text{ Eq. (7.2.2g)}$$

$$A_{f, reqd} = \frac{M_u}{\phi f_{fu} \left(d - \frac{\beta_1 c_b}{2} \right)} = \frac{(8.42)(12)}{(0.55)(76) \left(10.94 - \frac{(0.85)(2.09)}{2} \right)} = 0.24 \text{ in.}^2/\text{ft}$$

Note that this requirement is well less than the minimum reinforcement, as computed in the following.

$$\rho_{f, ts} = 0.0014 \leq 0.0018 \times \frac{60,000}{f_{fu}} \frac{E_s}{E_f} \leq 0.0036 \quad 440.1R, \text{ Eq. (9.1)}$$

$$\rho_{f, ts} = 0.0014 \leq 0.0018 \times \frac{60,000}{76,000} \frac{29,000}{6000} \leq 0.0036$$

$$\rho_{f, ts} = 0.0014 \leq 0.0069 \leq 0.0036, \text{ so } \rho_{f, ts} = 0.0036$$

$$A_{f, min} = \rho_{f, min} b h = (0.0036)(12)(12) = 0.52 \text{ in.}^2/\text{ft}$$

Select No. 5 at 7 in. spacing ($A_f = 0.53 \text{ in.}^2/\text{ft}$)

Verify assumption of tension-controlled behavior:

$$\rho_{fb} = 0.85 \beta_1 \frac{f'_c}{f_{fu}} \frac{E_f \epsilon_{cu}}{E_f \epsilon_{cu} + f_{fu}} \quad 440.1R, \text{ Eq. (7.2.1b)}$$

$$E_f \epsilon_{cu} = (6000)(0.003) = 18.00 \text{ ksi}$$

$$\rho_{fb} = 0.85(0.85) \frac{(4)}{(76)} \frac{(18.00)}{(18.00 + 76)} = 0.00728$$

$$\rho_f = \frac{A_f}{bd} = \frac{0.53}{(12)(10.94)} = 0.00404 \quad 440.1R, \text{ Eq. (7.2.1a)}$$

$$\frac{\rho_f}{\rho_{fb}} = \frac{0.00404}{0.00728} = 0.55 \quad \text{OK}$$

The slab may be designed to be 12 in. thick with No. 5 at 7 in. for $-M$. By observation, the same minimum reinforcement will be required for $+M$.

In addition to flexural strength, the slab should be examined for shear and the serviceability criteria of crack control, deflections, and creep rupture stress limits. Calculations related to these requirements are covered in other example problems in this chapter.

Further calculations show that this slab will be uncracked at service by a significant margin, and is even uncracked at ultimate conditions. The slab will work, but will be highly inefficient. Therefore, consider a more efficient slab design that is selected to be cracked at service.

4. Redesign the slab to be cracked at service loads.

When cracked, FRP-reinforced concrete slabs are seldom governed by flexural strength. Whereas a slab designed for flexural strength alone would have a ratio of service level moment to nominal moment strength (M_{serv}/M_n) of approximately 0.40 to 0.45, depending on the ratio of dead-to-live load, most FRP-reinforced slabs are governed by serviceability requirements and will exhibit ratios closer to 0.20 to 0.25. As a design approximation, design for a flexural strength corresponding to approximately twice the actual factored moment ($2.0M_u$).

Select a reinforcement ratio corresponding to a compression-controlled section, as this will promote the use of enough reinforcement to control cracking and reduce deflections.

Design for $2.0M_u$ and as a starting point, assume $\rho_f = 1.5\rho_{fb}$.

$$\rho_f = 1.5\rho_{fb} = 1.5(0.00728) = 0.01092$$

Calculate the stress in the tensile reinforcement (f_f) at ultimate conditions for the assumed value of ρ_f .

$$f_f = \sqrt{\frac{(E_f \epsilon_{cu})^2}{4} + \frac{0.85\beta_1 f'_c}{\rho_f} E_f \epsilon_{cu} - 0.5 E_f \epsilon_{cu}} \leq f_{fu} \quad 440.1R, \text{ Eq. (7.2.2d)}$$

$$f_f = \sqrt{\frac{(18.00)^2}{4} + \frac{0.85(0.85)(4)}{(0.01092)}(18.00) - 0.5(18.00)} \leq 76$$

$$f_f = 60.6 \text{ ksi}$$

Estimate dead load based on an assumed 8 in. slab thickness:

$$8 \text{ in. slab weighs } [(8)/(12)](150) = 100 \text{ lb/ft}^2$$

$$\text{Factored load } q_u = 1.2(100) + 1.6(50) = 200 \text{ lb/ft}^2$$

318-11, Eq. (9-2)

Negative moment at exterior face of first interior support (governs):

$$-M_u = \frac{q_u \ell_n^2}{10} = \frac{(0.200)(18)^2}{10} = 6.48 \text{ ft-kip/ft}$$

318-11, Sec. 8.3.3

Use the moment capacity equation to determine a depth for the slab.

$$M_u = \phi M_n = \phi \rho_f f_f \left(1 - 0.59 \frac{\rho_f f_f}{f'_c} \right) b d^2$$

440.1R, Eq. (7.2.2e)

$$2(6.48)(12) = (0.65)(0.01092)(60.6) \left(1 - 0.59 \frac{(0.01092)(60.6)}{(4)} \right) (12)d^2$$

$$d = 5.78 \text{ in.}$$

Assume No. 6 bars for flexural reinforcement.

$$h = (5.78) + (0.75) + \frac{(0.75)}{2} = 6.91 \text{ in.}$$

Round up to be conservative (7 in. thick slab [$h = 7$ in.]).

Correct dead load for 7 in. thickness:

$$7 \text{ in. slab weighs } [(7)/(12)](150) = 87.5 \text{ lb/ft}^2$$

$$\text{Factored load } q_u = 1.2(87.5) + 1.6(50) = 185 \text{ lb/ft}^2$$

318-11, Eq. (9-2)

The flexural capacity could be checked, but it should be satisfactory by inspection because the design was based on providing a capacity of $2.0M_u$. Thus, capacity calculations are not necessary.

Select reinforcement for the slab. Assume the same reinforcement for $-M$ and $+M$.

$$A_f = \rho_f bd = (0.01092)(12)(5.78) = 0.76 \text{ in.}^2/\text{ft}$$

440.1R, Eq. (7.2.1a)

Select No. 6 bars at 6 in. spacing ($A_f = 0.88 \text{ in.}^2/\text{ft}$).

5. Select temperature and shrinkage reinforcement for transverse direction.

$$\rho_{f,ts} = 0.0014 \leq 0.0018 \times \frac{60,000}{f_{fu}} \frac{E_s}{E_f} \leq 0.0036$$

440.1R, Eq. (9.1)

$$\rho_{f,ts} = 0.0014 \leq 0.0018 \times \frac{60,000}{76,000} \frac{29,000}{6000} \leq 0.0036$$

$$\rho_{f,ts} = 0.0014 \leq 0.0069 \leq 0.0036, \text{ so } \rho_{f,ts} = 0.0036$$

$$A_{f,ts} = \rho_{f,ts} bh = (0.0036)(12)(7.00) = 0.30 \text{ in.}^2/\text{ft}$$

Select No. 4 bars at 8 in. spacing ($A_f = 0.30 \text{ in.}^2/\text{ft}$).

Note: The slab should now be examined for shear, crack control, deflections, and creep rupture. Calculations related to these requirements are covered in other example problems in this chapter. If these design criteria are not satisfied, then the slab thickness may be increased incrementally or additional reinforcement added.

Example 5—Distribution of reinforcement for effective crack control

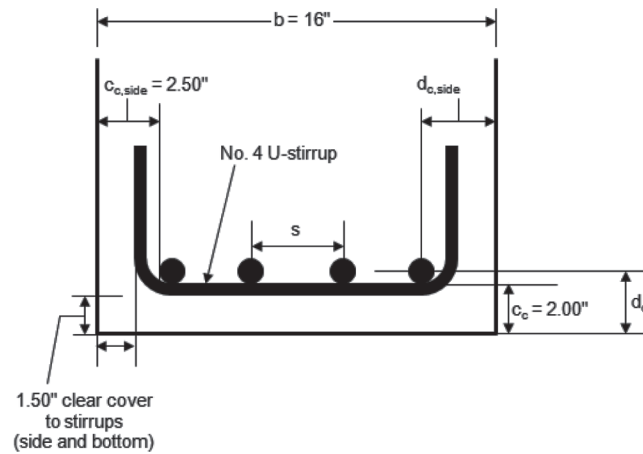
This example is similar to Example 9.1 of PCA Notes on ACI 318-08.

A rectangular beam is being designed for a factored moment $M_u = 131$ ft-kip. The beam has been sized as a 16 in. wide by 24 in. deep beam, and the required area of GFRP flexural reinforcement has been computed as $A_{f,reqd} = 2.27 \text{ in.}^2$. Determine an arrangement of flexural reinforcement that satisfies crack control requirements in 7.3.1. Assume bottom clear cover to the flexural reinforcement (c_c) of 2.0 in. (1.5 in. clear cover + 0.5 in. stirrup diameter). Assume side clear cover to the flexural reinforcement ($c_{c,side}$) of 2.5 in. (1.5 in. clear cover + 0.5 in. stirrup diameter + 0.5 in. to accommodate inner radius of stirrup bend). The unfactored service load moment is $M_s = 90$ ft-kip. Assume interior exposure conditions.

$$f'_c = 4000 \text{ psi}$$

$$f_{fu}^* = 80,000 \text{ psi}$$

$$E_f = 5800 \text{ ksi}$$



Calculations and discussion

Design material properties:

$$C_E = 0.8$$

$$f_{fu} = C_E f_{fu}^* = (0.8)(80) = 64 \text{ ksi}$$

1. Select reinforcement.

Four No.7 bars ($A_f = 2.40 \text{ in.}^2$)

No. 7 bar diameter: $d_b = 0.875 \text{ in.}$

2. Check limitation on value of d_c :

$$d_c \leq \frac{E_f w}{2 f_{fs} \beta k_b}$$

Assume a maximum allowable crack width w of 0.028 in.

Take $k_b = 1.4$.

The parameters β and f_{fs} must be determined from a linear-elastic cracked section analysis under service loads. Many of these calculations are covered in 7.3.2.2 and 7.4.1.

$$k = \sqrt{2\rho_f n_f + (\rho_f n_f)^2} - \rho_f n_f$$

$$d_c = c_c + \frac{d_b}{2} = 2.00 + \frac{0.875}{2} = 2.44 \text{ in.}$$

$$d = h - d_c = 24 - 2.44 = 21.56 \text{ in.}$$

$$\rho_f = \frac{A_f}{bd} = \frac{2.40}{(16)(21.56)} = 0.00696$$

$$E_c = 57,000 \sqrt{f'_c} = 57,000 \sqrt{4000} = 3.605 \times 10^6 \text{ psi} = 3605 \text{ ksi}$$

$$n_f = \frac{E_f}{E_c} = \frac{5800}{3605} = 1.609$$

$$\rho_f n_f = (0.00696)(1.609) = 0.01120$$

$$k = \sqrt{2\rho_f n_f + (\rho_f n_f)^2} - \rho_f n_f = \sqrt{2(0.01120) + (0.01120)^2} - 0.01120 = 0.139$$

$$I_{cr} = \frac{bd^3}{3} k^3 + n_f A_f d^2 (1-k)^2$$

Reference

440.1R, Table 6.2

440.1R, Eq. (6.2a)

440.6-08, Table 7.1

440.1R, Eq. (7.3.1b)

440.1R, Sec. 7.3.1

440.1R, Sec. 7.3.1

440.1R, Eq. (7.3.2b)

440.1R, Eq. (7.2.1a)

318-11, Sec. 8.5.1

440.1R, Eq. (7.3.2.2a)

$$= \frac{(16)(21.56)^3}{3} (0.139)^3 + (1.609)(2.40)(21.56)^2 (1 - 0.139)^2 = 1474 \text{ in.}^4$$

Service level stress in FRP reinforcement (refer to Eq. (7.4.1) for a similar calculation based on sustained service load):

$$f_{fs} = M_s \frac{n_f d (1 - k)}{I_{cr}} = ((90)(12)) \frac{(1.609)(21.56)(1 - 0.139)}{1474} = 21.9 \text{ ksi} \quad 440.1R, \text{ Eq. (7.4.1)}$$

$$\beta = \frac{h - kd}{d - kd} = \frac{24 - (0.139)(21.56)}{21.56 - (0.139)(21.56)} = 1.13$$

Once parameters have been calculated, check limit on d_c

$$d_c \leq \frac{E_f w}{2 f_{fs} \beta k_b} \quad 440.1R, \text{ Eq. (7.3.1b)}$$

$$2.44 \text{ in.} \leq \frac{(5800)(0.028)}{2(21.9)(1.13)(1.4)}$$

2.44 in. > 2.34 in. NG

Although the limit on d_c is not satisfied, continue to check the bar spacing for illustrative purposes in the following.

Check bar spacing against maximum spacing:

$$s_{max} = 1.15 \frac{E_f w}{f_{fs} k_b} - 2.5 c_c \leq 0.92 \frac{E_f w}{f_{fs} k_b} \quad 440.1R, \text{ Eq. (7.3.1a)}$$

$$s_{max} = 1.15 \frac{(5800)(0.028)}{(21.9)(1.4)} - 2.5(2.00) \leq 0.92 \frac{(5800)(0.028)}{(21.9)(1.4)}$$

$$s_{max} = 1.09 \leq 4.87, \text{ so } s_{max} = 1.09 \text{ in.}$$

Provided center-to-center bar spacing:

$$s_{provided} = \frac{b - 2d_{c,side}}{N - 1}$$

$$d_{c,side} = \text{side cover to center of exterior bars} = 2.5 + (1/2)(0.875) = 2.94 \text{ in.}$$

$$N = \text{number of bars} = 4$$

$$s_{provided} = \frac{16 - 2(2.94)}{4 - 1}$$

$$s_{provided} = 3.37 \text{ in.} > s_{max} = 1.09 \text{ in.} \quad \text{NG}$$

The selected reinforcement does not meet crack control requirements based on the calculations shown above. Both the cover (d_c) and spacing (s) limits are not satisfied.

Note that minimum clear bar spacing requirements must also be satisfied. In this case, maximum center-to-center bar spacing of 1.09 in. per Eq. (7.3.1a) is so small that minimum clear spacing (d_b , 1.0 in., or 4/3 times the maximum aggregate size) per ACI 318-11, Sec. 7.6, could not possibly be provided.

3. Choose a new reinforcement selection. Generally, if the aforementioned checks are not satisfied, then additional reinforcement will be required such that the FRP bar stress at service is reduced. Increase the amount of reinforcement and try two different possibilities:

$$\text{Three No. 9 bars } (A_f = 3.00 \text{ in.}^2; d_b = 1.128 \text{ in.})$$

$$\text{Five No. 7 bars } (A_f = 3.00 \text{ in.}^2; d_b = 0.875 \text{ in.})$$

440.6-08, Table 7.1

440.6-08, Table 7.1

Calculations are repeated for these two possibilities as well as the original selection checked previously. Values are presented in table format to save space and facilitate comparison.

Parameter	Unit	Four No. 7	Three No. 9	Five No.7
A_f	in. ²	2.40	3.00	3.00
d	in.	21.56	21.44	21.56
d_c	in.	2.44	2.56	2.44
ρ_f		0.00696	0.00875	0.00870
k		0.139	0.154	0.154
I_{cr}	in. ⁴	1474	1779	1801
f_{fs}	ksi	21.9	17.7	17.6
β		1.13	1.14	1.13
d_c (limit value)	in.	2.34	2.87	2.91
Check if $d_c \leq d_c$ (limit value)		NG	OK	OK
s_{max} (limit value)	in.	1.09	2.53	2.58
$d_{c,side}$	in.	2.94	3.06	2.94
$s_{provided}$	in.	3.37	4.94	2.53
Check if $s_{provided} \leq s_{max}$		NG	NG	OK

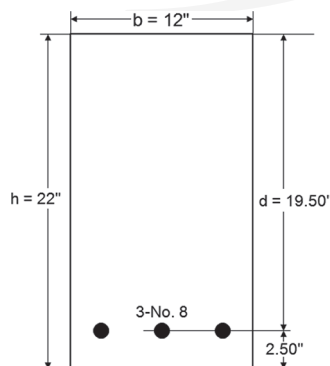
As can be seen in the table, the choice of three No. 9 bars provides sufficient additional reinforcement to reduce the stress in the reinforcing bars. The reinforcement, however, is spaced too far apart to meet the maximum spacing requirement, as the reinforcement is not sufficiently distributed to control crack widths.

The choice of five No. 7 bars provides the same amount of reinforcement as the choice of three No. 9 bars, but distributes the reinforcement better within the width of the cross section. The five bars would be spaced closely enough to control cracking, and far enough apart to provide minimum clear spacing required by ACI 318-11, Sec. 7.6.

Use five No. 7 bars distributed a single layer.

Example 6—Deflection of a simple-span nonprestressed rectangular beam

This example is similar to Example 10.1 of PCA Notes on ACI 318-08.



Required: analysis of deflections and comparison to ACI 318-11 allowable deflections. Consider long-term deflections at 3 months and 5 years (ultimate value).

Data:

$f'_c = 3000$ psi (normalweight concrete)

$E_f = 6500$ ksi

Superimposed dead load (not including beam weight) = 120 lb/ft

Live load = 300 lb/ft (20 percent sustained)

Span = 25 ft (simply-supported)

Calculations and discussion

No. 8 bar properties:

Reference

440.6-08, Table 7.1

$$d_b = 1.00 \text{ in.}$$

$$A_{f,bar} = 0.79 \text{ in.}^2$$

Reinforcement quantities needed for calculations:

$$A_f = (3)(0.79 \text{ in.}^2) = 2.37 \text{ in.}^2$$

$$\rho_f = \frac{A_f}{bd} = \frac{2.37}{(12)(19.50)} = 0.01013 \quad 440.1R, \text{ Eq. (7.2.1a)}$$

1. Check recommended minimum beam thickness.

Based on minimum thickness table, consider estimated depth:

$$h \approx \frac{\ell}{10} = \frac{(25)(12)}{10} = 30 \text{ in.} \quad 440.1R, \text{ Table 7.3.2.1}$$

Table 7.3.2.1 is intended to provide guidance for preliminary design, and does not guarantee that deflection limits will be met, so deflections should be computed.

2. Moments:

$$w_D = 0.120 + \frac{(12)(22)(0.150)}{144} = 0.395 \text{ kip/ft}$$

$$M_D = \frac{w_D \ell^2}{8} = \frac{(0.395)(25)^2}{8} = 30.86 \text{ ft-kip}$$

$$M_L = \frac{w_L \ell^2}{8} = \frac{(0.300)(25)^2}{8} = 23.44 \text{ ft-kip}$$

$$M_{sus} = M_D + 0.20(M_L) = 30.86 + (0.20)(23.44) = 35.55 \text{ ft-kip}$$

$$M_{D+L} = 30.86 + 23.44 = 54.30 \text{ ft-kip}$$

3. Modulus of elasticity and modular ratio:

$$E_c = 57,000\sqrt{f'_c} = 57,000\sqrt{3000} = 3.122 \times 10^6 \text{ psi} = 3122 \text{ ksi} \quad 318-11, \text{ Sec. 8.5.1}$$

$$n_f = \frac{E_f}{E_c} = \frac{6500}{3122} = 2.082$$

4. Gross and cracked section moment of inertia:

$$I_g = \frac{bh^3}{12} = \frac{(12)(22)^3}{12} = 10,648 \text{ in.}^4$$

$$\rho_f n_f = (0.01013)(2.082) = 0.02109$$

$$k = \sqrt{2\rho_f n_f + (\rho_f n_f)^2} - \rho_f n_f = \sqrt{2(0.02109) + (0.02109)^2} - 0.02109 = 0.185 \quad 440.1R, \text{ Eq. (7.3.2.2b)}$$

$$I_{cr} = \frac{bd^3}{3} k^3 + n_f A_f d^2 (1-k)^2 \quad 440.1R, \text{ Eq. (7.3.2.2a)}$$

$$= \frac{(12)(19.50)^3}{3} (0.185)^3 + (2.082)(2.37)(19.50)^2 (1-0.185)^2 = 1434 \text{ in.}^4$$

$$\frac{I_g}{I_{cr}} = \frac{10,648}{1434} = 7.43 \quad \frac{I_{cr}}{I_g} = \frac{1434}{10,648} = 0.135$$

5. Effective moments of inertia:

$$M_{cr} = \frac{7.5\lambda\sqrt{f'_c}I_g}{y_t} = \frac{7.5(1)(\sqrt{3000})(10,648)}{(1/2)(22)(12,000)} = 33.14 \text{ ft-kip} \quad 440.1R, \text{ Eq. (7.3.2.2d)}$$

Assuming that the member is loaded to the full dead load before any live load is applied, the effective moment of inertia may be computed on the basis of the dead load alone. (This assumption will yield a conservative estimate of live load deflection in the next step). Because $M_D < M_{cr}$, this beam is uncracked for this condition. Thus, the effective moment of inertia for dead load is I_g .

$$(I_e)_D = I_g = 10,648 \text{ in.}^4$$

Find the effective moment of inertia due to dead plus live load.

$$\frac{M_{cr}}{M_a} = \frac{M_{cr}}{M_{D+L}} = \frac{33.14}{54.30} = 0.610$$

$$\gamma = 1.72 - 0.72(M_{cr}/M_a) = 1.72 - 0.72(0.610) = 1.281 \quad 440.1R, \text{ Sec. 7.3.2.2}$$

$$(I_e)_{D+L} = \frac{I_{cr}}{1 - \gamma \left(\frac{M_{cr}}{M_a} \right)^2 \left[1 - \frac{I_{cr}}{I_g} \right]} = \frac{1434}{1 - (1.281)(0.610)^2 [1 - 0.135]} = 2440 \text{ in.}^4 \quad 440.1R, \text{ Eq. (7.3.2.2c)}$$

6. Immediate deflections:

$K = 1$ for simple spans

$$(\Delta_i)_D = \frac{K(5)M_D\ell^2}{48E_c(I_e)_D} = \frac{(1)(5)(30.86)(25)^2(12)^3}{48(3122)(10,648)} = 0.104 \text{ in.}$$

$$(\Delta_i)_{D+L} = \frac{K(5)M_{D+L}\ell^2}{48E_c(I_e)_{D+L}} = \frac{(1)(5)(54.30)(25)^2(12)^3}{48(3122)(2440)} = 0.802 \text{ in.}$$

The immediate live load deflection is found by subtracting the dead load deflection from the deflection due to both dead and live load.

$$(\Delta_i)_L = (\Delta_i)_{D+L} - (\Delta_i)_D = 0.802 - 0.104 = 0.698 \text{ in.}$$

It is conservative to find the immediate deflection due to sustained load by using the effective moment of inertia based on the full dead plus live load.

$$(\Delta_i)_{sus} = \frac{K(5)M_{sus}\ell^2}{48E_c(I_e)_{D+L}} = \frac{(1)(5)(35.55)(25)^2(12)^3}{48(3122)(2440)} = 0.525 \text{ in.}$$

$$(\Delta_i)_{L,unsustained} = (\Delta_i)_{D+L} - (\Delta_i)_{sus} = 0.802 - 0.525 = 0.277 \text{ in.}$$

7. Incremental portion of total deflection occurring after placement of nonstructural elements (sum of the long-term deflection due to all sustained loads and the immediate deflection due to any additional live load):

a. 3 months ($\xi = 1.0$) 318-11, Sec. 9.5.2.5

$$\Delta_{incr} = \Delta_{LT,sus} + \Delta_{L,unsustained} = 0.6\xi(\Delta_i)_{sus} + (\Delta_i)_{L,unsustained} = 0.6(1.0)(0.525) + 0.277 = 0.592 \text{ in.} \quad 440.1R, \text{ Eq. (7.3.2.3c)}$$

b. 5 years ($\xi = 2.0$) 318-11, Sec. 9.5.2.5



$$\Delta_{incr} = \Delta_{LT,sus} + \Delta_{L,unsustained} = 0.6\xi(\Delta_i)_{sus} + (\Delta_i)_{L,unsustained} = 0.6(2.0)(0.525) + 0.277 = 0.907 \text{ in.} \quad 440.1R, \text{ Eq. (7.3.2.3c)}$$

8. Compare computed deflections to allowable deflections.

Allowable deflections (immediate live load):

318-11, Table 9.5(b)

Flat roofs not supporting and not attached to nonstructural elements likely to be damaged by large deflections:

$$\{(\Delta_i)_L = 0.698 \text{ in.}\} \leq \left\{ \frac{\ell}{180} = \frac{(25)(12)}{180} = 1.67 \text{ in.} \right\} \text{ OK}$$

Floors not supporting and not attached to nonstructural elements likely to be damaged by large deflections:

$$\{(\Delta_i)_L = 0.698 \text{ in.}\} \leq \left\{ \frac{\ell}{360} = \frac{(25)(12)}{360} = 0.83 \text{ in.} \right\} \text{ OK}$$

Allowable deflections (incremental after placement of nonstructural elements):

318-11, Table 9.5(b)

Roof or floor construction supporting or attached to nonstructural elements not likely to be damaged by large deflections:

$$\{\Delta_{incr} = 0.907 \text{ in.}\} \leq \left\{ \frac{\ell}{240} = \frac{(25)(12)}{240} = 1.25 \text{ in.} \right\} \text{ OK}$$

Roof or floor construction supporting or attached to nonstructural elements likely to be damaged by large deflections (very stringent criteria):

$$\{\Delta_{incr} = 0.907 \text{ in.}\} > \left\{ \frac{\ell}{480} = \frac{(25)(12)}{480} = 0.63 \text{ in.} \right\} \text{ NG}$$

If nonstructural elements likely to be damaged by large deflections are to be supported by this member, it will need to be redesigned to have a greater flexural stiffness. Otherwise, the member is adequate.

Example 7—Creep rupture stress check under sustained loads

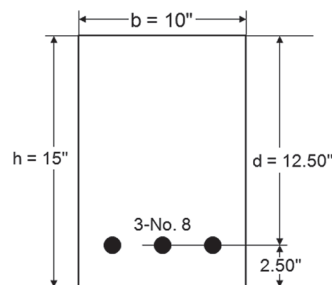
This example does not have a companion in PCA Notes on ACI 318-08 because creep rupture is an FRP phenomenon.

The rectangular beam shown is designed to carry service load moments $M_D = 18$ ft-kip and $M_L = 18$ ft-kip. Assume 20 percent of the live load is sustained. Verify that the beam satisfies the creep rupture stress limits in 7.4.1. Assume interior exposure conditions.

$$f'_c = 4000 \text{ psi}$$

$$f_{fu}^* = 80,000 \text{ psi}$$

$$E_f = 6000 \text{ ksi}$$



Calculations and discussion

No. 8 bar properties:

$$d_b = 1.00 \text{ in.}$$

$$A_{f,bar} = 0.79 \text{ in.}^2$$

Reference

440.6-08, Table 7.1

Reinforcement quantities needed for calculations:

$$A_f = (3)(0.79 \text{ in.}^2) = 2.37 \text{ in.}^2$$

$$\rho_f = \frac{A_f}{bd} = \frac{2.37}{(10)(12.50)} = 0.01896 \quad 440.1R, \text{ Eq. (7.2.1a)}$$

Design material properties:

$$C_E = 0.8 \quad 440.1R, \text{ Table 6.2}$$

$$f_{fu} = C_E f_{fu}^* = (0.8)(80) = 64 \text{ ksi} \quad 440.1R, \text{ Eq. (6.2a)}$$

1. Sustained load moment:

$$M_{sus} = M_D + 0.20(M_L) = 18 + (0.20)(18) = 21.6 \text{ ft-kip}$$

2. Modulus of elasticity and modular ratio:

$$E_c = 57,000\sqrt{f'_c} = 57,000\sqrt{4000} = 3.605 \times 10^6 \text{ psi} = 3605 \text{ ksi} \quad 318-11, \text{ Sec. 8.5.1}$$

$$n_f = \frac{E_f}{E_c} = \frac{6000}{3605} = 1.664$$

3. Cracked section moment of inertia:

$$\rho n_f = (0.01896)(1.664) = 0.03155$$

$$k = \sqrt{2\rho n_f + (\rho n_f)^2} - \rho n_f = \sqrt{2(0.03155) + (0.03155)^2} - 0.03155 = 0.222 \quad 440.1R, \text{ Eq. (7.3.2.2b)}$$

$$I_{cr} = \frac{bd^3}{3} k^3 + n_f A_f d^2 (1-k)^2 \quad 440.1R, \text{ Eq. (7.3.2.2a)}$$

$$= \frac{(10)(12.50)^3}{3} (0.222)^3 + (1.664)(2.37)(12.50)^2 (1-0.222)^2 = 444 \text{ in.}^4$$

4. Reinforcement stress under sustained service loads:

$$f_{fs,sus} = M_{s,sus} \frac{n_f d (1-k)}{I_{cr}} \quad 440.1R, \text{ Eq. (7.4.1)}$$

$$f_{fs,sus} = (21.6)(12) \frac{(1.664)(12.50)(1-0.222)}{444} = 9.45 \text{ ksi}$$

Allowable reinforcement stress:

$$\{f_{fs,sus} = 9.45 \text{ ksi}\} \leq \{0.20f_{fu} = 0.20(64) = 12.8 \text{ ksi}\} \quad \text{OK} \quad 440.1R, \text{ Table 7.4.1}$$

Example 8—Design for shear (members subject to shear and flexure only)

This example is similar to Example 12.1 of PCA Notes on ACI 318-08.

Determine the required size and spacing of vertical U-stirrups for an 18 ft span, simply-supported normalweight reinforced concrete beam. Assume interior exposure conditions.

$$b_w = 12 \text{ in.}$$

$$d = 19.5 \text{ in.}$$

$$f'_c = 4000 \text{ psi}$$

$$f_{fu}^* = 100,000 \text{ psi (stirrups)}$$

$$E_f = 6000 \text{ ksi (stirrups)}$$

$$w_u = 4.82 \text{ kip/ft (includes self-weight)}$$

$$\rho_f = 0.0270 \text{ (longitudinal reinforcement)}$$

$$r_b/d_b = 4 \text{ (assumed curvature of bent stirrup bars)}$$

Calculations and discussion

Design material properties:

$$C_E = 0.8$$

$$f_{fu} = C_E f_{fu}^* = (0.8)(100) = 80 \text{ ksi}$$

Reference

440.1R, Table 6.2

440.1R, Eq. (6.2a)

For the purposes of this example, the live load will be assumed to be present on the full span so that the design shear at the centerline of span is zero. (A design shear greater than zero at midspan is obtained by considering partial live loading of the span.)

1. Determine factored shear forces.

$$\text{At support: } V_u = 4.82 \left(\frac{18}{2} \right) = 43.38 \text{ kip}$$

$$\text{At distance } d \text{ from support: } V_u = 43.38 - 4.82 \left(\frac{19.5}{12} \right) = 35.55 \text{ kip}$$

2. Determine shear strength provided by concrete.

$$\phi V_c = \phi \left(\frac{5}{2} k \right) 2 \sqrt{f'_c} b_w d \quad 440.1R, \text{ Eq. (8.2b)}$$

$$E_c = 57,000 \sqrt{f'_c} = 57,000 \sqrt{4000} = 3.605 \times 10^6 \text{ psi} = 3605 \text{ ksi} \quad 318-11, \text{ Sec. 8.5.1}$$

$$n_f = \frac{E_f}{E_c} = \frac{6000}{3605} = 1.664$$

$$\rho_f n_f = (0.0270)(1.664) = 0.04493$$

$$k = \sqrt{2\rho_f n_f + (\rho_f n_f)^2} - \rho_f n_f = \sqrt{2(0.04493) + (0.04493)^2} - 0.04493 = 0.258 \quad 440.1R, \text{ Eq. (7.3.2.2b)}$$

$$\phi V_c = (0.75) \left(\frac{5}{2} (0.258) \right) 2 \frac{\sqrt{4000}}{1000} (12)(19.5) = 14.32 \text{ kip}$$

$$V_u = 35.55 \text{ kip} > \phi V_c / 2 = 7.16 \text{ kip}$$

Therefore, shear reinforcement is required.

440.1R, Sec. 8.2.2

3. Compute $V_u - \phi V_c$ at critical section.

$$V_u - \phi V_c = 35.55 - 14.32 = 21.23 \text{ kip} < \phi 8 \sqrt{f'_c} b_w d = 88.8 \text{ kip} \quad \text{OK} \quad 440.1R, \text{ Sec. 8.2.3}$$

4. Determine distance x_c from support beyond which shear reinforcement is not required for strength ($V_u = \phi V_c$):

$$x_c = \frac{V_u @ \text{support} - \phi V_c}{w_u} = \frac{43.38 - 14.32}{4.82} = 6.03 \text{ ft}$$

Determine distance x_m from support beyond which shear reinforcement is not required ($V_u = \phi V_c / 2$):

$$x_m = \frac{V_u @ \text{support} - (\phi V_c / 2)}{w_u} = \frac{43.38 - (14.32 / 2)}{4.82} = 7.51 \text{ ft}$$

Therefore, only minimum shear reinforcement is required between 6.03 ft and 7.51 ft from the supports. Shear reinforcement is not required past 7.51 ft from the supports.

5. Determine design tensile stress in shear reinforcement.

Tensile strength of bent bars:

$$f_{fb} = \left(0.05 \cdot \frac{r_b}{d_b} + 0.3 \right) f_{fu} \leq f_{fu} \quad 440.1R, \text{ Eq. (6.2.1)}$$

$$f_{fb} = (0.05 \cdot 4 + 0.3) f_{fu} \leq f_{fu}$$

$$f_{fb} = (0.50) f_{fu} \leq f_{fu}$$

$$f_{fb} = (0.50)(80) = 40 \text{ ksi}$$

The design tensile strength is based on a strain of 0.004:

$$f_{fv} = 0.004 E_f \leq f_{fb} \quad 440.1R, \text{ Eq. (8.2d)}$$

$$f_{fv} = 0.004(6000) \leq 40$$

$$f_{fv} = 24 \leq 40$$

$$f_{fv} = 24 \text{ ksi}$$

6. Determine required spacing of vertical U-stirrups at the critical section.

$$\frac{A_{fv}}{s} = \frac{(V_u - \phi V_c)}{\phi f_{fv} d} = \frac{(35.55 - 14.32)}{(0.75)(24)(19.5)} = 0.0605 \text{ in.}^2/\text{in.} \quad \text{440.1R, Eq. (8.2e)}$$

Assuming No. 4 U-stirrups ($A_{fv} = 0.40 \text{ in.}^2$)

$$s = \frac{0.40}{0.0605} = 6.61 \text{ in.}$$

Check maximum permissible spacing of stirrups:

$$s = d/2 = 9.75 \text{ in.} \leq 24 \text{ in.} \quad \text{440.1R, Sec. 8.3}$$

because $V_u - \phi V_c = 21.23 \text{ kip} < \phi 4\sqrt{f'_c} b_w d = 44.4 \text{ kip}$ OK 318-11, Sec. 11.4.5

Maximum stirrup spacing based on minimum shear reinforcement:

$$s = \frac{A_{fv, min} f_{fv}}{50 b_w} = \frac{(0.40)(24)(1000)}{50(12)} = 16 \text{ in.} \quad \text{440.1R, Eq. (8.2.2)}$$

Therefore, the spacing at the critical section is restricted to the smallest of 6.61, 9.75, and 16 in. Select spacing of 6 in. at the critical section.

Determine the distance x where a transition can be made to a spacing of 9 in. (to satisfy strength and maximum spacing requirement calculated above as $d/2 = 9.75 \text{ in.}$):

$$\frac{A_{fv}}{s} = \frac{(V_u - \phi V_c)}{\phi f_{fv} d} \quad \text{440.1R, Eq. (8.2e)}$$

$$\frac{0.40}{9} = \frac{(V_u - \phi V_c)}{(0.75)(24)(19.5)}$$

$$V_u - \phi V_c = 15.60 \text{ kip}$$

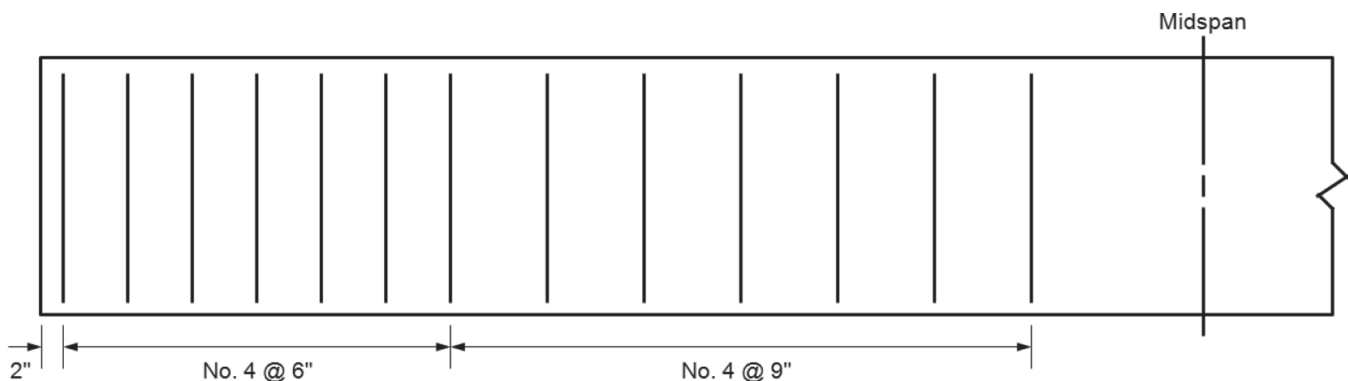
$$V_u = 15.60 + 14.32 = 29.92 \text{ kip}$$

$$x = \frac{V_u @ \text{support} - V_u}{w_u} = \frac{43.38 - 29.92}{4.82} = 2.79 \text{ ft}$$

Therefore, a transition may be made from 6 to 9 in. spacing at 2.79 ft from the support.

7. Select a stirrup spacing arrangement that satisfies previous calculations.

Place first stirrup at 2 in. from support. Use 6 in. spacing to 3 ft-2 in. from support. Use 9 in. spacing to 7 ft-8 in. from support.



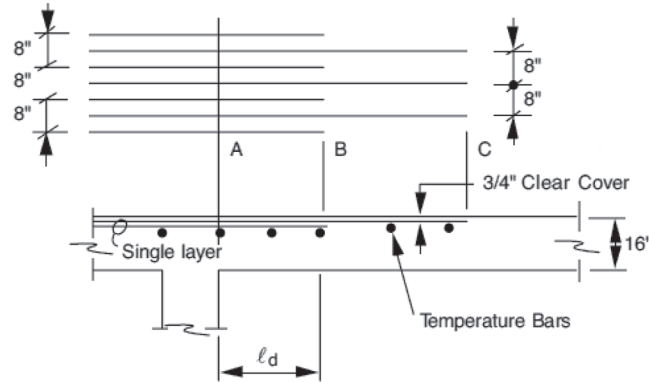
Note: Many designers would carry the reinforcement spacing of 9 in. through midspan, even though it is not required by calculations.

Example 9—Development of bars in tension (compression-controlled or transition zone section)

This example is similar to Example 4.2 of PCA Notes on ACI 318-08.

Calculate the required tension development length for the No. 8 glass FRP (GFRP) bars (alternate short bars) embedded in the normalweight concrete one-way slab shown in the following figure to develop the full moment capacity at Section A.

Assume $f'_c = 4000$ psi, $f_{fu}^* = 80,000$ psi, and $E_f = 6000$ ksi. Assume interior exposure conditions.


Calculations and discussion

Assume short bars are developed within distance AB while long bars are developed within BC.

No. 8 bar properties:

$$d_b = 1.00 \text{ in.}$$

$$A_{f,bar} = 0.79 \text{ in.}^2$$

Design material properties:

$$C_E = 0.8$$

$$f_{fu} = C_E f_{fu}^* = (0.8)(80) = 64 \text{ ksi}$$

1. Determine the type of section.

$$d = 16 - 0.75 - (1.00/2) = 14.75 \text{ in.}$$

$$A_f = (0.79 \text{ in.}^2)/(4 \text{ in. spacing}) = 0.198 \text{ in.}^2/\text{in.} = 2.37 \text{ in.}^2/\text{ft of slab}$$

$$\rho_f = \frac{A_f}{bd} = \frac{2.37}{(12)(14.75)} = 0.01339$$

$$\rho_{fb} = 0.85\beta_1 \frac{f'_c}{f_{fu}} \frac{E_f \epsilon_{cu}}{E_f \epsilon_{cu} + f_{fu}}$$

$$E_f \epsilon_{cu} = (6000)(0.003) = 18.00 \text{ ksi}$$

$$\rho_{fb} = 0.85(0.85) \frac{(4)}{(64)} \frac{(18.00)}{(18.00 + 64)} = 0.00991$$

$$\frac{\rho_f}{\rho_{fb}} = \frac{0.01339}{0.00991} = 1.35$$

Because $\rho_{fb} < \rho_f < 1.4\rho_{fb}$, the section is in the transition zone.

2. Determine stress in tensile reinforcement at ultimate conditions.

$$f_f = \sqrt{\frac{(E_f \epsilon_{cu})^2}{4} + \frac{0.85\beta_1 f'_c}{\rho_f} E_f \epsilon_{cu} - 0.5 E_f \epsilon_{cu}} \leq f_{fu}$$

$$f_f = \sqrt{\frac{(18.00)^2}{4} + \frac{0.85(0.85)(4)}{(0.01339)} (18.00) - 0.5(18.00)} \leq 64$$

$$f_f = 54.0 \text{ ksi}$$

Reference

440.6-08, Table 7.1

440.1R, Table 6.2

440.1R, Eq. (6.2a)

440.1R, Eq. (7.2.1a)

440.1R, Eq. (7.2.1b)

440.1R, Eq. (7.2.3)

440.1R, Eq. (7.2.2d)

3. Determine development length.

$$\ell_d = \frac{\alpha \frac{f_{fr}}{\sqrt{f'_c}} - 340}{13.6 + \frac{C}{d_b}} d_b \tag{440.1R, Eq. (10.3a)}$$

The bar stress that needs to be developed is the stress at the ultimate condition. There is no need to develop the full strength of the bar in this case.

$$f_{fr} = f_f = 54.0 \text{ ksi} \tag{440.1R, Sec. 10.3}$$

Bar location modification factor should be taken as $\alpha = 1.5$ because more than 12 in. of concrete is cast below the reinforcement. 440.1R, Sec. 10.1.1

Center-to-center spacing of bars being developed = 8 in.

$$C = \min\left(d_c, \frac{\text{ctr-to-ctr spacing}}{2}\right) \leq 3.5d_b \tag{440.1R, Sec. 10.1}$$

$$C = \min\left(0.75 + \frac{1.00}{2}, \frac{8}{2}\right) \leq 3.5(1.00) = \min(1.25, 4.00) \leq 3.50$$

$C = 1.25$ in.

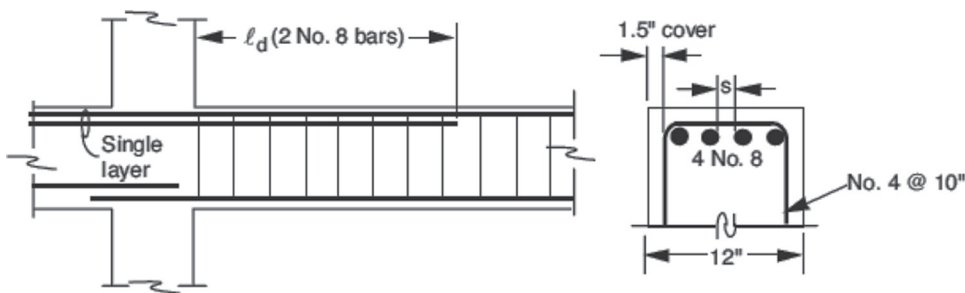
$$\ell_d = \frac{\alpha \frac{f_{fr}}{\sqrt{f'_c}} - 340}{13.6 + \frac{C}{d_b}} d_b = \frac{(1.5) \frac{(54.0)(1000)}{\sqrt{4000}} - 340}{13.6 + \frac{1.25}{1.00}} (1.00) = 63.3 \text{ in.}$$

The required development length is 63.3 in.

Example 10—Development of bars in tension (tension-controlled section)

This example is similar to Example 4.3 of PCA Notes on ACI 318-08.

Calculate the length required to develop the inner two No. 8 glass FRP (GFRP) bars at the column face in the following figure. The two No. 8 outer bars are to be made continuous along full length of beam. Use $f'_c = 4000$ psi (normalweight concrete), $f_{fu}^* = 80,000$ psi, and $E_f = 6000$ ksi. Assume $d = 27.50$ in. Assume interior exposure conditions.



Calculations and discussion

No. 8 bar properties:

$$d_b = 1.00 \text{ in.}$$

$$A_{f,bar} = 0.79 \text{ in.}^2$$

Design material properties:

$$C_E = 0.8$$

$$f_{fu} = C_E f_{fu}^* = (0.8)(80) = 64 \text{ ksi}$$

Reference

440.6-08, Table 7.1

440.1R, Table 6.2

440.1R, Eq. (6.2a)

1. Determine the type of section.

$$A_f = (4)(0.79 \text{ in.}^2) = 3.16 \text{ in.}^2$$



$$\rho_f = \frac{A_f}{bd} = \frac{3.16}{(12)(27.50)} = 0.00958 \quad 440.1R, \text{ Eq. (7.2.1a)}$$

$$\rho_{fb} = 0.85\beta_1 \frac{f'_c}{f_{fu}} \frac{E_f \epsilon_{cu}}{E_f \epsilon_{cu} + f_{fu}} \quad 440.1R, \text{ Eq. (7.2.1b)}$$

$$E_f \epsilon_{cu} = (6000)(0.003) = 18.00 \text{ ksi}$$

$$\rho_{fb} = 0.85(0.85) \frac{(4)}{(64)} \frac{(18.00)}{(18.00 + 64)} = 0.00991$$

$$\frac{\rho_f}{\rho_{fb}} = \frac{0.00958}{0.00991} = 0.97$$

Because $\rho_f \leq \rho_{fb}$, the section is tension-controlled.

440.1R, Eq. (7.2.3)

2. Determine stress in tensile reinforcement at ultimate conditions.

Because section is tension-controlled, $f_f = f_{fu} = 64 \text{ ksi}$

3. Determine development length.

$$\ell_d = \frac{\alpha \frac{f_{fr}}{\sqrt{f'_c}} - 340}{13.6 + \frac{C}{d_b}} d_b \quad 440.1R, \text{ Eq. (10.3a)}$$

$$f_{fr} = f_f = 64.0 \text{ ksi}$$

440.1R, Sec. 10.3

Bar location modification factor should be taken as $\alpha = 1.5$ because more than 12 in. of concrete is cast below the reinforcement.

440.1R, Sec. 10.1.1

Clear spacing of bars being developed = $[12 - 2(1.50) - 2(0.50) - 4(1.00)]/3 = 1.33 \text{ in.}$

$$C = \min\left(d_c, \frac{\text{ctr-to-ctr spacing}}{2}\right) \leq 3.5d_b \quad 440.1R, \text{ Sec. 10.1}$$

$$= \min\left(1.50 + 0.50 + \frac{1.00}{2}, \frac{0.50 + 1.33 + 0.50}{2}\right) \leq 3.5(1.00) = \min(2.50, 1.17) \leq 3.50$$

$C = 1.17 \text{ in.}$

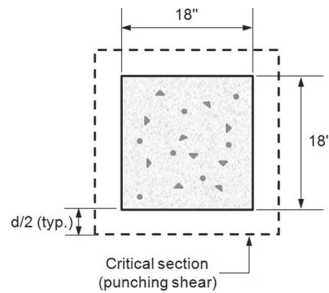
$$\ell_d = \frac{\alpha \frac{f_{fr}}{\sqrt{f'_c}} - 340}{13.6 + \frac{C}{d_b}} d_b = \frac{(1.5) \frac{(64)(1000)}{\sqrt{4000}} - 340}{13.6 + \frac{1.17}{1.00}} (1.00) = 79.5 \text{ in.}$$

The required development length is 79.5 in.

Example 11—Shear strength of slab at column support

This example is similar to Example 16.1 of PCA Notes on ACI 318-08.

Determine two-way action shear strength at an interior column support of a flat plate slab system for the following design conditions.



Column dimensions = 18 in. x 18 in.

Slab effective depth $d = 6.5$ in.

Specified concrete strength $f'_c = 4000$ psi (normalweight concrete)

$E_f = 5800$ ksi

$\rho_f = 0.0120$ (flexural reinforcement in column strips in both directions, top mat of reinforcement)

Calculations and discussion

1. Two-way action shear (punching shear) without shear reinforcement:

$$V_u \leq \phi V_n$$

$$V_u \leq \phi V_c \quad (V_f = 0)$$

2. Determine shear strength provided by concrete.

$$\phi V_c = \phi \left(\frac{5}{2} k \right) 4 \sqrt{f'_c} b_o d$$

$$E_c = 57,000 \sqrt{f'_c} = 57,000 \sqrt{4000} = 3.605 \times 10^6 \text{ psi} = 3605 \text{ ksi}$$

$$\rho_f n_f = \rho_f \frac{E_f}{E_c} = (0.0120) \left(\frac{5800}{3605} \right) = (0.0120)(1.609) = 0.01931$$

$$k = \sqrt{2\rho_f n_f + (\rho_f n_f)^2} - \rho_f n_f = \sqrt{2(0.01931) + (0.01931)^2} - 0.01931 = 0.178$$

$$b_o = 4(18 + 3.25 + 3.25) = 98 \text{ in.}$$

$$\phi V_c = (0.75) \left(\frac{5}{2} (0.178) \right) 4 \frac{\sqrt{4000}}{1000} (98)(6.5) = 53.83 \text{ kip}$$

Reference

440.1R, Sec. 8.1

440.1R, Sec. 8.2

440.1R, Eq. (8.4a)

318-11, Sec. 8.5.1

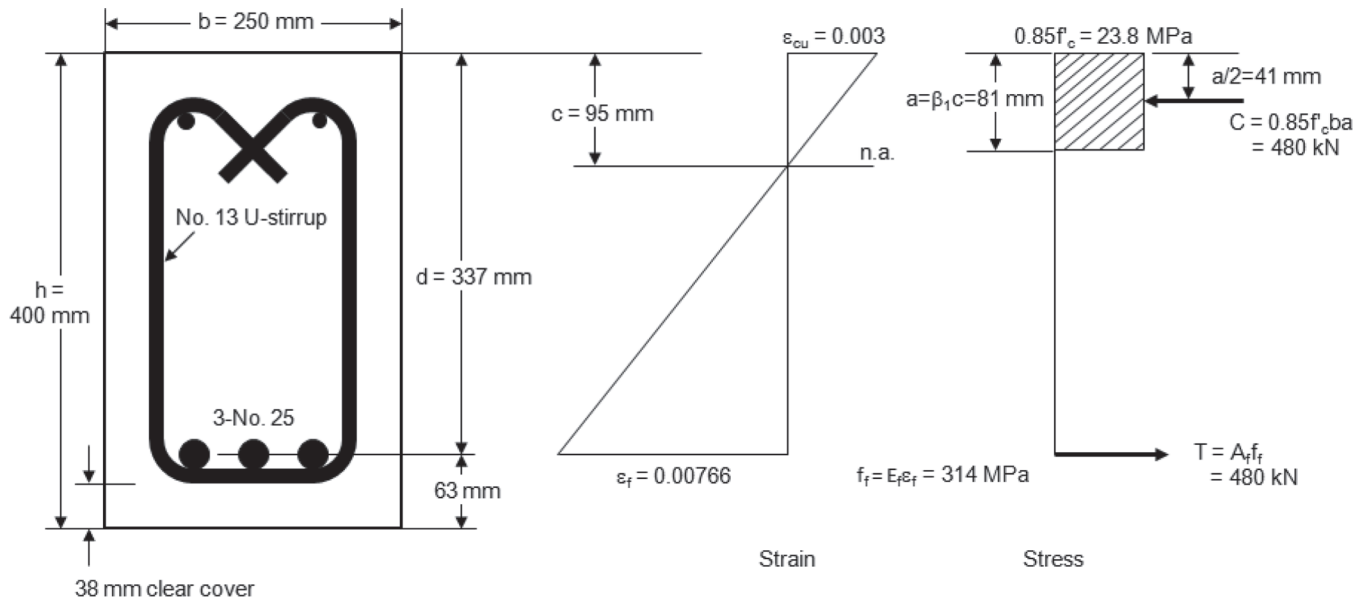
440.1R, Eq. (7.3.2.2b)

440.1R, Sec. 8.4

Example 1M—Flexural (moment) strength using equivalent rectangular concrete stress distribution (compression-controlled section)

This example is similar to Example 6.1 of PCA Notes on ACI 318-08.

For the beam section shown, calculate moment strength based on static equilibrium using the equivalent rectangular concrete stress distribution as shown in Fig. 7.2 of this guide. Assume $f'_c = 28$ MPa, $f_{fu}^* = 550$ MPa, and $E_f = 41,000$ MPa. Assume interior exposure conditions and neglect compression reinforcement.



Calculations and discussion

No. 25 bar properties:

$$d_b = 25.4 \text{ mm}$$

$$A_{f,bar} = 510 \text{ mm}^2$$

Design material properties:

$$C_E = 0.8$$

$$f_{fu} = C_E f_{fu}^* = (0.8)(550) = 440 \text{ MPa}$$

1. Determine the strength reduction factor.

$$d = 400 - 38 - 12.7 - (25.4/2) = 337 \text{ mm}$$

$$A_f = (3)(510 \text{ mm}^2) = 1530 \text{ mm}^2$$

$$\rho_f = \frac{A_f}{bd} = \frac{1530}{(250)(337)} = 0.01816$$

$$\rho_{fb} = 0.85\beta_1 \frac{f'_c}{f_{fu}} \frac{E_f \epsilon_{cu}}{E_f \epsilon_{cu} + f_{fu}}$$

$$E_f \epsilon_{cu} = (41,000)(0.003) = 123 \text{ MPa}$$

$$\rho_{fb} = 0.85(0.85) \frac{(28)}{(440)} \frac{(123)}{(123 + 440)} = 0.01004$$

$$\rho_f / \rho_{fb} = \frac{0.01816}{0.01004} = 1.81$$

Because $\rho_f \geq 1.4\rho_{fb}$, the section is compression-controlled.

$$\phi = 0.65$$

2. Determine stress in tensile reinforcement at ultimate conditions.

$$f_f = \sqrt{\frac{(E_f \epsilon_{cu})^2}{4} + \frac{0.85\beta_1 f'_c}{\rho_f} E_f \epsilon_{cu} - 0.5 E_f \epsilon_{cu}} \leq f_{fu}$$

$$f_f = \sqrt{\frac{(123)^2}{4} + \frac{0.85(0.85)(28)}{(0.01814)} (123) - 0.5(123)} \leq 440$$

Reference

440.6-08, Table 7.1

440.1R, Table 6.2

440.1R, Eq. (6.2a)

440.1R, Eq. (7.2.1a)

440.1R, Eq. (7.2.1b)

440.1R, Eq. (7.2.3)

440.1R, Eq. (7.2.2d)

$f_f = 314 \text{ MPa}$

3. Determine nominal flexural strength M_n and design flexural strength ϕM_n .

$$a = \frac{A_f f_f}{0.85 f'_c b} = \frac{(1530)(314)}{0.85(28)(250)} = 81 \text{ mm} \quad \text{440.1R, Eq. (7.2.2b)}$$

$$M_n = A_f f_f \left(d - \frac{a}{2} \right) = (1530)(314) \left(337 - \frac{81}{2} \right) = 142.4 \times 10^6 \text{ N-mm} = 142.4 \text{ kN-m} \quad \text{440.1R, Eq. (7.2.2a)}$$

Alternatively, compute M_n directly:

$$M_n = \rho_f f_f \left(1 - 0.59 \frac{\rho_f f_f}{f'_c} \right) b d^2 \quad \text{440.1R, Eq. (7.2.2e)}$$

$$= (0.01814)(314) \left(1 - 0.59 \frac{(0.01814)(314)}{28} \right) (250)(337)^2 = 142.3 \times 10^6 \text{ N-mm} = 142.3 \text{ kN-m}$$

$$\phi M_n = (0.65)(142.3) = 92.5 \text{ kN-m}$$

4. Minimum reinforcement.

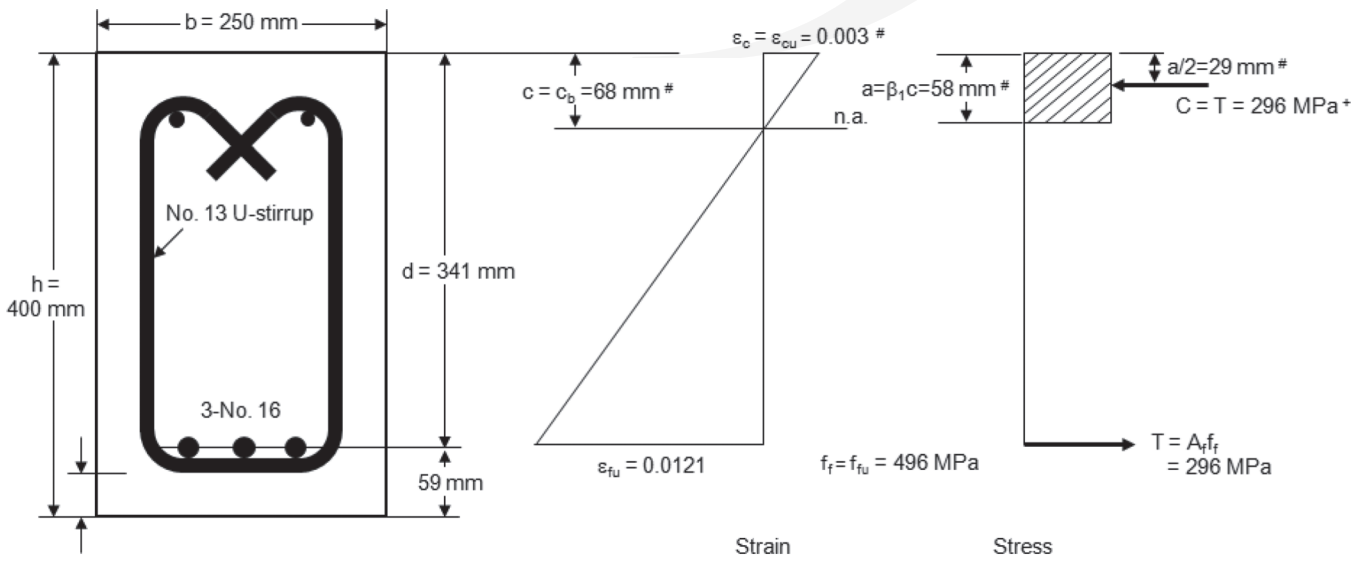
The minimum reinforcement provisions do not apply because the section is not tension-controlled. 440.1R, Sec. 7.2.4

Note: While the general procedure and principles used in this example are applicable for an FRP-reinforced beam of any cross-sectional shape, the specific equations used in this example are restricted to singly-reinforced rectangular cross sections (or flanged sections that exhibit rectangular section behavior) with reinforcement in a single layer.

Example 2M—Flexural (moment) strength using equivalent rectangular concrete stress distribution (tension-controlled section)

This example is similar to Example 6.1 of PCA Notes on ACI 318-08.

For the beam section shown, calculate moment strength based on static equilibrium using the equivalent rectangular concrete stress distribution as shown in Fig. 7.2 of this guide. Assume $f'_c = 28 \text{ MPa}$, $f_{fu}^* = 620 \text{ MPa}$, and $E_f = 41,000 \text{ MPa}$. Assume interior exposure conditions and neglect compression reinforcement.



* Conservatively assumed for design simplification. True values for c , a , and ϵ_c will be smaller, since actual NA will be higher.
 † Compression force must equal tension force. C cannot be calculated as $0.85f'_c b a$, since the correct value of a is not known.

Calculations and discussion

No. 16 bar properties:
 $d_b = 15.9 \text{ mm}$
 $A_{f,bar} = 199 \text{ mm}^2$

Reference

440.6-08, Table 7.1



Design material properties:

$$C_E = 0.8$$

440.1R, Table 6.2

$$f_{fu} = C_E f_{fu}^* = (0.8)(620) = 496 \text{ MPa}$$

440.1R, Eq. (6.2a)

1. Determine the strength reduction factor.

$$d = 400 - 38 - 12.7 - (15.9/2) = 341 \text{ mm}$$

$$A_f = (3)(199 \text{ mm}^2) = 597 \text{ mm}^2$$

$$\rho_f = \frac{A_f}{bd} = \frac{597}{(250)(341)} = 0.00700$$

440.1R, Eq. (7.2.1a)

$$\rho_{fb} = 0.85\beta_1 \frac{f'_c}{f_{fu}} \frac{E_f \epsilon_{cu}}{E_f \epsilon_{cu} + f_{fu}}$$

440.1R, Eq. (7.2.1b)

$$E_f \epsilon_{cu} = (41,000)(0.003) = 123 \text{ MPa}$$

$$\rho_{fb} = 0.85(0.85) \frac{(28)}{(496)} \frac{(123)}{(123 + 496)} = 0.00810$$

$$\frac{\rho_f}{\rho_{fb}} = \frac{0.00700}{0.00810} = 0.86$$

Because $\rho_f \leq \rho_{fb}$, the section is tension-controlled and $\phi = 0.55$.

440.1R, Eq. (7.2.3)

2. Determine stress in tensile reinforcement at ultimate conditions.

Because section is tension-controlled, $f_f = f_{fu} = 496 \text{ MPa}$

3. Determine nominal flexural strength M_n and design flexural strength ϕM_n .

$$c_b = \left(\frac{\epsilon_{cu}}{\epsilon_{cu} + \epsilon_{fu}} \right) d = \left(\frac{0.003}{0.003 + \frac{496}{41,000}} \right) (341) = 68 \text{ mm}$$

440.1R, Eq. (7.2.2h)

$$M_n = A_f f_{fu} \left(d - \frac{\beta_1 c_b}{2} \right) = (597)(496) \left(341 - \frac{(0.85)(68)}{2} \right) = 92.4 \times 10^6 \text{ N-mm} = 92.4 \text{ kN-m}$$

440.1R, Eq. (7.2.2g)

$$\phi M_n = (0.55)(92.4) = 50.8 \text{ kN-m}$$

4. Minimum reinforcement

The minimum reinforcement provisions apply since the section is tension-controlled.

440.1R, Sec. 7.2.4

$$A_{f,min} = \frac{0.41\sqrt{f'_c}}{f_{fu}} b_w d \geq \frac{2.3}{f_{fu}} b_w d$$

440.1R, Eq. (7.2.4)

$$\begin{aligned} A_{f,min} &= \frac{0.41\sqrt{28}}{496} (250)(341) \geq \frac{2.3}{496} (250)(341) \\ &= 373 \geq 395 \end{aligned}$$

$$A_{f,min} = 395 \text{ mm}^2$$

$$A_f(\text{provided}) = 597 \text{ mm}^2 > A_{f,min} = 395 \text{ mm}^2 \quad \text{OK}$$

Note: Whereas the general procedure and principles used in this example are applicable for an FRP-reinforced beam of any cross-sectional shape, the specific equations used in this example are restricted to singly-reinforced rectangular cross sections (or flanged sections that exhibit rectangular section behavior) with reinforcement in a single layer.

The procedure used in this example, described in 7.2.2, is approximate and conservative. A more detailed analysis of a tension-controlled cross section would require the computation of the neutral axis location based on the principles of strain compatibility and a numerical constitutive model for the concrete (for example, parabolic and Hognestad). This type of analysis can be computationally intensive and is generally not suitable for hand calculations. For problems such as the one shown in this example, differences in results (computed flexural strength) are likely to be negligible. A strain compatibility analysis is suggested for cases where there are multiple layers of reinforcement or when different FRP bar types are mixed (7.2.5.1).

Example 3M—Design of a rectangular beam with tension reinforcement only

This example is similar to Example 7.1 of PCA Notes on ACI 318-08.

Design a rectangular beam of width $b = 300$ mm to have adequate flexural strength. The beam must resist service load moments $M_D = 76$ kN-m and $M_L = 47$ kN-m. Assume interior exposure conditions.

$$f'_c = 28 \text{ MPa}$$

$$f_{fu}^* = 550 \text{ MPa}$$

$$E_f = 45,000 \text{ MPa}$$

Calculations and discussion

Design material properties:

$$C_E = 0.8$$

$$f_{fu} = C_E f_{fu}^* = (0.8)(550) = 440 \text{ MPa}$$

1. A common starting point for design of a reinforced concrete member of unknown dimensions is the assumption of a reinforcement ratio.

As a starting point, assume $\rho_f = 1.5\rho_{fb}$.

$$\rho_{fb} = 0.85\beta_1 \frac{f'_c}{f_{fu}} \frac{E_f \epsilon_{cu}}{E_f \epsilon_{cu} + f_{fu}}$$

$$E_f \epsilon_{cu} = (45,000)(0.003) = 135 \text{ MPa}$$

$$\rho_{fb} = 0.85(0.85) \frac{(28)}{(440)} \frac{(135)}{(135 + 440)} = 0.01079$$

$$\rho_f = 1.5\rho_{fb} = 1.5(0.01079) = 0.01619$$

Because $\rho_f \geq 1.4\rho_{fb}$, the section is compression-controlled.

$$\phi = 0.65$$

2. Compute bd^2 required.

First, determine the required design moment strength:

$$\phi M_{n,reqd} = M_u = 1.2M_D + 1.6M_L = 1.2(76) + 1.6(47) = 166.4 \text{ kN-m}$$

Calculate the stress in the tensile reinforcement (f_f) at ultimate conditions for the assumed value of ρ_f .

$$f_f = \sqrt{\frac{(E_f \epsilon_{cu})^2}{4} + \frac{0.85\beta_1 f'_c}{\rho_f} E_f \epsilon_{cu} - 0.5E_f \epsilon_{cu}} \leq f_{fu}$$

$$f_f = \sqrt{\frac{(135)^2}{4} + \frac{0.85(0.85)(28)}{(0.01619)}(135) - 0.5(135)} \leq 440$$

$$f_f = 349 \text{ MPa}$$

Use the moment capacity equation to determine required dimensions for the cross section.

$$M_u = \phi M_n = \phi \rho_f f_f \left(1 - 0.59 \frac{\rho_f f_f}{f'_c}\right) bd^2$$

$$(166.4)(10^6) = (0.65)(0.01619)(349) \left(1 - 0.59 \frac{(0.01619)(349)}{(28)}\right) bd^2$$

Reference

440.1R, Table 6.2

440.1R, Eq. (6.2a)

440.1R, Eq. (7.2.1b)

440.1R, Eq. (7.2.3)

318-11, Eq. (9-2)

440.1R, Eq. (7.2.2d)

440.1R, Eq. (7.2.2e)

$$bd^2 = 51.43 \times 10^6 \text{ mm}^3$$

3. Size member so that $(bd^2)_{provided} \geq (bd^2)_{required}$.

Recall $b = 300 \text{ mm}$, so $d = \sqrt{\frac{51.43 \times 10^6}{300}} = 414 \text{ mm}$

4. Now, determine the required reinforcement, select bars, and determine depth.

$$A_{f,reqd} = \rho_f b d = (0.01619)(300)(414) = 2011 \text{ mm}^2$$

Select four No. 25 bars ($A_f = 2040 \text{ mm}^2$)

Note: Examining alternative designs using other bar sizes may require changing the assumed value of f_{tu}^ to a value appropriate for the selected bar size.*

No. 25 bar diameter: $d_b = 25.4 \text{ mm}$

440.6-08, Table 7.1

For interior exposure, clear cover is 38 mm

440.5-08, Table 3.1

Assuming No. 13 stirrups:

$$h = (414) + (38) + (12.7) + \frac{(25.4)}{2} = 477 \text{ mm}$$

Round up to be conservative. So, select a 300 x 500 mm beam.

5. Determine capacity of cross section.

$$d = 500 - \left[(38) + (12.7) + \frac{(25.4)}{2} \right] = 437 \text{ mm}$$

$$\rho_f = \frac{A_f}{bd} = \frac{2040}{(300)(437)} = 0.01556$$

440.1R, Eq. (7.2.1a)

$$\frac{\rho_f}{\rho_{fb}} = \frac{0.01556}{0.01079} = 1.44$$

Because $\rho_f \geq 1.4\rho_{fb}$, $\phi = 0.65$.

440.1R, Eq. (7.2.3)

$$f_f = \sqrt{\frac{(E_f \epsilon_{cu})^2}{4} + \frac{0.85\beta_1 f'_c}{\rho_f} E_f \epsilon_{cu}} - 0.5 E_f \epsilon_{cu} \leq f_{fu}$$

440.1R, Eq. (7.2.2d)

$$f_f = \sqrt{\frac{(135)^2}{4} + \frac{0.85(0.85)(28)}{(0.01556)}(135)} - 0.5(135) \leq 440$$

$$f_f = 357 \text{ MPa}$$

$$M_n = \rho_f f_f \left(1 - 0.59 \frac{\rho_f f_f}{f'_c} \right) b d^2$$

440.1R, Eq. (7.2.2e)

$$= (0.01556)(357) \left(1 - 0.59 \frac{(0.01556)(357)}{28} \right) (300)(437)^2 = 281.0 \times 10^6 \text{ N-mm} = 281.0 \text{ kN-m}$$

$$\phi M_n = (0.65)(281.0) = 182.3 \text{ kN-m} > M_u = 166.4 \text{ kN-m} \quad \text{OK}$$

Note: Many designs for FRP-reinforced concrete are governed by serviceability requirements related to crack control, deflections, and creep rupture, rather than by flexural strength requirements. Calculations related to these serviceability requirements are covered in other example problems in this chapter.

Example 4M—Design of one-way solid slab

This example is similar to Example 7.2 of PCA Notes on ACI 318-08.

Determine the required thickness and reinforcement for a one-way slab continuous over three or more equal spans. Center-to-center span $\ell = 5.8$ m and clear span $\ell_n = 5.5$ m. Assume interior exposure conditions.

$$f'_c = 28 \text{ MPa}$$

$$f_{fu}^* = 650 \text{ MPa}$$

$$E_f = 41,000 \text{ MPa}$$

Service loads: $w_D =$ slab self-weight (no superimposed dead load), $w_L = 24 \text{ kN/m}^2$

Calculations and discussion

Design material properties:

$$C_E = 0.8$$

$$f_{fu} = C_E f_{fu}^* = (0.8)(650) = 520 \text{ MPa}$$

1. Determine required slab thickness.

Based on minimum thickness table, consider estimated depth.

End span will control thickness:

$$h \approx \frac{\ell}{17} = \frac{(5.8)(1000)}{17} = 341 \text{ mm}$$

440.1R, Table 7.3.2.1

Table 7.3.2.1 is only intended to provide guidance for initial design, therefore, assume $h = 300$ mm.

2. Compute the design moments using approximate moment analysis permitted by ACI 318-11, Sec. 8.3.3. Design will be based on the end span because it will yield the highest moments.

Assume the end of the end span is integral with the support.

300 mm slab weighs $[(300)/(1000)](24) = 7.2 \text{ kN/m}^2$

Factored load $q_u = 1.2(7.2) + 1.6(2.4) = 12.5 \text{ kN/m}^2$

318-11, Eq. (9-2)

Positive moment at discontinuous end integral with support:

$$+M_u = \frac{q_u \ell_n^2}{14} = \frac{(12.5)(5.5)^2}{14} = 27.0 \text{ kN-m/m}$$

318-11, Sec. 8.3.3

Negative moment at exterior face of first interior support:

$$-M_u = \frac{q_u \ell_n^2}{10} = \frac{(12.5)(5.5)^2}{10} = 37.8 \text{ kN-m/m}$$

318-11, Sec. 8.3.3

3. Determine required reinforcement and select bars.

Assume section is tension-controlled. For this case, $f_f = f_{fu} = 520 \text{ MPa}$ and $\phi = 0.55$.

For interior exposure, clear cover is 19 mm.

440.5-08, Table 3.1

Assume No. 16 bars for flexural reinforcement.

No. 16 bar diameter: $d_b = 15.9 \text{ mm}$

440.6-08, Table 7.1

$$d = 300 - \left[(19) + \frac{(15.9)}{2} \right] = 273 \text{ mm}$$

$$c_b = \left(\frac{\epsilon_{cu}}{\epsilon_{cu} + \epsilon_{fu}} \right) d = \left(\frac{0.003}{0.003 + \frac{520}{41,000}} \right) (273) = 52 \text{ mm}$$

440.1R, Eq. (7.2.2h)

Use moment strength equation to solve for area of reinforcement.

Consider $-M$ because it governs.

Reference

440.1R, Table 6.2

440.1R, Eq. (6.2a)

$$M_u = \phi M_{n,reqd} = \phi A_{f,reqd} f_{fu} \left(d - \frac{\beta_1 c_b}{2} \right) \quad 440.1R, \text{ Eq. (7.2.2g)}$$

$$A_{f,reqd} = \frac{M_u}{\phi f_{fu} \left(d - \frac{\beta_1 c_b}{2} \right)} = \frac{(37.8)(10^6)}{(0.55)(520) \left(273 - \frac{(0.85)(52)}{2} \right)} = 527 \text{ mm}^2/\text{m}$$

Note that this requirement is well less than the minimum reinforcement, as computed in the following.

$$\rho_{f,ts} = 0.0014 \leq 0.0018 \times \frac{414 E_s}{f_{fu} E_f} \leq 0.0036 \quad 440.1R, \text{ Eq. (9.1)}$$

$$\rho_{f,ts} = 0.0014 \leq 0.0018 \times \frac{414 \cdot 200,000}{520 \cdot 41,000} \leq 0.0036$$

$$\rho_{f,ts} = 0.0014 \leq 0.0070 \leq 0.0036, \text{ so } \rho_{f,ts} = 0.0036$$

$$A_{f,min} = \rho_{f,min} b h = (0.0036)(1000)(300) = 1080 \text{ mm}^2/\text{m}$$

Select No. 16 at 180 mm spacing ($A_f = 1106 \text{ mm}^2/\text{m}$)

Verify assumption of tension-controlled behavior:

$$\rho_{fb} = 0.85 \beta_1 \frac{f'_c}{f_{fu}} \frac{E_f \epsilon_{cu}}{E_f \epsilon_{cu} + f_{fu}} \quad 440.1R, \text{ Eq. (7.2.1b)}$$

$$E_f \epsilon_{cu} = (41,000)(0.003) = 123 \text{ MPa}$$

$$\rho_{fb} = 0.85(0.85) \frac{(28)}{(520)} \frac{(123)}{(123 + 520)} = 0.00744$$

$$\rho_f = \frac{A_f}{bd} = \frac{1106}{(1000)(273)} = 0.00405 \quad 440.1R, \text{ Eq. (7.2.1a)}$$

$$\frac{\rho_f}{\rho_{fb}} = \frac{0.00405}{0.00744} = 0.54 \quad \text{OK}$$

The slab may be designed to be 300 mm thick with No. 16 at 180 mm for $-M$. By observation, the same minimum reinforcement will be required for $+M$.

In addition to flexural strength, the slab should be examined for shear and the serviceability criteria of crack control, deflections, and creep rupture stress limits. Calculations related to these requirements are covered in other example problems in this chapter.

Further calculations show that this slab will be uncracked at service by a significant margin, and is even uncracked at ultimate conditions. The slab will work, but will be highly inefficient. Therefore, consider a more efficient slab design that is selected to be cracked at service.

4. Redesign the slab to be cracked at service loads.

When cracked, FRP-reinforced concrete slabs are seldom governed by flexural strength. Whereas a slab designed for flexural strength alone would have a ratio of service level moment to nominal moment strength (M_{serv}/M_n) of approximately 0.40 to 0.45, depending on the ratio of dead-to-live load, most FRP-reinforced slabs are governed by serviceability requirements and will exhibit ratios closer to 0.20 to 0.25. As a design approximation, design for a flexural strength corresponding to approximately twice the actual factored moment ($2.0M_u$).

Select a reinforcement ratio corresponding to a compression-controlled section, as this will promote the use of enough reinforcement to control cracking and reduce deflections.

Design for $2.0M_u$ and as a starting point, assume $\rho_f = 1.5\rho_{fb}$.

$$\rho_f = 1.5\rho_{fb} = 1.5(0.00744) = 0.01116$$

Calculate the stress in the tensile reinforcement (f_f) at ultimate conditions for the assumed value of ρ_f .

$$f_f = \sqrt{\frac{(E_f \epsilon_{cu})^2}{4} + \frac{0.85\beta_1 f'_c}{\rho_f} E_f \epsilon_{cu} - 0.5 E_f \epsilon_{cu}} \leq f_{fu} \quad 440.1R, \text{ Eq. (7.2.2d)}$$

$$f_f = \sqrt{\frac{(123)^2}{4} + \frac{0.85(0.85)(28)}{(0.01116)}(123) - 0.5(123)} \leq 520$$

$$f_f = 415 \text{ MPa}$$

Estimate dead load based on an assumed 200 mm slab thickness:

$$200 \text{ mm slab weighs } [(200)/(1000)](24) = 4.8 \text{ kN/m}^2$$

$$\text{Factored load } q_u = 1.2(4.8) + 1.6(2.4) = 9.6 \text{ kN/m}^2 \quad 318-11, \text{ Eq. (9-2)}$$

Negative moment at exterior face of first interior support (governs):

$$-M_u = \frac{q_u \ell_n^2}{10} = \frac{(9.6)(5.5)^2}{10} = 29.0 \text{ kN-m/m} \quad 318-11, \text{ Sec. 8.3.3}$$

Use the moment capacity equation to determine a depth for the slab.

$$M_u = \phi M_n = \phi \rho_f f_f \left(1 - 0.59 \frac{\rho_f f_f}{f'_c}\right) b d^2 \quad 440.1R, \text{ Eq. (7.2.2e)}$$

$$2(29.0)(10^6) = (0.65)(0.01116)(415) \left(1 - 0.59 \frac{(0.01116)(415)}{(28)}\right) (1000)d^2$$

$$d = 146 \text{ mm}$$

Assume No. 19 bars for flexural reinforcement.

$$h = (146) + (19) + \frac{(19.1)}{2} = 175 \text{ mm}$$

Round up to be conservative (180 mm thick slab [$h = 180 \text{ mm}$]).

Correct dead load for 180 mm thickness:

$$180 \text{ mm slab weighs } [(180)/(1000)](24) = 4.3 \text{ kN/m}^2$$

$$\text{Factored load } q_u = 1.2(4.3) + 1.6(2.4) = 9.0 \text{ kN/m}^2 \quad 318-11, \text{ Eq. (9-2)}$$

The flexural capacity could be checked, but it should be satisfactory by inspection because the design was based on providing a capacity of $2.0M_u$. Thus, capacity calculations are not necessary.

Select reinforcement for the slab.

Assume the same reinforcement for $-M$ and $+M$.

$$A_f = \rho_f b d = (0.01116)(1000)(146) = 1629 \text{ mm}^2/\text{m}$$

Select No. 19 bars at 150 mm spacing ($A_f = 1890 \text{ mm}^2/\text{m}$).

$$440.1R, \text{ Eq. (7.2.1a)}$$

5. Select temperature and shrinkage reinforcement for transverse direction.

$$\rho_{f,ts} = 0.0014 \leq 0.0018 \times \frac{414 E_s}{f_{fu} E_f} \leq 0.0036 \quad 440.1R, \text{ Eq. (9.1)}$$

$$\rho_{f,ts} = 0.0014 \leq 0.0018 \times \frac{414 \cdot 200,000}{520 \cdot 41,000} \leq 0.0036$$

$$\rho_{f,ts} = 0.0014 \leq 0.0070 \leq 0.0036, \text{ so } \rho_{f,ts} = 0.0036$$

$$A_{f,ts} = \rho_{f,ts} b h = (0.0036)(1000)(180) = 648 \text{ mm}^2/\text{m}$$

Select No. 13 bars at 180 mm spacing ($A_f = 717 \text{ mm}^2/\text{m}$).

Note: The slab should now be examined for shear, crack control, deflections, and creep rupture. Calculations related to these requirements are covered in other example problems in this chapter. If these design criteria are not satisfied, then the slab thickness may be increased incrementally or additional reinforcement added.

Example 5M—Distribution of reinforcement for effective crack control

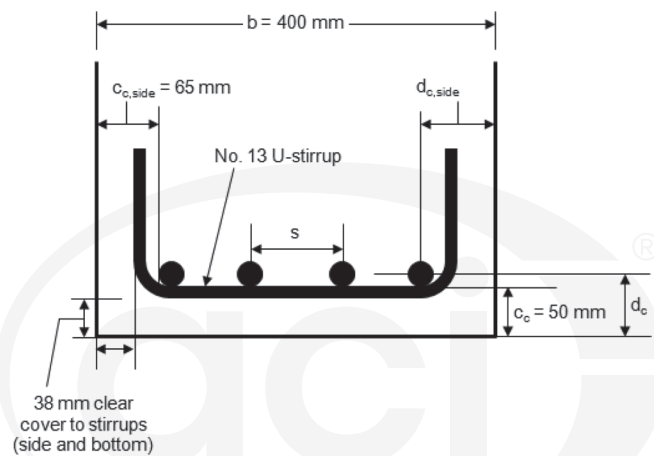
This example is similar to Example 9.1 of PCA Notes on ACI 318-08.

A rectangular beam is being designed for a factored moment $M_u = 177 \text{ kN-m}$. The beam has been sized as a 400 mm wide by 600 mm deep beam, and the required area of GFRP flexural reinforcement has been computed as $A_{f,reqd} = 1460 \text{ mm}^2$. Determine an arrangement of flexural reinforcement that satisfies crack control requirements in 7.3.1. Assume bottom clear cover to the flexural reinforcement (c_c) of 50 mm (approximately 38 mm clear cover + 13 mm stirrup diameter). Assume side clear cover to the flexural reinforcement ($c_{c,side}$) of 65 mm (approximately 38 mm clear cover + 13 mm stirrup diameter + 13 mm to accommodate inner radius of stirrup bend). The unfactored service load moment is $M_s = 122 \text{ kN-m}$. Assume interior exposure conditions.

$$f'_c = 28 \text{ MPa}$$

$$f_{fu}^* = 550 \text{ MPa}$$

$$E_f = 40,000 \text{ MPa}$$



Calculations and discussion

Design material properties:

$$C_E = 0.8$$

$$f_{fu} = C_E f_{fu}^* = (0.8)(550) = 440 \text{ MPa}$$

1. Select reinforcement.

Four No. 22 bars ($A_f = 1550 \text{ mm}^2$)

No. 22 bar diameter: $d_b = 22.2 \text{ mm}$

2. Check limitation on value of d_c :

$$d_c \leq \frac{E_f w}{2 f_s \beta k_b} \quad 440.1R, \text{ Eq. (7.3.1b)}$$

Assume a maximum allowable crack width w of 0.70 mm.

440.1R, Sec. 7.3.1

Take $k_b = 1.4$.

440.1R, Sec. 7.3.1

The parameters β and f_s must be determined from a linear-elastic cracked section analysis under service loads. Many of these calculations are covered in 7.3.2.2 and 7.4.1.

$$k = \sqrt{2\rho_f n_f + (\rho_f n_f)^2} - \rho_f n_f \quad 440.1R, \text{ Eq. (7.3.2b)}$$

$$d_c = c_c + \frac{d_b}{2} = 50 + \frac{22.2}{2} = 61 \text{ mm}$$

$$d = h - d_c = 600 - 61 = 539 \text{ mm}$$

Reference

440.1R, Table 6.2

440.1R, Eq. (6.2a)

440.6-08, Table 7.1

$$\rho_f = \frac{A_f}{bd} = \frac{1550}{(400)(539)} = 0.00719 \quad 440.1R, \text{ Eq. (7.2.1a)}$$

$$E_c = 4700\sqrt{f'_c} = 4700\sqrt{28} = 24,900 \text{ MPa} \quad 318-11, \text{ Sec. 8.5.1}$$

$$n_f = \frac{E_f}{E_c} = \frac{41,000}{24,900} = 1.647$$

$$\rho_f n_f = (0.00719)(1.647) = 0.01184$$

$$k = \sqrt{2\rho_f n_f + (\rho_f n_f)^2} - \rho_f n_f = \sqrt{2(0.01184) + (0.01184)^2} - 0.01184 = 0.142$$

$$I_{cr} = \frac{bd^3}{3} k^3 + n_f A_f d^2 (1-k)^2 \quad 440.1R, \text{ Eq. (7.3.2.2a)}$$

$$= \frac{(400)(539)^3}{3} (0.142)^3 + (1.647)(1550)(539)^2 (1-0.142)^2 = 605.7 \times 10^6 \text{ mm}^4$$

Service level stress in FRP reinforcement (refer to Eq. (7.4.1) for a similar calculation based on sustained service load)

$$f_{fs} = M_s \frac{n_f d (1-k)}{I_{cr}} = ((122)(10^6)) \frac{(1.647)(539)(1-0.142)}{605.7 \times 10^6} = 153 \text{ MPa} \quad 440.1R, \text{ Eq. (7.4.1)}$$

$$\beta = \frac{h - kd}{d - kd} = \frac{600 - (0.142)(539)}{539 - (0.142)(539)} = 1.13$$

Once parameters have been calculated, check limit on d_c

$$d_c \leq \frac{E_f w}{2 f_{fs} \beta k_b} \quad 440.1R, \text{ Eq. (7.3.1b)}$$

$$61 \text{ mm} \leq \frac{(41,000)(0.70)}{2(153)(1.13)(1.4)}$$

$$61 \text{ mm} > 59 \text{ mm} \quad \text{NG}$$

Although the limit on d_c is not satisfied, continue to check the bar spacing for illustrative purposes in the following.

Check bar spacing against maximum spacing:

$$s_{max} = 1.15 \frac{E_f w}{f_{fs} k_b} - 2.5c_c \leq 0.92 \frac{E_f w}{f_{fs} k_b} \quad 440.1R, \text{ Eq. (7.3.1a)}$$

$$s_{max} = 1.15 \frac{(41,000)(0.70)}{(153)(1.4)} - 2.5(50) \leq 0.92 \frac{(41,000)(0.70)}{(153)(1.4)}$$

$$s_{max} = 29 \leq 123, \text{ so } s_{max} = 29 \text{ mm}$$

Provided center-to-center bar spacing:

$$s_{provided} = \frac{b - 2d_{c,side}}{N - 1}$$

$$d_{c,side} = \text{side cover to center of exterior bars} = 65 + (1/2)(22.2) = 76 \text{ mm}$$

$$N = \text{number of bars} = 4$$

$$s_{provided} = \frac{400 - 2(76)}{4 - 1}$$

$$s_{provided} = 83 \text{ mm} > s_{max} = 29 \text{ mm} \quad \text{NG}$$

The selected reinforcement does not meet crack control requirements based on the calculations shown above. Both the cover (d_c) and spacing (s) limits are not satisfied.

Note that minimum clear bar spacing requirements must also be satisfied. In this case, maximum center-to-center bar spacing of 1.09 in. per Eq. (7.3.1a) is so small that minimum clear spacing (d_b , 25 mm, or 4/3 times the maximum aggregate size) per ACI 318-11, Sec. 7.6, could not possibly be provided (318-11, Sec. 7.6).

3. Choose a new reinforcement selection. Generally, if the aforementioned checks are not satisfied, then additional reinforcement will be required such that the FRP bar stress at service is reduced. Increase the amount of reinforcement and try two different possibilities:

Three No. 29 bars ($A_f = 1940 \text{ mm}^2$; $d_b = 28.7 \text{ mm}$)

440.6-08, Table 7.1

Five No. 22 bars ($A_f = 1940 \text{ mm}^2$; $d_b = 22.2 \text{ mm}$)

440.6-08, Table 7.1

Calculations are repeated for these two possibilities as well as the original selection checked previously. Values are presented in table format to save space and facilitate comparison.

Parameter	Unit	Four No. 22	Three No. 29	Five No. 22
A_f	mm ²	1550	1940	1940
d	mm	539	536	539
d_c	mm	61	64	61
ρ_f		0.00719	0.00905	0.00900
k		0.142	0.158	0.158
I_{cr}	mm ⁴	605.7×10^6	731.8×10^6	740.5×10^6
f_{fs}	MPa	153	124	123
β		1.13	1.14	1.13
d_c (limit value)	mm	59	73	74
Check if $d_c \leq d_c$ (limit value)		NG	OK	OK
s_{max} (limit value)	mm	29	65	67
$d_{c,side}$	mm	76	79	76
$s_{provided}$	mm	83	121	62
Check if $s_{provided} \leq s_{max}$		NG	NG	OK

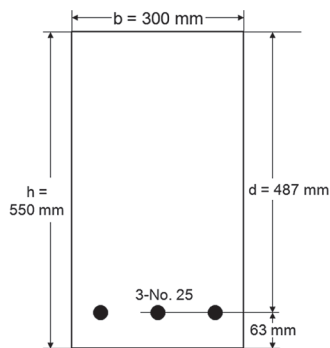
As can be seen in the table, the choice of three No. 29 bars provides sufficient additional reinforcement to reduce the stress in the reinforcing bars. The reinforcement, however, is spaced too far apart to meet the maximum spacing requirement, as the reinforcement is not sufficiently distributed to control crack widths.

The choice of five No. 22 bars provides the same amount of reinforcement as the choice of three No. 29 bars, but distributes the reinforcement better within the width of the cross section. The five bars would be spaced closely enough to control cracking, and far enough apart to provide minimum clear spacing required by ACI 318-11, Sec. 7.6.

Use five No. 22 bars distributed a single layer.

Example 6M—Deflection of a simple-span nonprestressed rectangular beam

This example is similar to Example 10.1 of PCA Notes on ACI 318-08.



Required: analysis of deflections and comparison to ACI 318-11 allowable deflections. Consider long-term deflections at 3 months and 5 years (ultimate value).

Data:

$$f'_c = 21 \text{ MPa (normalweight concrete)}$$

$$E_f = 45,000 \text{ MPa}$$

$$\text{Superimposed dead load (not including beam weight)} = 1.8 \text{ kN/m}$$

$$\text{Live load} = 4.4 \text{ kN/m (20 percent sustained)}$$

$$\text{Span} = 7.5 \text{ m (simply-supported)}$$

Calculations and discussion

No. 25 bar properties:

$$d_b = 25.4 \text{ mm}$$

$$A_{f,bar} = 510 \text{ mm}^2$$

Reinforcement quantities needed for calculations:

$$A_f = (3)(510 \text{ mm}^2) = 1530 \text{ mm}^2$$

$$\rho_f = \frac{A_f}{bd} = \frac{1530}{(300)(487)} = 0.01047$$

1. Check recommended minimum beam thickness.

Based on minimum thickness table, consider estimated depth:

$$h \approx \frac{\ell}{10} = \frac{(7.5)(1000)}{10} = 750 \text{ mm}$$

Table 7.3.2.1 is intended to provide guidance for preliminary design, and does not guarantee that deflection limits will be met, so deflections will be computed.

2. Moments:

$$w_D = 1.8 + \frac{(300)(550)(24)}{1000} = 5.8 \text{ kN/m}$$

$$M_D = \frac{w_D \ell^2}{8} = \frac{(5.8)(7.5)^2}{8} = 40.8 \text{ kN-m}$$

$$M_L = \frac{w_L \ell^2}{8} = \frac{(4.4)(7.5)^2}{8} = 30.9 \text{ kN-m}$$

$$M_{sus} = M_D + 0.20(M_L) = 40.8 + (0.20)(30.9) = 47.0 \text{ kN-m}$$

$$M_{D+L} = 40.8 + 30.9 = 71.7 \text{ kN-m}$$

3. Modulus of elasticity and modular ratio:

$$E_c = 4700\sqrt{f'_c} = 4700\sqrt{21} = 21,500 \text{ MPa}$$

$$n_f = \frac{E_f}{E_c} = \frac{45,000}{21,500} = 2.093$$

Reference

440.6-08, Table 7.1

440.1R, Eq. (7.2.1a)

440.1R, Table 7.3.2.1

318-11, Sec. 8.5.1

4. Gross and cracked section moment of inertia:

$$I_g = \frac{bh^3}{12} = \frac{(300)(550)^3}{12} = 4.159 \times 10^9 \text{ mm}^4$$

$$\rho_f n_f = (0.01047)(2.093) = 0.02191$$

$$k = \sqrt{2\rho_f n_f + (\rho_f n_f)^2} - \rho_f n_f = \sqrt{2(0.02191) + (0.02191)^2} - 0.02191 = 0.189 \quad 440.1R, \text{ Eq. (7.3.2.2b)}$$

$$I_{cr} = \frac{bd^3}{3} k^3 + n_f A_f d^2 (1-k)^2 \quad 440.1R, \text{ Eq. (7.3.2.2a)}$$

$$= \frac{(300)(487)^3}{3} (0.189)^3 + (2.093)(1530)(487)^2 (1-0.189)^2 = 0.578 \times 10^9 \text{ mm}^4$$

$$\frac{I_g}{I_{cr}} = \frac{4.159 \times 10^9}{0.578 \times 10^9} = 7.20 \quad \frac{I_{cr}}{I_g} = \frac{0.578 \times 10^9}{4.159 \times 10^9} = 0.139$$

5. Effective moments of inertia:

$$M_{cr} = \frac{0.62\lambda\sqrt{f'_c}I_g}{y_t} = \frac{0.62(1)(\sqrt{21})(4.159 \times 10^9)}{(1/2)(550)(10^6)} = 43.0 \text{ kN-m} \quad 440.1R, \text{ Eq. (7.3.2.2d)}$$

Assuming that the member is loaded to the full dead load before any live load is applied, the effective moment of inertia may be computed on the basis of the dead load alone. (This assumption will yield a conservative estimate of live load deflection in the next step). Because $M_D < M_{cr}$, this beam is uncracked for this condition. Thus, the effective moment of inertia for dead load is I_g .

$$(I_e)_D = I_g = 4.159 \times 10^9 \text{ mm}^4$$

Find the effective moment of inertia due to dead plus live load.

$$\frac{M_{cr}}{M_a} = \frac{M_{cr}}{M_{D+L}} = \frac{43.0}{71.7} = 0.600$$

$$\gamma = 1.72 - 0.72(M_{cr}/M_a) = 1.72 - 0.72(0.600) = 1.288 \quad 440.1R, \text{ Sec. 7.3.2.2}$$

$$(I_e)_{D+L} = \frac{I_{cr}}{1 - \gamma \left(\frac{M_{cr}}{M_a} \right)^2 \left[1 - \frac{I_{cr}}{I_g} \right]} \quad 440.1R, \text{ Eq. (7.3.2.2c)}$$

$$= \frac{0.578 \times 10^9}{1 - (1.288)(0.600)^2 [1 - 0.139]} = 0.962 \times 10^9 \text{ mm}^4$$

6. Immediate deflections:

$K = 1$ for simple spans

$$(\Delta_i)_D = \frac{K(5)M_D \ell^2}{48E_c(I_e)_D} = \frac{(1)(5)(40.8)(7.5)^2(10^{12})}{48(21,500)(4.159 \times 10^9)} = 2.7 \text{ mm}$$

$$(\Delta_i)_{D+L} = \frac{K(5)M_{D+L} \ell^2}{48E_c(I_e)_{D+L}} = \frac{(1)(5)(71.7)(7.5)^2(10^{12})}{48(21,500)(0.962 \times 10^9)} = 20.3 \text{ mm}$$

The immediate live load deflection is found by subtracting the dead load deflection from the deflection due to both dead and live load.

$$(\Delta_i)_L = (\Delta_i)_{D+L} - (\Delta_i)_D = 20.3 - 2.7 = 17.6 \text{ mm}$$

It is conservative to find the immediate deflection due to sustained load by using the effective moment of inertia based on the full dead plus live load.

$$(\Delta_i)_{sus} = \frac{K(5)M_{sus}\ell^2}{48E_c(I_e)_{D+L}} = \frac{(1)(5)(47.0)(7.5)^2(10^{12})}{48(21,500)(0.962 \times 10^9)} = 13.3 \text{ mm}$$

$$(\Delta_i)_{L,unsustained} = (\Delta_i)_{D+L} - (\Delta_i)_{sus} = 20.3 - 13.3 = 7.0 \text{ mm}$$

7. Incremental portion of total deflection occurring after placement of nonstructural elements (sum of the long-term deflection due to all sustained loads and the immediate deflection due to any additional live load):

a. 3 months ($\xi = 1.0$)

318-11, Sec. 9.5.2.5

$$\Delta_{incr} = \Delta_{LT,sus} + \Delta_{L,unsustained} = 0.6\xi(\Delta_i)_{sus} + (\Delta_i)_{L,unsustained} = 0.6(1.0)(13.3) + 7.0 = 15.0 \text{ mm}$$

440.1R, Eq. (7.3.2.3c)

b. 5 years ($\xi = 2.0$)

318-11, Sec. 9.5.2.5

$$\Delta_{incr} = \Delta_{LT,sus} + \Delta_{L,unsustained} = 0.6\xi(\Delta_i)_{sus} + (\Delta_i)_{L,unsustained} = 0.6(2.0)(13.3) + 7.0 = 23.0 \text{ mm}$$

440.1R, Eq. (7.3.2.3c)

8. Compare computed deflections to allowable deflections.

Allowable deflections (immediate live load):

318-11, Table 9.5(b)

Flat roofs not supporting and not attached to nonstructural elements likely to be damaged by large deflections:

$$\{(\Delta_i)_L = 17.6 \text{ mm}\} \leq \left\{ \frac{\ell}{180} = \frac{(7.5)(1000)}{180} = 41.7 \text{ mm} \right\} \text{ OK}$$

Floors not supporting and not attached to nonstructural elements likely to be damaged by large deflections:

$$\{(\Delta_i)_L = 17.6 \text{ mm}\} \leq \left\{ \frac{\ell}{360} = \frac{(7.5)(1000)}{360} = 20.8 \text{ mm} \right\} \text{ OK}$$

Allowable deflections (incremental after placement of nonstructural elements):

318-11, Table 9.5(b)

Roof or floor construction supporting or attached to nonstructural elements not likely to be damaged by large deflections:

$$\{\Delta_{incr} = 23.0 \text{ mm}\} \leq \left\{ \frac{\ell}{240} = \frac{(7.5)(1000)}{240} = 31.3 \text{ mm} \right\} \text{ OK}$$

Roof or floor construction supporting or attached to nonstructural elements likely to be damaged by large deflections (very stringent criteria):

$$\{\Delta_{incr} = 23.0 \text{ mm}\} > \left\{ \frac{\ell}{480} = \frac{(7.5)(1000)}{480} = 15.6 \text{ mm} \right\} \text{ NG}$$

If nonstructural elements likely to be damaged by large deflections are to be supported by this member, it will need to be redesigned to have a greater flexural stiffness. Otherwise, the member is adequate.

Example 7M—Creep rupture stress check under sustained loads

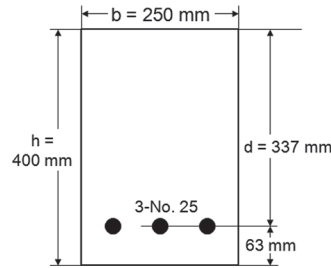
This example does not have a companion in PCA Notes on ACI 318-08 because creep rupture is an FRP phenomenon.

The rectangular beam shown is designed to carry service load moments $M_D = 24 \text{ kN-m}$ and $M_L = 24 \text{ kN-m}$. Assume 20 percent of the live load is sustained. Verify that the beam satisfies the creep rupture stress limits in 7.4.1. Assume interior exposure conditions.

$$f'_c = 28 \text{ MPa}$$

$$f_{fu}^* = 550 \text{ MPa}$$

$$E_f = 41,000 \text{ MPa}$$



Calculations and discussion

No. 25 bar properties:

$$d_b = 25.4 \text{ mm}$$

$$A_{f,bar} = 510 \text{ mm}^2$$

Reinforcement quantities needed for calculations:

$$A_f = (3)(510 \text{ mm}^2) = 1530 \text{ mm}^2$$

$$\rho_f = \frac{A_f}{bd} = \frac{1530}{(250)(337)} = 0.01816$$

Design material properties:

$$C_E = 0.8$$

$$f_{fu} = C_E f_{fu}^* = (0.8)(550) = 440 \text{ MPa}$$

1. Sustained load moment:

$$M_{sus} = M_D + 0.20(M_L) = 24 + (0.20)(24) = 28 \text{ kN-m}$$

2. Modulus of elasticity and modular ratio:

$$E_c = 4700\sqrt{f'_c} = 4700\sqrt{28} = 24,900 \text{ MPa}$$

$$n_f = \frac{E_f}{E_c} = \frac{41,000}{24,900} = 1.647$$

3. Cracked section moment of inertia:

$$\rho n_f = (0.01816)(1.647) = 0.02991$$

$$k = \sqrt{2\rho_f n_f + (\rho_f n_f)^2} - \rho_f n_f = \sqrt{2(0.02991) + (0.02991)^2} - 0.02991 = 0.216$$

$$I_{cr} = \frac{bd^3}{3} k^3 + n_f A_f d^2 (1-k)^2$$

$$= \frac{(250)(337)^3}{3} (0.216)^3 + (1.647)(1530)(337)^2 (1-0.216)^2 = 0.208 \times 10^9 \text{ mm}^4$$

4. Reinforcement stress under sustained service loads:

$$f_{fs,sus} = M_{s,sus} \frac{n_f d (1-k)}{I_{cr}}$$

$$f_{fs,sus} = (28.8)(10^6) \frac{(1.647)(337)(1-0.216)}{0.208 \times 10^9} = 60 \text{ MPa}$$

Allowable reinforcement stress:

Reference

440.6-08, Table 7.1

440.1R, Eq. (7.2.1a)

440.1R, Table 6.2

440.1R, Eq. (6.2a)

318-11, Sec. 8.5.1

440.1R, Eq. (7.3.2.2b)

440.1R, Eq. (7.3.2.2a)

440.1R, Eq. (7.4.1)

440.1R, Table 7.4.1

$$\{f_{s,sus} = 60 \text{ MPa}\} \leq \{0.20f_{fu} = 0.20(440) = 88 \text{ MPa}\} \quad \text{OK}$$

Example 8M—Design for shear (members subject to shear and flexure only)

This example is similar to Example 12.1 of PCA Notes on ACI 318-08.

Determine the required size and spacing of vertical U-stirrups for an 5.5 m span, simply-supported normalweight reinforced concrete beam. Assume interior exposure conditions.

$$b_w = 300 \text{ mm}$$

$$d = 500 \text{ mm}$$

$$f'_c = 28 \text{ MPa}$$

$$f_{fu}^* = 700 \text{ MPa (stirrups)}$$

$$E_f = 41,000 \text{ MPa (stirrups)}$$

$$w_u = 70.8 \text{ kN/m (includes self-weight)}$$

$$\rho_f = 0.0272 \text{ (longitudinal reinforcement)}$$

$$r_b/d_b = 4 \text{ (assumed curvature of bent stirrup bars)}$$

Calculations and discussion

Design material properties:

$$C_E = 0.8$$

$$f_{fu} = C_E f_{fu}^* = (0.8)(700) = 560 \text{ MPa}$$

For the purposes of this example, the live load will be assumed to be present on the full span so that the design shear at the centerline of span is zero. (A design shear greater than zero at midspan is obtained by considering partial live loading of the span.)

1. Determine factored shear forces.

$$\text{At support: } V_u = 70.8 \left(\frac{5.5}{2} \right) = 194.7 \text{ kN}$$

$$\text{At distance } d \text{ from support: } V_u = 194.7 - 70.8 \left(\frac{500}{1000} \right) = 159.3 \text{ kN}$$

2. Determine shear strength provided by concrete.

$$\phi V_c = \phi \left(\frac{5}{2} k \right) 2 \sqrt{f'_c} b_w d \quad 440.1R, \text{ Eq. (8.2b)}$$

$$E_c = 4700 \sqrt{f'_c} = 4700 \sqrt{28} = 24,900 \text{ MPa} \quad 318-11, \text{ Sec. 8.5.1}$$

$$n_f = \frac{E_f}{E_c} = \frac{41,000}{24,900} = 1.647$$

$$\rho_f n_f = (0.0272)(1.647) = 0.04480$$

$$k = \sqrt{2\rho_f n_f + (\rho_f n_f)^2} - \rho_f n_f = \sqrt{2(0.04480) + (0.04480)^2} - 0.04480 = 0.258 \quad 440.1R, \text{ Eq. (7.3.2.2b)}$$

$$\phi V_c = (0.75) \left(\frac{0.258}{5} \right) 2 \sqrt{28} (300)(500) \left(\frac{1}{1000} \right) = 61.4 \text{ kN}$$

$$V_u = 159.3 \text{ kN} > \phi V_c / 2 = 31.2 \text{ kN}$$

Therefore, shear reinforcement is required. 440.1R, Sec. 8.2.2

3. Compute $V_u - \phi V_c$ at critical section.

$$V_u - \phi V_c = 159.3 - 61.4 = 97.9 \text{ kN} < \phi 0.66 \sqrt{f'_c} b_w d = 393 \text{ kN} \quad \text{OK} \quad 440.1R, \text{ Sec. 8.2.3}$$

4. Determine distance x_c from support beyond which shear reinforcement is not required for strength ($V_u = \phi V_c$):

Reference

440.1R, Table 6.2

440.1R, Eq. (6.2a)

$$x_c = \frac{V_u @ \text{support} - \phi V_c}{w_u} = \frac{194.7 - 61.4}{70.8} = 1.88 \text{ m}$$

Determine distance x_m from support beyond which shear reinforcement is not required ($V_u = \phi V_c/2$):

$$x_m = \frac{V_u @ \text{support} - (\phi V_c/2)}{w_u} = \frac{194.7 - (61.4/2)}{70.8} = 2.32 \text{ m}$$

Therefore, only minimum shear reinforcement is required between 1.88 m and 2.32 m from the supports. Shear reinforcement is not required past 2.32 m from the supports.

5. Determine design tensile stress in shear reinforcement.

Tensile strength of bent bars:

$$f_{fb} = \left(0.05 \cdot \frac{r_b}{d_b} + 0.3 \right) f_{fu} \leq f_{fu} \quad 440.1R, \text{ Eq. (6.2.1)}$$

$$f_{fb} = (0.05 \cdot 4 + 0.3) f_{fu} \leq f_{fu}$$

$$f_{fb} = (0.50) f_{fu} \leq f_{fu}$$

$$f_{fb} = (0.50)(560) = 280 \text{ MPa}$$

The design tensile strength is based on a strain of 0.004:

$$f_{fv} = 0.004 E_f \leq f_{fb} \quad 440.1R, \text{ Eq. (8.2d)}$$

$$f_{fv} = 0.004(41,000) \leq 280$$

$$f_{fv} = 164 \leq 280$$

$$f_{fv} = 164 \text{ MPa}$$

6. Determine required spacing of vertical U-stirrups at the critical section.

$$\frac{A_{fv}}{s} = \frac{(V_u - \phi V_c)}{\phi f_{fv} d} = \frac{(159.3 - 61.4)1000}{(0.75)(164)(500)} = 1.59 \text{ mm}^2/\text{mm} \quad 440.1R, \text{ Eq. (8.2e)}$$

Assuming No. 13 U-stirrups ($A_{fv} = 258 \text{ mm}^2$)

$$s = \frac{258}{1.59} = 162 \text{ mm}$$

Check maximum permissible spacing of stirrups:

$$s = d/2 = 250 \text{ mm} \leq 600 \text{ mm}$$

$$\text{because } V_u - \phi V_c = 97.9 \text{ kN} < \phi 4 \sqrt{f'_c b_w} d = 196 \text{ kN} \quad \text{OK}$$

440.1R, Sec. 8.3
318-11, Sec. 11.4.5

Maximum stirrup spacing based on minimum shear reinforcement:

$$s = \frac{A_{fv, \text{min}} f_{fv}}{0.35 b_w} = \frac{(258)(164)}{0.35(300)} = 403 \text{ mm} \quad 440.1R, \text{ Eq. (8.2.2)}$$

Therefore, the spacing at the critical section is restricted to the smallest of 162, 250, and 403 mm. Select spacing of 150 mm at the critical section.

Determine the distance x where a transition can be made to a spacing of 250 mm (to satisfy strength and maximum spacing requirement calculated above as $d/2 = 250 \text{ mm}$):

$$\frac{A_{fv}}{s} = \frac{(V_u - \phi V_c)}{\phi f_{fv} d} \quad 440.1R, \text{ Eq. (8.2e)}$$

$$\frac{258}{250} = \frac{(V_u - \phi V_c)}{(0.75)(164)(500)1000}$$

$$V_u - \phi V_c = 63.5 \text{ kN}$$

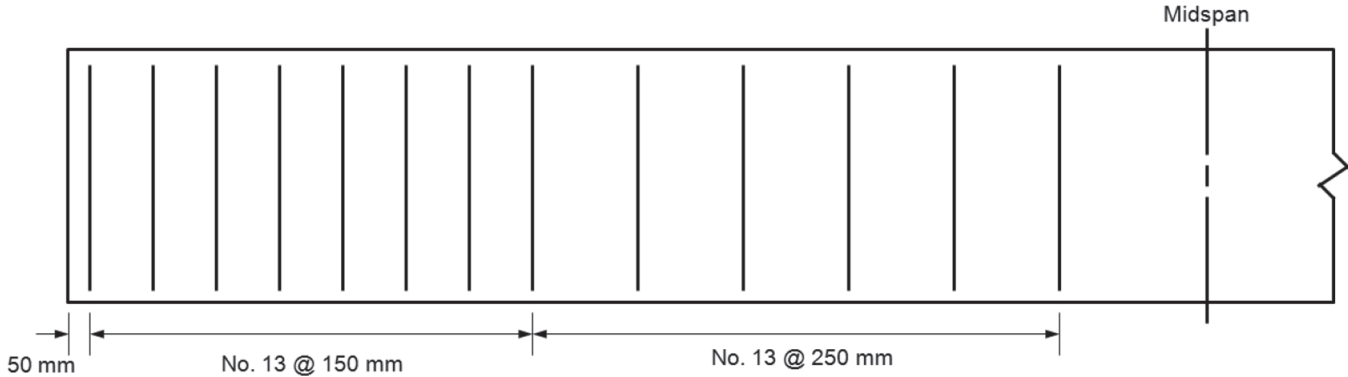
$$V_u = 63.5 + 61.4 = 124.9 \text{ kN}$$

$$x = \frac{V_u @ \text{support} - V_u}{w_u} = \frac{194.7 - 124.9}{70.8} = 0.99 \text{ m}$$

Therefore, a transition may be made from 150 to 250 mm spacing at 0.99 m from the support.

7. Select a stirrup spacing arrangement that satisfies previous calculations.

Place first stirrup at 50 mm from support. Use 150 mm spacing to 1.10 m from support. Use 250 mm spacing to 2.3 m from support.



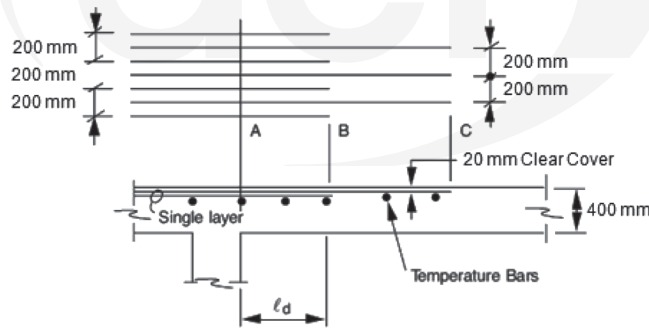
Note: Many designers would carry the reinforcement spacing of 250 mm through midspan, even though it is not required by calculations.

Example 9M—Development of bars in tension (compression-controlled or transition zone section)

This example is similar to Example 4.2 of PCA Notes on ACI 318-08.

Calculate the required tension development length for the No. 25 glass FRP (GFRP) bars (alternate short bars) embedded in the normalweight concrete one-way slab shown in the following figure to develop the full moment capacity at Section A.

Assume $f'_c = 28$ MPa, $f_{fu}^* = 550$ MPa, and $E_f = 41,000$ MPa. Assume interior exposure conditions.



Calculations and discussion

Assume short bars are developed within distance AB while long bars are developed within BC.

No. 25 bar properties:

$$d_b = 25.4 \text{ mm}$$

$$A_{f,bar} = 510 \text{ mm}^2$$

Design material properties:

$$C_E = 0.8$$

$$f_{fu} = C_E f_{fu}^* = (0.8)(550) = 440 \text{ MPa}$$

1. Determine the type of section.

$$d = 400 - 20 - (25.4/2) = 367 \text{ mm}$$

$$A_f = (510 \text{ mm}^2)/(100 \text{ mm spacing}) = 5.10 \text{ mm}^2/\text{mm} = 5100 \text{ mm}^2/\text{m of slab}$$

$$\rho_f = \frac{A_f}{bd} = \frac{5100}{(1000)(367)} = 0.01390$$

Reference

440.6-08, Table 7.1

440.1R, Table 6.2
440.1R, Eq. (6.2a)

440.1R, Eq. (7.2.1a)

$$\rho_{fb} = 0.85\beta_1 \frac{f'_c}{f_{fu}} \frac{E_f \epsilon_{cu}}{E_f \epsilon_{cu} + f_{fu}} \quad 440.1R, \text{ Eq. (7.2.1b)}$$

$$E_f \epsilon_{cu} = (41,000)(0.003) = 123 \text{ MPa}$$

$$\rho_{fb} = 0.85(0.85) \frac{(28)}{(440)} \frac{(123)}{(123 + 440)} = 0.01004$$

$$\frac{\rho_f}{\rho_{fb}} = \frac{0.01390}{0.01004} = 1.38$$

Because $\rho_{fb} < \rho_f < 1.4\rho_{fb}$, the section is in the transition zone.

440.1R, Eq. (7.2.3)

2. Determine stress in tensile reinforcement at ultimate conditions.

$$f_f = \sqrt{\frac{(E_f \epsilon_{cu})^2}{4} + \frac{0.85\beta_1 f'_c}{\rho_f} E_f \epsilon_{cu} - 0.5E_f \epsilon_{cu}} \leq f_{fu} \quad 440.1R, \text{ Eq. (7.2.2d)}$$

$$f_f = \sqrt{\frac{(123)^2}{4} + \frac{0.85(0.85)(28)}{(0.01390)}(123) - 0.5(123)} \leq 440$$

$$f_f = 366 \text{ MPa}$$

3. Determine development length.

$$\ell_d = \frac{\alpha \frac{f_{fr}}{0.083\sqrt{f'_c}} - 340}{13.6 + \frac{C}{d_b}} d_b \quad 440.1R, \text{ Eq. (10.3a)}$$

The bar stress that needs to be developed is the stress at the ultimate condition. There is no need to develop the full strength of the bar in this case.

$$f_{fr} = f_f = 366 \text{ MPa}$$

440.1R, Sec. 10.3

Bar location modification factor should be taken as $\alpha = 1.5$ because more than 300 mm of concrete is cast below the reinforcement.

ACI 440.1R, Sec. 10.1.1

Center-to-center spacing of bars being developed = 200 mm

$$C = \min\left(d_c, \frac{\text{ctr-to-ctr spacing}}{2}\right) \leq 3.5d_b \quad 440.1R, \text{ Sec. 10.1}$$

$$C = \min\left(20 + \frac{25.4}{2}, \frac{200}{2}\right) \leq 3.5(25.4) = \min(33, 100) \leq 89$$

$$C = 33 \text{ mm}$$

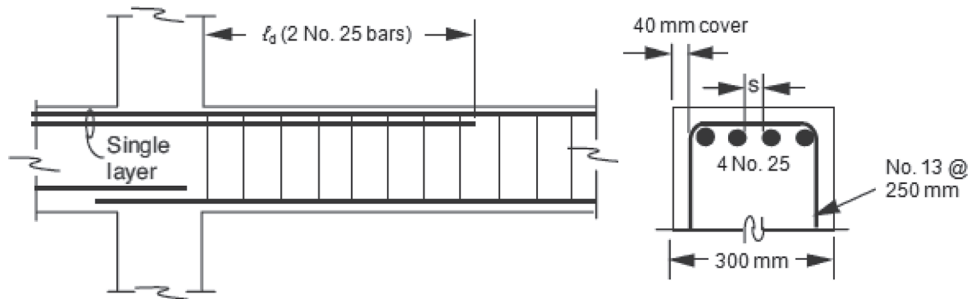
$$\ell_d = \frac{\alpha \frac{f_{fr}}{0.083\sqrt{f'_c}} - 340}{13.6 + \frac{C}{d_b}} d_b = \frac{(1.5) \frac{(366)}{0.083\sqrt{28}} - 340}{13.6 + \frac{33}{25.4}} (25.4) = 1550 \text{ mm}$$

The required development length is 1550 mm.

Example 10M—Development of bars in tension (tension-controlled section)

This example is similar to Example 4.3 of PCA Notes on ACI 318-08.

Calculate the length required to develop the inner two No. 25 glass FRP (GFRP) bars at the column face in the following figure. The two No. 25 outer bars are to be made continuous along full length of beam. Use $f'_c = 28$ MPa (normalweight concrete), $f_{fu}^* = 550$ MPa, and $E_f = 41,000$ MPa. Assume $d = 700$ mm. Assume interior exposure conditions.



Calculations and discussion

No. 25 bar properties:

$$d_b = 25.4 \text{ mm}$$

$$A_{f,bar} = 510 \text{ mm}^2$$

Design material properties:

$$C_E = 0.8$$

$$f_{fu} = C_E f_{fu}^* = (0.8)(550) = 440 \text{ MPa}$$

1. Determine the type of section.

$$A_f = (4)(510 \text{ mm}^2) = 2040 \text{ mm}^2$$

$$\rho_f = \frac{A_f}{bd} = \frac{2010}{(300)(700)} = 0.00957$$

$$\rho_{fb} = 0.85\beta_1 \frac{f'_c}{f_{fu}} \frac{E_f \epsilon_{cu}}{E_f \epsilon_{cu} + f_{fu}}$$

$$E_f \epsilon_{cu} = (41,000)(0.003) = 123 \text{ MPa}$$

$$\rho_{fb} = 0.85(0.85) \frac{(28)}{(440)} \frac{(123)}{(123 + 440)} = 0.01004$$

$$\frac{\rho_f}{\rho_{fb}} = \frac{0.00957}{0.01004} = 0.95$$

Because $\rho_f \leq \rho_{fb}$, the section is tension-controlled.

2. Determine stress in tensile reinforcement at ultimate conditions.

Because section is tension-controlled, $f_f = f_{fu} = 440$ MPa

3. Determine development length.

$$l_d = \frac{\alpha \frac{f_{fr}}{0.083\sqrt{f'_c}} - 340}{13.6 + \frac{C}{d_b}} d_b$$

$$f_{fr} = f_f = 440 \text{ MPa}$$

Bar location modification factor should be taken as $\alpha = 1.5$ because more than 300 mm of concrete is cast below the reinforcement.

$$\text{Clear spacing of bars being developed} = [300 - 2(40) - 2(12.7) - 4(25.4)]/3 = 31 \text{ mm}$$

Reference

440.6-08, Table 7.1

440.1R, Table 6.2

440.1R, Eq. (6.2a)

440.1R, Eq. (7.2.1a)

440.1R, Eq. (7.2.1b)

440.1R, Eq. (7.2.3)

440.1R, Eq. (10.3a)

440.1R, Sec. 10.3

ACI 440.1R, Sec. 10.1.1

$$C = \min\left(d_c, \frac{\text{ctr-to-ctr spacing}}{2}\right) \leq 3.5d_b \quad 440.1R, \text{ Sec. 10.1}$$

$$= \min\left(40 + 12.7 + \frac{25.4}{2}, \frac{12.7 + 31 + 12.7}{2}\right) \leq 3.5(25.4) = \min(65, 28) \leq 89$$

$$C = 28 \text{ mm}$$

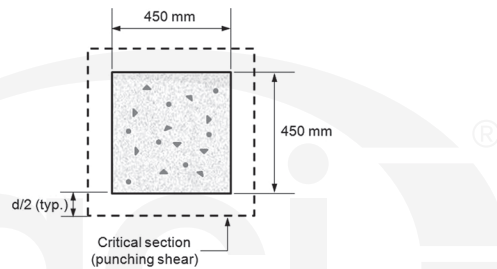
$$\ell_d = \frac{\alpha \frac{f_{fr}}{0.083\sqrt{f'_c}} - 340}{13.6 + \frac{C}{d_b}} d_b = \frac{(1.5) \frac{(440)}{0.083\sqrt{28}} - 340}{13.6 + \frac{28}{25.4}} (25.4) = 2010 \text{ mm}$$

The required development length is 2010 mm.

Example 11M—Shear strength of slab at column support

This example is similar to Example 16.1 of PCA Notes on ACI 318-08.

Determine two-way action shear strength at an interior column support of a flat plate slab system for the following design conditions.



Column dimensions = 450 mm x 450 mm

Slab effective depth $d = 165$ mm

Specified concrete strength $f'_c = 28$ MPa (normalweight concrete)

$E_f = 40,000$ MPa

$\rho_f = 0.0120$ (flexural reinforcement in column strips in both directions, top mat of reinforcement)

Calculations and discussion

1. Two-way action shear (punching shear) without shear reinforcement:

$$V_u \leq \phi V_n$$

$$V_u \leq \phi V_c \quad (V_f = 0)$$

440.1R, Sec. 8.1

440.1R, Sec. 8.2

2. Determine shear strength provided by concrete.

$$\phi V_c = \phi \left(\frac{k}{5}\right) 4\sqrt{f'_c} b_o d \quad 440.1R, \text{ Eq. (8.4b)}$$

$$E_c = 4700\sqrt{f'_c} = 4700\sqrt{28} = 24,900 \text{ MPa} \quad 318-11, \text{ Sec. 8.5.1}$$

$$\rho_f n_f = \rho_f \frac{E_f}{E_c} = (0.0120) \left(\frac{40,000}{24,900}\right) = (0.0120)(1.606) = 0.01927$$

$$k = \sqrt{2\rho_f n_f + (\rho_f n_f)^2} - \rho_f n_f = \sqrt{2(0.01927) + (0.01927)^2} - 0.01927 = 0.178 \quad 440.1R, \text{ Eq. (7.3.2.2b)}$$

$$b_o = 4(450 + 82.5 + 82.5) = 2460 \text{ mm} \quad 440.1R, \text{ Sec. 8.4}$$

$$\phi V_c = (0.75) \left(\frac{0.178}{5}\right) 4\sqrt{28} (2460) (165) \left(\frac{1}{1000}\right) = 229 \text{ kN}$$

Reference

CHAPTER 12—REFERENCES

ACI committee documents and documents published by other organizations are listed first by document number, full title, and year of publication followed by authored documents listed alphabetically.

American Concrete Institute

216.1-07/TMS-0216-07—Code Requirements for Determining Fire Resistance of Concrete and Masonry Construction Assemblies

318-71—Building Code Requirements for Reinforced Concrete and Commentary

318-99—Building Code Requirements for Structural Concrete and Commentary

318-08—Building Code Requirements for Structural Concrete and Commentary

318-11—Building Code Requirements for Structural Concrete and Commentary

360R-10—Guide to Design of Slabs-on-Ground

435R-95(00)—Control of Deflection in Concrete Structures (Appendix B added 2003)

440R-07—Report on Fiber-Reinforced Polymer (FRP) Reinforcement for Concrete Structures

440.3R-04—Guide Test Methods for Fiber-Reinforced Polymers (FRPs) for Reinforcing or Strengthening Concrete Structures

440.4R-04(11)—Prestressing Concrete Structures with FRP Tendons (Reapproved 2011)

440.5-08—Specification for Construction with Fiber-Reinforced Polymer Reinforcing Bars

440.6-08—Specification for Carbon and Glass Fiber-Reinforced Polymer Bar Materials for Concrete Reinforcement

ASTM International

ASTM D7205/D7205M-06(2011)—Standard Test Method for Tensile Properties of Fiber Reinforced Polymer Matrix Composite Bars

ASTM D7337/D733M-12—Standard Test Method for Tensile Creep Rupture of Fiber Reinforced Polymer Matrix Composite Bars

ASTM D7617/D7617M-11—Standard Test Method for Transverse Shear Strength of Fiber-reinforced Polymer Matrix Composite Bars

ASTM D7705/D7705M-12—Standard Test Method for Alkali Resistance of Fiber Reinforced Polymer (FRP) Matrix Composite Bars used in Concrete Construction

ASTM E119-12a—Standard Test Methods for Fire Tests of Building Construction and Materials.

Canadian Standards Association

CAN/CSA-S6-06—Canadian Highway Bridge Design Code

CAN/CSA S6S1-10—Canadian Highway Bridge Design Code

CAN/CSA-S806-12—Design and Construction of Building Components with Fibre-Reinforced Polymers

Canadian Standards Association/Underwriters Laboratory Canada

CAN/ULC-S101-M89—Standard Methods of Fire Endurance Tests of Building Construction and Materials

International Organization for Standardization

ISO 834-1:1999—Fire-Resistance Tests – Elements of Building Construction – Part 1: General Requirements

Authored documents

Adimi, R.; Rahman, H.; Benmokrane, B.; and Kobayashi, K., 1998, “Effect of Temperature and Loading Frequency on the Fatigue Life of a CFRP Bar in Concrete,” *Proceedings of the Second International Conference on Composites in Infrastructure (ICCI-98)*, Tucson, AZ, V. 2, pp. 203-210.

Afifi, M. Z.; Mohamed, H. M.; and Benmokrane, B., 2013, “Axial Capacity of Circular Concrete Columns Reinforced with Glass-FRP Bars and Spirals,” *11th International Conference on Fibre Reinforced Polymer (FRP) Reinforcement for Concrete Structures (FRPRCS-11)*, Porto, Portugal, June 26-28, 10 pp.

Ahmed, E. A.; El-Salakawy, E. F.; and Benmokrane, B., 2010a, “Shear Performance of RC Bridge Girders Reinforced with Carbon FRP Stirrups,” *Journal of Bridge Engineering*, V. 15, No. 1, pp. 44-54. doi: 10.1061/(ASCE)BE.1943-5592.0000035

Ahmed, E. A.; El-Salakawy, E. F.; and Benmokrane, B., 2010b, “Performance Evaluation of GFRP Shear Reinforcement for Concrete Beams,” *ACI Structural Journal*, V. 107, No. 1, Jan.-Feb., pp. 53-62.

Ahmad, S. H.; Zia, P.; Yu, T.; and Xie, Y., 1993, “Punching Shear Tests of Slabs Reinforced with 3-D Carbon Fiber Fabric,” *Concrete International*, V. 16, No. 6, June, pp. 36-41.

Al-Dulaijan, S. U.; Nanni, A.; Al-Zahrani, M. M.; and Bakis, C. E., 1996, “Bond Evaluation of Environmentally Conditioned GFRP/Concrete System,” *Proceedings of the Second International Conference on Advanced Composite Materials in Bridges and Structures (ACMBS-2)*, M. M. El-Badry, ed., Canadian Society for Civil Engineering, Montreal, QC, Canada, pp. 845-852.

Almusallam, T. H.; Al-Salloum, Y.; Alsayed, S.; and Amjad, M., 1997, “Behavior of Concrete Beams Doubly Reinforced by FRP Bars,” *Proceedings of the Third International Symposium on Non-Metallic (FRP) Reinforcement for Concrete Structures (FRPRCS-3)*, Japan Concrete Institute, Tokyo, Japan, V. 2, pp. 471-478.

Al-Zahrani, M. M.; Nanni, A.; Al-Dulaijan, S. U.; and Bakis, C. E., 1996, “Bond of FRP to Concrete for Rods with Axisymmetric Deformations,” *Proceedings of the Second International Conference on Advanced Composite Materials in Bridges and Structures (ACMBS-II)*, Montreal, QC, Canada, pp. 853-860.

Ando, N.; Matsukawa, H.; Hattori, A.; and Mashima, A., 1997, “Experimental Studies on the Long-Term Tensile Properties of FRP Tendons,” *Proceedings of the Third International Symposium on Non-Metallic (FRP) Reinforcement for Concrete Structures (FRPRCS-3)*, V. 2, Japan Concrete Institute, Tokyo, Japan, pp. 203-210.

Arockiasamy, M.; Amer, A.; and Shahawy, M., 1998, “Environmental and Long-Term Studies on CFRP Cables

and CFRP Reinforced Concrete Beams,” *Proceedings of the First International Conference on Durability of Composites for Construction*, B. Benmokrane and H. Rahman, eds., Sherbrooke, QC, Canada, pp. 599-610.

Bakis, C. E., 1993, “FRP Composites: Materials and Manufacturing,” *Fiber-Reinforced-Plastic for Concrete Structures: Properties and Applications*, A. Nanni, ed., Elsevier, Amsterdam, pp. 13-58.

Bakis, C. E., and Boothby, T. E., 2004, “Evaluation of Crack Width and Bond Strength in GFRP Reinforced Beams Subjected to Sustained Loads,” *Proceedings of the 4th International Conference on Advanced Composite Materials in Bridges and Structures—ACMBS-IV*, M. El-Badry and L. Dunaszegi, eds. (CD-ROM)

Bakis, C. E.; Freimanis, A. J.; Gremel, D.; and Nanni, A., 1998, “Effect of Resin Material on Bond and Tensile Properties of Unconditioned and Conditioned FRP Reinforcement Rods,” *Proceedings of the First International Conference on Durability of Composites for Construction*, B. Benmokrane and H. Rahman, eds., Sherbrooke, QC, Canada, pp. 525-535.

Bakis, C.; Ospina, C.; Bradberry, T.; Benmokrane, B.; Gross, S.; Newhook, J.; and Thiagarajan, G., 2006, “Evaluation of Crack Widths in Concrete Flexural Members Reinforced with FRP Bars,” *Proceedings of the 3rd International Conference on FRP Composites in Civil Engineering*, A. Mirmiran and A. Nanni, eds., Florida International University, Miami, FL, pp. 307-310.

Bank, L. C., 1993, “Properties of FRP Reinforcement for Concrete,” *Fiber-Reinforced-Plastic (FRP) Reinforcement for Concrete Structures: Properties and Applications, Developments in Civil Engineering*, V. 42, A. Nanni, ed., Elsevier, Amsterdam, pp. 59-86.

Bank, L. C., and Puterman, M., 1997, “Microscopic Study of Surface Degradation of Glass Fiber-Reinforced Polymer Rods Embedded in Concrete Castings Subjected to Environmental Conditioning,” *High Temperature and Environmental Effects on Polymeric Composites*, V. 2, ASTM STP 1302, T. S. Gates and A.-H. Zureick, eds., ASTM International, West Conshohocken, PA, pp. 191-205.

Bank, L. C.; Puterman, M.; and Katz, A., 1998, “The Effect of Material Degradation on Bond Properties of FRP Reinforcing Bars in Concrete,” *ACI Materials Journal*, V. 95, No. 3, May-June, pp. 232-243.

Bank, L. C., and Xi, Z., 1995, “Punching Shear Behavior of Pultruded FRP Grating Reinforced Concrete Slabs,” *Proceedings of the 2nd International Symposium on Non-Metallic (FRP) Reinforcement for Concrete Structures*, Ghent, Belgium, pp. 360-367.

Banthia, N.; Al-Asaly, M.; and Ma, S., 1995, “Behavior of Concrete Slabs Reinforced with Fiber-Reinforced Plastic Grid,” *Journal of Materials in Civil Engineering*, V. 7, No. 4, Nov., pp. 252-257. doi: 10.1061/(ASCE)0899-1561(1995)7:4(252)

Barkatt, A.; Bank, L. C.; Prian, L.; and Gentry, T. R.; 1998, “Accelerated Test Methods to Determine the Long-Term Behavior of Composite Highway Structures Subject to Environmental Loading,” *Journal of Composites, Technology and Research*, V. 20, No. 1, Jan., pp. 38-50. doi: 10.1520/CTR10499J

Beaulieu-Michaud, M.-C. B.; Mohamed, H. M.; and Benmokrane, B., 2013, “Conception, Construction et Monitoring d’une Dalle de Grande Dimension en Béton Armé de Polymères Renforcés de Fibre (PRF),” *Proceedings of the CSCE Annual General Meeting & Conference, Montreal, Québec, Canada, May 29-June 1, 10 pp.*

Belarbi, A., and Wang, H., 2012, “Durability of FRP Bars Embedded in Fiber-Reinforced-Concrete,” *Journal of Composites for Construction*, V. 16, No. 4, pp. 371-380. doi: 10.1061/(ASCE)CC.1943-5614.0000270

Bellakehal, H.; Zaidi, A.; Masmoudi, R.; and Bouhicha, M., 2013, “Combined Effect of Sustained Load and Freeze-Thaw Cycles on One-Way Concrete Slabs Reinforced with Glass Fibre-Reinforced Polymer,” *Canadian Journal of Civil Engineering*, V. 40, No. 11, pp. 1060-1067. doi: 10.1139/cjce-2012-0514

Benmokrane, B., 1997, “Bond Strength of FRP Rebar Splices,” *Proceedings of the Third International Symposium on Non-Metallic (FRP) Reinforcement for Concrete Structures (FRPRCS-3)*, V. 2, Japan Concrete Institute, Tokyo, Japan, pp. 405-412.

Benmokrane, B.; Ahmed, E.; Dulude, C.; and Boucher, E., 2012, “Design, Construction, and Monitoring of the First Worldwide Two Way Flat Slab Parking Garage Reinforced with GFRP Bars,” *Sixth International Conference on FRP Composites in Civil Engineering*, Rome, Italy, June 13-15, 8 pp.

Benmokrane, B.; Chaallal, O.; and Masmoudi, R., 1996, “Flexural Response of Concrete Beams Reinforced with FRP Reinforcing Bars,” *ACI Structural Journal*, V. 93, No. 1, Jan.-Feb., pp. 46-55.

Benmokrane, B.; El-Salakawy, E.; Desgagné, G.; and Lackey, T., 2004, “FRP Bars for Bridges,” *Concrete International*, V. 26, No. 8, pp. 84-90.

Benmokrane, B.; El-Salakawy, E.; El-Gamal, S.; and Goulet, S., 2007, “Construction and Testing of an Innovative Concrete Bridge Deck Totally Reinforced with Glass FRP Bars: Val-Alain Bridge on Highway 20 East,” *Journal of Bridge Engineering*, V. 12, No. 5, Sept., pp. 632-645. doi: 10.1061/(ASCE)1084-0702(2007)12:5(632)

Benmokrane, B., and Mohamed, M. H., 2014, “Extending the Service Life of Water Treatment Structures: Glass Fiber-Reinforced Polymer Bars Used in Water Treatment Plant,” *Concrete International*, V. 36, No. 2, Feb., pp. 40-45.

Benmokrane, B., and Rahman, H., eds., 1998, “Durability of Fiber Reinforced Polymer (FRP) Composites for Construction,” *Proceedings of the First International Conference (CDCC '98)*, QC, Canada, Feb., 692 pp.

Bisby, L. A., and Kodur, V. K. R., 2007, “Evaluating the Fire Endurance of Concrete Slabs Reinforced with FRP Bars: Considerations for a Holistic Approach,” *Composites. Part B, Engineering*, V. 38, No. 5-6, pp. 547-558. doi: 10.1016/j.compositesb.2006.07.013

Bisby, L. A.; Green, M. F.; and Kodur, V. K. R., 2005, “Response to Fire of Concrete Structures that Incorporate FRP,” *Progress in Structural Engineering and Materials*, V. 7, No. 3, pp. 136-149. doi: 10.1002/pse.198

Bischoff, P., 2005, "Reevaluation of Deflection Prediction for Concrete Beams Reinforced with Steel and Fiber-Reinforced Polymer Bars," *Journal of Structural Engineering*, V. 131, No. 5, May, pp. 752-767. doi: 10.1061/(ASCE)0733-9445(2005)131:5(752)

Bischoff, P. H., and Gross, S. P., 2011, "Equivalent Moment of Inertia Based on Integration of Curvature," *Journal of Composites for Construction*, V. 15, No. 3, pp. 263-273. doi: 10.1061/(ASCE)CC.1943-5614.0000164

Bischoff, P. H.; Gross, S. P.; and Ospina, C. E., 2009, "The Story Behind the Proposed ACI 440 Changes for Prediction of Deflections in Reinforced Concrete," *Serviceability of Concrete Members Reinforced with Internal/External FRP Reinforcement*, ACI SP-264, T. Alkhardji, P. H. Bischoff, and C. E. Ospina, eds., American Concrete Institute, Farmington Hills, MI, pp. 53-76.

Bischoff, P. H., and Scanlon, A., 2007, "Effective Moment of Inertia for Calculating Deflections of Concrete Members Containing Steel Reinforcement and Fiber-Reinforced Polymer Reinforcement," *ACI Structural Journal*, V. 104, No. 1, pp. 68-75.

Boyle, H. C., and Karbhari, V. M., 1994, "Investigation of Bond Behavior between Glass Fiber Composite Reinforcements and Concrete," *Journal of Polymer-Plastic Technology Engineering*, V. 33, No. 6, pp. 733-753. doi: 10.1080/03602559408013105

Branson, D. E., 1965, "Instantaneous and Time-Dependent Deflections of Simple and Continuous Reinforced Concrete Beams," *HPR Report No. 7*, Alabama Highway Department, Bureau of Public Roads, Montgomery, AL, Part 1, 78 pp.

Brown, V., 1997, "Sustained Load Deflections in GFRP-Reinforced Concrete Beams," *Proceedings of the Third International Symposium on Non-Metallic (FRP) Reinforcement for Concrete Structures (FRPRCS-3)*, V. 2, Japan Concrete Institute, Tokyo, Japan, pp. 495-502.

Brown, V., and Bartholomew, C., 1996, "Long-Term Deflections of GFRP-Reinforced Concrete Beams," *Proceedings of the First International Conference on Composites in Infrastructure (ICCI-96)*, H. Saadatmanesh and M. R. Ehsani, eds., Tucson, AZ, pp. 389-400.

Burgoyne, C., ed., 2001, "Non-Metallic Reinforcement for Concrete Structures—FRPRCS-5," *Proceedings*, International Conference, Cambridge, UK.

Clarke, J., and Sheard, P., 1998, "Designing Durable FRP Reinforced Concrete Structures," *Proceedings of the First International Conference on Durability of Composites for Construction*, B. Benmokrane and H. Rahman, eds., Sherbrooke, QC, Canada, pp. 13-24.

Chen, Y.; Davalos, J. F.; Ray, I.; and Kim, H.-Y., 2007, "Accelerated Aging Tests for Evaluations of Durability Performance of FRP Reinforcing Bars for Concrete Structures," *Composite Structures*, V. 78, No. 1, Mar., pp. 101-111. doi: 10.1016/j.compstruct.2005.08.015

Chowdhury, E. U.; Eedson, R.; Bisby, L. A.; Green, M. F.; Bénichou, N.; and Kodur, V. K. R., 2011, "Mechanical Characterization of FRP Materials at High Temperature," *Fire Technology*, V. 45, No. 4, pp. 1-18.

Conrad, J. O.; Bakis, C. E.; Boothby, T. E.; and Nanni, A., 1998, "Durability of Bond of Various FRP Rods in Concrete," *Proceedings of the First International Conference on Durability of Composites for Construction*, B. Benmokrane and H. Rahman, eds., Sherbrooke, QC, Canada, pp. 299-310.

Coomarasamy, A., and Goodman, S., 1997, "Investigation of the Durability Characteristics of Fiber Reinforced Polymer (FRP) Materials in Concrete Environment," *American Society for Composites—Twelfth Technical Conference*, Dearborn, MI.

Cosenza, E.; Manfredi, G.; and Nanni, A., eds., 2001, "Composites in Construction: A Reality," *Proceedings, International Workshop*, Capri, Italy, ASCE, Reston, VA, 277 pp.

Curtis, P. T., 1989, "The Fatigue Behavior of Fibrous Composite Materials," *Journal of Strain Analysis*, V. 24, No. 4, pp. 235-244. doi: 10.1243/03093247V244235

Dally, J. W., and Riley, W. F., 1991, *Experimental Stress Analysis*, third edition, McGraw Hill, New York, 672 pp.

Daniali, S., 1992, "Development Length for Fiber-Reinforced Plastic Bars," *Advanced Composite Materials in Bridges and Structures*, K. W. Neale and P. Labossiere, eds., pp. 179-188.

Darwin, D.; Zuo, J.; Tholen, M.; and Idun, E., 1996, "Development Length Criteria for Conventional and High Relative Rib Area Reinforcing Bars," *ACI Structural Journal*, V. 93, No. 3, May-June, pp. 347-359.

De Luca, A.; Matta, F.; and Nanni, A., 2010, "Behavior of Full-Scale Glass Fiber-Reinforced Polymer Reinforced Concrete Columns under Axial Load," *ACI Structural Journal*, V. 107, No. 5, Sept-Oct., pp. 589-596.

DeSimone, M. V., 2009, "Deflections of Continuous GFRP-Reinforced Concrete Beams," MSCE thesis, Department of Civil and Environmental Engineering, Villanova University, Villanova, PA.

Deutsches Institut für Normung e.V., 2012, "German Standards for Testing of Hardened Concrete, Part 1—Impermeability to Water," DIN 1048, pp. 9-10.

Devalapura, R. K.; Greenwood, M. E.; Gauchel, J. V.; and Humphrey, T. J., 1996, *Advanced Composite Materials in Bridges and Structures*, M. M. El-Badry, ed., Canadian Society for Civil Engineering, Montreal, QC, Canada, pp. 107-116.

Dolan, C. W.; Rizkalla, S.; and Nanni, A., eds., 1999, *Fourth International Symposium on Fiber Reinforced Polymer Reinforcement for Reinforced Concrete Structures*, SP-188, C. W. Dolan, S. H. Rizkalla, and A. Nanni, eds., American Concrete Institute, Farmington Hills, MI, 1182 pp.

Dowden, D. M., and Dolan, C. W., 1997, "Comparison of Experimental Shear Data with Code Predictions for FRP Prestressed Beams," *Proceedings of the Third International Symposium on Non-Metallic (FRP) Reinforcement for Concrete Structures (FRPRCS-3)*, V. 2, Japan Concrete Institute, Tokyo, Japan, pp. 687-694.

Drouin, B.; Latour, G.; and Mohamed, H., 2011, "More than 10 Years Successful Field Applications of FRP Bars in Canada," *CDCC 2011, The Fourth International Conference on Durability & Sustainability of Fiber Reinforced Polymer*

(FRP) Composites for Construction and Rehabilitation, Quebec City, QC, Canada, July, 6 pp.

Dulude, C.; Hassan, M.; Ahmed, E. A.; and Benmokrane, B., 2013, "Punching Shear Behavior of Two-Way Flat Concrete Slabs Reinforced with GFRP Bars," *ACI Structural Journal*, V. 110, No. 5, Sept.-Oct., pp. 723-734.

Ehsani, M. R., 1993, "Glass-Fiber Reinforcing Bars," *Alternative Materials for the Reinforcement and Prestressing of Concrete*, J. L. Clarke, Blackie Academic & Professional, London, UK, pp. 35-54.

Ehsani, M. R.; Saadatmanesh, H.; and Tao, S., 1995, "Bond of Hooked Glass Fiber Reinforced Plastic (GFRP) Reinforcing Bars to Concrete," *ACI Materials Journal*, V. 92, No. 4, July-Aug., pp. 391-400.

Ehsani, M. R.; Saadatmanesh, H.; and Tao, S., 1996a, "Design Recommendation for Bond of GFRP Rebars to Concrete," *Journal of Structural Engineering*, V. 122, No. 3, pp. 247-254. doi: 10.1061/(ASCE)0733-9445(1996)122:3(247)

Ehsani, M. R.; Saadatmanesh, H.; and Tao, S., 1996b, "Bond Behavior and Design Recommendations for Fiber-Glass Reinforcing Bars," *Proceedings of the First International Conference on Composites in Infrastructure (ICCI-96)*, H. Saadatmanesh and M. R. Ehsani, eds., Tucson, AZ, pp. 466-476.

El-Badry, M., ed., 1996, "Advanced Composite Materials in Bridges and Structures (ACMBS-II)," *Proceedings of the Second International Conference*, Montreal, QC, Canada, 1027 pp.

El-Ghandour, A. W.; Pilakoutas, K.; and Waldron, P., 2003, "Punching Shear Behavior of Fiber Reinforced Polymers Reinforced Concrete Flat Slabs: Experimental Study," *Journal of Composites for Construction*, V. 7, No. 3, pp. 258-265. doi: 10.1061/(ASCE)1090-0268(2003)7:3(258)

El-Salakawy, E. F., and Benmokrane, B., 2003, "Design and Testing of a Highway Concrete Bridge Deck Reinforced with Glass and Carbon FRP Bars," *ACI Special Publication, Field Applications of FRP Reinforcement: Case Studies, SP-215-2*, Aug., pp. 37-54.

El-Salakawy, E. F.; Benmokrane, B.; and Desgagné, G., 2003, "Fibre-Reinforced Polymer Composite Bars for the Concrete Deck Slab of Wotton Bridge," *Canadian Journal of Civil Engineering*, V. 30, No. 5, pp. 861-870. doi: 10.1139/103-055

El-Salakawy, E. F.; Benmokrane, B.; El-Ragaby, A.; and Nadeau, D., 2005, "Field Investigation on the First Bridge Deck Slab Reinforced with Glass FRP Bars Constructed in Canada," *Journal of Composites for Construction*, V. 9, No. 6, Dec., pp. 470-479. doi: 10.1061/(ASCE)1090-0268(2005)9:6(470)

Faza, S. S., and GangaRao, H. V. S., 1990, "Bending and Bond Behavior of Concrete Beams Reinforced with Plastic Rebars," *Transportation Research Record*, V. 1290, pp. 185-193.

Faza, S. S., and GangaRao, H. V. S., 1992, "Pre- and Post-Cracking Deflection Behaviour of Concrete Beams Reinforced with Fibre-Reinforced Plastic Rebars," *Advanced Composite Materials in Bridges and Structures*, K. W. Neale

and P. Labossiere, eds., Canadian Society for Civil Engineering, Montreal, QC, Canada, pp. 151-160.

Faza, S. S., and GangaRao, H. V. S., 1993a, "Theoretical and Experimental Correlation of Behavior of Concrete Beams Reinforced with Fiber Reinforced Plastic Rebars," *Fiber-Reinforced-Plastic Reinforcement for Concrete Structures—International Symposium*, SP-138, A. Nanni and C. W. Dolan, eds., American Concrete Institute, Farmington Hills, MI, pp. 599-614.

Faza, S. S., and GangaRao, H. V. S., 1993b, "Glass FRP Reinforcing Bars for Concrete," *Fiber-Reinforced-Plastic (FRP) Reinforcement for Concrete Structures: Properties and Applications, Developments in Civil Engineering*, V. 42, A. Nanni, ed., Elsevier, Amsterdam, pp. 167-188.

fib, 2007, "FRP Reinforcement in RC Structures," *Bulletin No. 40*, Federal Institute of Technology, Lausanne, Switzerland.

fib, 2010, *Model Code for Concrete Structures (MC2010)*, Ernst and Son, Federal Institute of Technology, Lausanne, Switzerland.

Figueiras, J.; Juvandes, L.; and Furia, R., eds., 2001, "Composites in Construction," *Proceedings of the International Conference Composites in Construction—CCC2001*, Portugal.

Freimanis, A. J.; Bakis, C. E.; Nanni, A.; and Gremel, D., 1998, "A Comparison of Pullout and Tensile Behaviors of FRP Reinforcement for Concrete," *Proceedings of the Second International Conference on Composites in Infrastructure (ICCI-98)*, V. 2, Tucson, AZ, pp. 52-65.

Frosch, R. J., 1999, "Another Look at Cracking and Crack Control in Reinforced Concrete," *ACI Structural Journal*, V. 96, No. 3, May-June, pp. 437-442.

GangaRao, H. V. S., and Vijay, P. V., 1997a, "Design of Concrete Members Reinforced with GFRP Bars," *Proceedings of the Third International Symposium on Non-Metallic (FRP) Reinforcement for Concrete Structures (FRPRCS-3)*, V. 1, Japan Concrete Institute, Tokyo, Japan, pp. 143-150.

GangaRao, H. V. S., and Vijay, P. V., 1997b, "Aging of Structural Composites under Varying Environmental Conditions," *Proceedings of the Third International Symposium on Non-Metallic (FRP) Reinforcement for Concrete Structures (FRPRCS-3)*, V. 2, Japan Concrete Institute, Tokyo, Japan, pp. 91-98.

Gao, D.; Benmokrane, B.; and Masmoudi, R., 1998a, "A Calculating Method of Flexural Properties of FRP-Reinforced Concrete Beam: Part 1: Crack Width and Deflection," *Technical Report*, Department of Civil Engineering, University of Sherbrooke, Sherbrooke, QC, Canada, 24 pp.

Gao, D.; Benmokrane, B.; and Tighiouart, B., 1998b, "Bond Properties of FRP Rebars to Concrete," *Technical Report*, Department of Civil Engineering, University of Sherbrooke, Sherbrooke, QC, Canada, 27 pp.

Gentry, T. R., and Husain, M., 1999, "Thermal Compatibility of Concrete and Composite Reinforcements," *Journal of Composites for Construction*, V. 3, No. 2, pp. 82-86. doi: 10.1061/(ASCE)1090-0268(1999)3:2(82)

Gergely, P., and Lutz, L. A., 1968, "Maximum Crack Width in Reinforced Concrete Flexural Members," *Causes*,

Mechanism, and Control of Cracking in Concrete, SP-20, American Concrete Institute, Farmington Hills, MI, pp. 87-117.

Gerritse, A., 1992, "Durability Criteria for Non-Metallic Tendons in an Alkaline Environment," *Proceedings of the First International Conference on Advance Composite Materials in Bridges and Structures (ACMBS-I)*, Canadian Society of Civil Engineers, Sherbrooke, QC, Canada, pp. 129-137.

Gremel, D., 2012, "Ensuring Electrical Isolation in Elevate Rail," *Concrete International*, V. 34, No. 2, Feb., pp. 22-25.

Gross, S.; Yost, J.; and Kevgas, G., 2003, "Time-Dependent Behavior of Normal and High Strength Concrete Beams Reinforced with GFRP Bars Under Sustained Loads," *High Performance Materials in Bridges*, ASCE, Reston, VA, pp. 451-462.

Hassan, M.; Ahmed, E. A.; and Benmokrane, B., 2013a, "Punching-Shear Strength of Normal- and High-Strength Concrete Flat Slabs Reinforced with GFRP Bars," *Journal of Composites for Construction*, V. 17, No. 6, Sept., 12 pp.

Hassan, M.; Ahmed, E. A.; and Benmokrane, B., 2013b, "Punching Shear Strength of Glass Fiber-Reinforced Polymer Reinforced Concrete Flat Slabs," *Canadian Journal of Civil Engineering*, V. 40, No. 10, pp. 951-960. doi: 10.1139/cjce-2012-0177

Hayes, M. D.; Garcia, K.; Verghese, N.; and Lesko, J., 1998, "The Effect of Moisture on the Fatigue Behavior of a Glass/Vinyl Ester Composite," *Proceedings of the Second International Conference on Composites in Infrastructure (ICCI-98)*, V. 1, Tucson, AZ, pp. 1-12.

Hughes, B. W., and Porter, M. L., 1996, "Experimental Evaluation of Non-Metallic Dowel Bars in Highway Pavements," *Proceedings of the First International Conference on Composites in Infrastructure (ICCI-96)*, H. Saadatmanesh and M. R. Ehsani, eds., Tucson, AZ, pp. 440-450.

Humar, J., and Razaqpur, A. G., eds., 2000, "Advanced Composite Materials in Bridges and Structures," *Proceedings of the third International Conference*, Ottawa, ON, Canada.

Iyer, S. L., and Sen, R., eds., 1991, "Advanced Composite Materials in Civil Engineering Structures," *Proceedings of the Specialty Conference*, ASCE, Reston, VA, 443 pp.

Jaeger, L. G.; Mufti, A.; and Tadros, G., 1997, "The Concept of the Overall Performance Factor in Rectangular-Section Reinforced Concrete Beams," *Proceedings of the Third International Symposium on Non-Metallic (FRP) Reinforcement for Concrete Structures (FRPRCS-3)*, V. 2, Japan Concrete Institute, Tokyo, Japan, pp. 551-558.

Japan Society of Civil Engineers, 1997a, *Proceedings of the Third International Symposium on Non-Metallic (FRP) Reinforcement for Concrete Structures (FRPRCS-3)*, V. 2, Japan Concrete Institute, Tokyo, Japan, pp. 511-518.

Japan Society of Civil Engineers, 1997b, "Recommendation for Design and Construction of Concrete Structures Using Continuous Fiber Reinforcing Materials," *Concrete Engineering Series* No. 23, 325 pp.

Japan Society of Civil Engineers Subcommittee on Continuous Fiber Reinforcement, 1992, *Proceedings of the Utilization of FRP-Rods for Concrete Reinforcement*, Japan Society of Civil Engineers, Tokyo, Japan, 314 pp.

Joint ACI-ASCE Committee 426, 1973, "The Shear Strength of Reinforced Concrete Members," *Journal of the Structural Division*, V. 99, No. 6, pp. 1091-1197.

Kamal, A., and Boulfiza, M., 2011, "Durability of GFRP Rebars in Simulated Concrete Solutions under Accelerated Aging Conditions," *Journal of Composites for Construction*, V. 15, No. 4, pp. 473-481. doi: 10.1061/(ASCE)CC.1943-5614.0000168

Katz, A., 1998, "Effect of Helical Wrapping on Fatigue Resistance of GFRP," *Journal of Composites for Construction*, V. 2, No. 3, pp. 121-125. doi: 10.1061/(ASCE)1090-0268(1998)2:3(121)

Katz, A., 2000, "Bond to Concrete of FRP Rebars after Cyclic Loading," *Journal of Composites for Construction*, V. 4, No. 3, pp. 137-144. doi: 10.1061/(ASCE)1090-0268(2000)4:3(137)

Katz, A., 2004, "Environmental Impact of Steel and Fiber-Reinforced Polymer Reinforced Pavements," *Journal of Composites for Construction*, V. 8, No. 6, pp. 481-488. doi: 10.1061/(ASCE)1090-0268(2004)8:6(481)

Katz, A.; Berman, N.; and Bank, L. C., 1999, "Effect of High Temperature on the Bond Strength of FRP Rebars," *Journal of Composites for Construction*, V. 3, No. 2, pp. 73-81. doi: 10.1061/(ASCE)1090-0268(1999)3:2(73)

Kobayashi, K., and Fujisaki, T., 1995, "Compressive Behavior of FRP Reinforcement in Non-Prestressed Concrete Members," *Proceedings of the Second International RILEM Symposium on Non-Metallic (FRP) Reinforcement for Concrete Structures (FRPRCS-2)*, Ghent, Belgium, pp. 267-274.

Kocaoz, S.; Samaranyake, V. A.; and Nanni, A., 2005, "Tensile Characterization of Glass FRP Bars," *Composites. Part B, Engineering*, V. 36, No. 2, Jan., pp. 127-134. doi: 10.1016/j.compositesb.2004.05.004

Kodur, V. K. R., and Bisby, L. A., 2005, "Evaluation of Fire Endurance of Concrete Slabs Reinforced with Fiber-Reinforced Polymer Bars," *Journal of Structural Engineering*, V. 131, No. 1, Jan., pp. 34-43. doi: 10.1061/(ASCE)0733-9445(2005)131:1(34)

Lee, J. H.; Yoon, Y. S.; and Mitchell, D., 2009, "Improving Punching Shear Behavior of Glass Fiber-Reinforced Polymer Reinforced Slabs," *ACI Structural Journal*, V. 106, No. 4, July-Aug., pp. 427-434.

Litherland, K. L.; Oakley, D. R.; and Proctor, B. A., 1981, "The Use of Accelerated Aging Procedures to Predict the Long Term Strength of GRC Composites," *Cement and Concrete Research*, V. 11, No. 3, pp. 455-466. doi: 10.1016/0008-8846(81)90117-4

Liu, R., and Pantelides, C. P., 2012, "Shear Capacity of Concrete Slabs Reinforced with Glass-Fiber-Reinforced Polymer Bars using the Modified Compression Field Theory," *PCI Journal*, V. 57, No. 3, pp. 83-99. doi: 10.15554/pci.06012012.83.99

Liu, R., and Pantelides, C. P., 2013, "Shear Strength of GFRP Reinforced Precast Lightweight Concrete Panels," *Construction & Building Materials*, V. 48, No. 11, July, pp. 51-58. doi: 10.1016/j.conbuildmat.2013.06.057

Mallick, P. K., 1988, *Fiber Reinforced Composites, Materials, Manufacturing, and Design*, Marcell Dekker, Inc., New York, 469 pp.

Maluk, C.; Bisby, L. A.; Terrasi, G.; and Green, M. F., 2011, "Bond Strength of CFRP and Steel Bars in Concrete at Elevated Temperature," *Advances in Fire Design of Concrete Structures*, SP-279, American Concrete Institute, Farmington Hills, MI, pp. 1-36. doi: 10.14359/51682965

Mandell, J. F., 1982, "Fatigue Behavior of Fiber-Resin Composites," *Developments in Reinforced Plastics*, V. 2, Applied Science Publishers, London, pp. 67-107.

Mandell, J. F., and Meier, U., 1983, "Effects of Stress Ratio Frequency and Loading Time on the Tensile Fatigue of Glass-Reinforced Epoxy," *Long Term Behavior of Composites*, ASTM STP 813, ASTM International, West Conshohocken, PA, pp. 55-77.

Masmoudi, R.; Masmoudi, A.; Ouezdou, M.; and Daoud, A., 2011, "Long-Term Bond Performance of GFRP Bars in Concrete under Temperature Ranging From 20 °C to 80 °C," *Construction & Building Materials*, V. 25, No. 2, pp. 486-493. doi: 10.1016/j.conbuildmat.2009.12.040

Masmoudi, R.; Zaidi, A.; and Gérard, P., 2005, "Transverse Thermal Expansion of FRP Bars Embedded in Concrete," *Journal of Composites for Construction*, V. 9, No. 5, pp. 377-387. doi: 10.1061/(ASCE)1090-0268(2005)9:5(377)

Matthys, S., and Taerwe, L., 2000, "Concrete Slabs Reinforced with FRP Grids. II: Punching Resistance," *Journal of Composites for Construction*, V. 4, No. 3, pp. 154-161. doi: 10.1061/(ASCE)1090-0268(2000)4:3(154)

McClure, G., and Mohammadi, Y., 1995, "Compression Creep of Pultruded E-Glass-Reinforced-Plastic Angles," *Journal of Materials in Civil Engineering*, V. 7, No. 4, Nov., pp. 269-276. doi: 10.1061/(ASCE)0899-1561(1995)7:4(269)

Meier, U., 1992, "Carbon Fiber Reinforced Polymers: Modern Materials in Bridge Engineering," *Journal of the International Association for Bridge and Structural Engineering*, V. 2, No. 1, pp. 7-12. doi: 10.2749/101686692780617020

Michaluk, C. R.; Rizkalla, S.; Tadros, G.; and Benmokrane, B., 1998, "Flexural Behavior of One-Way Concrete Slabs Reinforced by Fiber Reinforced Plastic Reinforcement," *ACI Structural Journal*, V. 95, No. 3, May-June, pp. 353-364.

Mindess, S.; Young, J. F.; and Darwin, D., 2003, *Concrete*, second edition, Prentice-Hall, Upper Saddle River, NJ, 644 pp.

Mosley, C. P., 2002, "Bond Performance of Fiber Reinforced Plastic (FRP) Reinforcement in Concrete," MS thesis, Purdue University, West Lafayette, IN.

Mota, C.; Alminar, S.; and Svecova, D., 2006, "Critical Review of Deflection Formulas for FRP-RC Members," *Journal of Composites for Construction*, V. 10, No. 3, pp. 183-194. doi: 10.1061/(ASCE)1090-0268(2006)10:3(183)

Mufti, A.; Onofrei, M.; Benmokrane, B.; Banthia, N.; Boulfiza, M.; Newhook, J. P.; Bakht, B.; Tadros, G.; and Brett, P., 2007, "Field Study of Glass-Fibre-Reinforced Polymer Durability in Concrete," *Canadian Journal of Civil Engineering*, V. 34, No. 3, pp. 355-366. doi: 10.1139/106-138

Mufti, A. A.; Newhook, J.; Benmokrane, B.; Tadros, G.; and Vogel, H. M., 2011, "Durability of GFRP Rods in Field Demonstration Projects across Canada," *Proceedings of*

the 4th International Conference on Durability and Sustainability of Fibre Reinforced Polymer (FRP) Composites for Construction and Rehabilitation, CDCC2011, Quebec City, Canada, July 20-22, 9 pp.

Mutsuyoshi, H.; Uehara, K.; and Machida, A., 1990, "Mechanical Properties and Design Method of Concrete Beams Reinforced with Carbon Fiber Reinforced Plastics," *Transaction of the Japan Concrete Institute*, V. 12, Japan Concrete Institute, Tokyo, Japan, pp. 231-238.

Nagasaka, T.; Fukuyama, H.; and Tanigaki, M., 1993, "Shear Performance of Concrete Beams Reinforced with FRP Stirrups," *Fiber-Reinforced-Plastic Reinforcement for Concrete Structures—International Symposium*, SP-138, A. Nanni and C. W. Dolan, eds., American Concrete Institute, Farmington Hills, MI, pp. 789-811.

Nanni, A., ed., 1993a, "Fiber-Reinforced-Plastic (FRP) Reinforcement for Concrete Structures: Properties and Applications," *Developments in Civil Engineering*, V. 42, 450 pp.

Nanni, A., 1993b, "Flexural Behavior and Design of RC Members Using FRP Reinforcement," *Journal of Structural Engineering*, V. 119, No. 11, pp. 3344-3359. doi: 10.1061/(ASCE)0733-9445(1993)119:11(3344)

Nanni, A., 2001, "Relevant Field Applications of FRP Composites in Concrete Structures," *Proceedings of the International Conference Composites in Construction—CCC2001*, J. Figueiras, L. Juvandes, and R. Faria, eds., Portugal, pp. 661-670.

Nanni, A.; Bakis, C. E.; Al-Zahrani, M. M.; Al-Dulaijan, S. U.; and Boothby, T. E., 1998a, "Effect of Cyclic Loading on Bond Behavior of GFRP Rods Embedded in Concrete Beams," *Journal of Composites, Technology and Research*, V. 20, No. 1, pp. 29-37. doi: 10.1520/CTR10498J

Nanni, A.; Rizkalla, S.; Bakis, C. E.; Conrad, J. O.; and Abdelrahman, A. A., 1998b, "Characterization of GFRP Ribbed Rod Used for Reinforced Concrete Construction," *Proceedings of the International Composites Exhibition (ICE-98)*, Nashville, TN, pp. 16A/1-6.

Nanni, A.; Bakis, C. E.; and Boothby, T. E., 1995, "Test Methods for FRP-Concrete Systems Subjected to Mechanical Loads: State of the Art Review," *Journal of Reinforced Plastics and Composites*, V. 14, pp. 524-588.

Nanni, A., and Dolan, C. W., eds., 1993, *Fiber-Reinforced-Plastic Reinforcement for Concrete Structures—International Symposium*, SP-138, American Concrete Institute, Farmington Hills, MI, 977 pp.

Nanni, A.; Nenner, J.; Ash, K.; and Liu, J., 1997, "Experimental Bond Behavior of Hybrid Rods for Concrete Reinforcement," *Structural Engineering & Mechanics*, V. 5, No. 4, pp. 339-353. doi: 10.12989/sem.1997.5.4.339

National Research Council, 1991, "Life Prediction Methodologies for Composite Materials," Committee on Life Prediction Methodologies for Composites, NMAB-460, National Materials Advisory Board, Washington, DC, 66 pp.

Nawy, E., and Neuwerth, G., 1977, "Fiberglass Reinforced Concrete Slabs and Beams," *Journal of the Structural Division*, V. 103, No. 2, Feb., pp. 421-440.

Neale, K. W., and Labossiere, P., eds., 1992, "Advanced Composite Materials in Bridges and Structures," *Proceed-*

ings of the First International Conference (ACMBS-I), Sherbrooke, QC, Canada, 705 pp.

Nigro, E.; Bilotta, A.; Cefarelli, G.; Manfredi, G.; and Cosenza, E., 2012, "Performance under Fire Situations of Concrete Members Reinforced with FRP Rods: Bond Models and Design Nomograms," *Journal for Composites in Construction*, V. 16, No. 4, pp. 395-406.

Nigro, E.; Cefarelli, G.; Bilotta, A.; Manfredi, G.; and Cosenza, E., 2011a, "Fire Resistance of Concrete Slabs Reinforced with FRP Bars. Part I: Experimental Investigations on the Mechanical Behavior," *Composites. Part B, Engineering*, V. 42, No. 6, pp. 1739-1750. doi: 10.1016/j.compositesb.2011.02.025

Nigro, E.; Cefarelli, G.; Bilotta, A.; Manfredi, G.; and Cosenza, E., 2011b, "Fire Resistance of Concrete Slabs Reinforced with FRP Bars. Part II: Experimental Results and Numerical Simulations on the Thermal Field," *Composites. Part B, Engineering*, V. 42, No. 6, pp. 1751-1763. doi: 10.1016/j.compositesb.2011.02.026

Nigro, E.; Cefarelli, G.; Bilotta, A.; Manfredi, G.; and Cosenza, E., 2013, "Adhesion at High Temperature of FRP Bars Straight or Bent at the end of Concrete Slabs," *Journal of Structural Fire Engineering*, V. 4, No. 2, June, pp. 71-86. doi: 10.1260/2040-2317.4.2.71

Noritake, K.; Kakihara, R.; Kumagai, S.; and Mizutani, J., 1993, "Technora, an Aramid FRP Rod," *Fiber-Reinforced-Plastic (FRP) Reinforcement for Concrete Structures: Properties and Applications, Developments in Civil Engineering*, V. 42, A. Nanni, ed., Elsevier, Amsterdam, pp. 267-290.

Odagiri, T.; Matsumoto, K.; and Nakai, H., 1997, "Fatigue and Relaxation Characteristics of Continuous Aramid Fiber Reinforced Plastic Rods," *Proceedings of the Third International Symposium on Non-Metallic (FRP) Reinforcement for Concrete Structures (FRPRCS-3)*, V. 2, Japan Concrete Institute, Tokyo, Japan, pp. 227-234.

Okamoto, T.; Nagasaka, T.; and Tanigaki, M., 1994, "Shear Capacity of Concrete Beams Using FRP Reinforcement," *Journal of Structural Construction Engineering*, No. 455, pp. 127-136.

Orangun, C.; Jirsa, J. O.; and Breen, J. E., 1977, "A Reevaluation of Test Data on Development Length and Splices," *ACI Journal Proceedings*, V. 74, No. 3, Mar., pp. 114-122.

Ospina, C. E., 2005, "Alternative Model for Concentric Punching Capacity Evaluation of Reinforced Concrete Two-Way Slabs," *Concrete International*, V. 27, No. 9, Sept., pp. 53-57.

Ospina, C. E.; Alexander, S.; and Cheng, J. J., 2001, "Behaviour of Concrete Slabs with Fibre-Reinforced Polymer Reinforcement," *Structural Engineering Report No. 242*, Department of Civil and Environmental Engineering, University of Alberta, AB, Canada, 355 pp.

Ospina, C. E.; Alexander, S. D. B.; and Cheng, J. J. R., 2003, "Punching of Two-way Concrete Slabs with Fiber-Reinforced Polymer Reinforcing Bars or Grids," *ACI Structural Journal*, V. 100, No. 5, Sept.-Oct., pp. 589-598.

Ospina, C. E., and Bakis, C. E., 2007, "Indirect Flexural Crack Control of Concrete Beams and One-Way Slabs Reinforced with FRP Bars," *Proceedings of the 8th International*

Symposium on Fiber Reinforced Polymer Reinforcement for Concrete Structures (FRPRCS-8), T.C. Triantafillou, ed., University of Patras, Greece. (CD-ROM).

Ospina, C. E., and Gross, S. P., 2005, "Rationale for the ACI 440.1R-06 Indirect Deflection Control Design provisions," *Proceedings of the 7th International Symposium on Fiber-Reinforced Polymer (FRP) Reinforcement for Concrete Structures (FRPRCS-7)*, SP-230, C. Shield, J. Busel, S. Walkup, and D. Gremel, eds., American Concrete Institute, Farmington Hills, MI, pp. 651-670.

Pantelides, C. P.; Besser, B. T.; and Liu, R., 2012a, "One-Way Shear Behavior of Lightweight Concrete Panels Reinforced with GFRP Bars," *Journal of Composites for Construction*, V. 16, No. 1, Feb., pp. 2-9. doi: 10.1061/(ASCE)CC.1943-5614.0000240

Pantelides, C. P.; Liu, R.; and Reaveley, L. D., 2012b, "Lightweight Concrete Precast Bridge Deck Panels Reinforced with Glass Fiber-Reinforced Polymer Bars," *ACI Structural Journal*, V. 109, No. 6, Nov.-Dec., pp. 879-888.

Pantelides, C. P.; Gibbons, M. E.; and Reaveley, L. D., 2013, "Axial Load Behavior of Concrete Columns Confined with GFRP Spirals," *Journal of Composites for Construction*, V. 17, No. 3, June, pp. 305-313. doi: 10.1061/(ASCE)CC.1943-5614.0000357

Pearson, C.; Donchev, T.; and Limbachiya, M., 2011, "An Investigation into the Sustainability of FRP Reinforcement Bars," *CDC-11 4th International Conference on Durability and Sustainability of Fibre Reinforced Polymer (FRP) Composites for Construction and Rehabilitation*, Quebec City, Canada, July, pp. 71-80.

Porter, M. L., and Barnes, B. A., 1998, "Accelerated Aging Degradation of Glass Fiber Composites," *Second International Conference on Composites in Infrastructure*, V. II, H. Saadatmanesh and M. R. Eshani, eds., University of Arizona, Tucson, AZ, pp. 446-459.

Porter, M. L.; Hughes, B. W.; Barnes, B. A.; and Viswanath, K. P., 1993, "Non-Corrosive Tie Reinforcing and Dowel Bars for Highway Pavement Slabs," *Report No. HR-343*, Iowa Highway Research Board and Iowa Department of Transportation, Ames, IA.

Porter, M. L.; Mehus, J.; Young, K. A.; O'Neil, E. F.; and Barnes, B. A., 1997, "Aging for Fiber Reinforcement in Concrete," *Proceedings of the Third International Symposium on Non-Metallic (FRP) Reinforcement for Concrete Structures (FRPRCS-3)*, V. 2, Japan Concrete Institute, Tokyo, Japan, pp. 59-66.

Portland Cement Association, 1990, "Concrete Floors on Ground," Skokie, IL, 36 pp.

Portland Cement Association, 2008, *Notes on ACI 318-08 Building Code Requirements for Structural Concrete*, M. Kamara, L. Novak, and B. Rabbat, eds., Portland Cement Association, Skokie, IL, 1028 pp.

Priestley, M. N.; Seible, F.; and Calvi, G. M., 1996, *Seismic Design and Retrofit of Bridges*, John Wiley and Sons, New York, 704 pp.

Rahman, A. H.; Kingsley, C. Y.; and Crimi, J., 1996, "Durability of FRP Grid Reinforcement," *Advanced Composite Materials in Bridges and Structures*, M. M. El-Badry, ed.,

Canadian Society for Civil Engineering, Montreal, QC, Canada, pp. 681-690.

Rahman, A. H., and Kingsley, C. Y., 1996, "Fatigue Behavior of a Fiber-Reinforced-Plastic Grid as Reinforcement for Concrete," *Proceedings of the First International Conference on Composites in Infrastructure (ICCI-96)*, H. Saadatmanesh and M. R. Ehsani, eds., Tucson, AZ, pp. 427-439.

Rahman, H.; Adimi, R.; and Crimi, J., 1997, "Fatigue Behavior of a Carbon FRP Grid Encased in Concrete," *Proceedings of the Third International Symposium on Non-Metallic (FRP) Reinforcement for Concrete Structures (FRPRCS-3)*, V. 2, Japan Concrete Institute, Tokyo, Japan, pp. 219-226.

Rasheed, H. A.; Nayal, R.; and Melhem, H. G., 2004, "Response Prediction of Concrete Beams Reinforced with FRP Bars," *Composite Structures*, V. 65, No. 2, pp. 193-204. doi: 10.1016/j.compstruct.2003.10.016

Razaqpur, A. G.; Svecova, D.; and Cheung, M. S., 2000, "Rational Method for Calculating Deflection of Fiber-Reinforced Polymer Reinforced Beams," *ACI Structural Journal*, V. 97, No. 1, Jan.-Feb., pp. 175-185.

Rizkalla, S. H., 1997, "A New Generation of Civil Engineering Structures and Bridges," *Proceedings of the Third International Symposium on Non-Metallic (FRP) Reinforcement for Concrete Structures (FRPRCS-3)*, V. 1, Japan Concrete Institute, Tokyo, Japan, pp. 113-128.

Robert, M. and Benmokrane, B., 2010, "Behaviour of GFRP Reinforcing Bars Subjected to Extreme Temperature," *Journal of Composites for Construction*, V. 14, No. 4, pp. 353-360

Robert, M., and Benmokrane, B., 2013, "Combined Effects of Saline Solution and Moist Concrete on Long-Term Durability of GFRP Reinforcing Bars," *Journal of Construction and Building Materials*, V. 38, Jan, pp. 274-284. doi: 10.1016/j.conbuildmat.2012.08.021

Robert, M.; Cousin, P.; and Benmokrane, B., 2009, "Durability of GFRP Reinforcing Bars Embedded in Moist Concrete," *Journal of Composites for Construction*, V. 13, No. 2, pp. 66-73. doi: 10.1061/(ASCE)1090-0268(2009)13:2(66)

Rostasy, F. S., 1997, "On Durability of FRP in Aggressive Environments," *Proceedings of the Third International Symposium on Non-Metallic (FRP) Reinforcement for Concrete Structures (FRPRCS-3)*, V. 2, Japan Concrete Institute, Tokyo, Japan, pp. 107-114.

Roylance, M., and Roylance, O., 1981, "Effect of Moisture on the Fatigue Resistance of an Aramid-Epoxy Composite," *Organic Coatings and Plastics Chemistry*, American Chemical Society, Washington, DC, V. 45, pp. 784-788.

Saadatmanesh, H., and Ehsani, M. R., eds., 1998, "Fiber Composites in Infrastructure," *Proceedings of the Second International Conference on Composites in Infrastructure (ICCI-98)*, Tucson, AZ.

Saadatmanesh, H., and Tannous, F. E., 1999a, "Relaxation, Creep, and Fatigue Behavior of Carbon Fiber-Reinforced Plastic Tendons," *ACI Materials Journal*, V. 96, No. 2, Mar.-Apr., pp. 143-153.

Saadatmanesh, H., and Tannous, F. E., 1999b, "Long-Term Behavior of Aramid Fiber-Reinforced Plastic Tendons," *ACI Materials Journal*, V. 96, No. 3, May-June, pp. 297-305.

Santoh, N., 1993, "CFCC (Carbon Fiber Composite Cable)," *Fiber-Reinforced-Plastic (FRP) Reinforcement for Concrete Structures: Properties and Applications, Developments in Civil Engineering*, V. 42, A. Nanni, ed., Elsevier, Amsterdam, pp. 223-247.

Sasaki, I.; Nishizaki, I.; Sakamoto, H.; Katawaki, K.; and Kawamoto, Y., 1997, "Durability Evaluation of FRP Cables by Exposure Tests," *Proceedings of the Third International Symposium on Non-Metallic (FRP) Reinforcement for Concrete Structures (FRPRCS-3)*, V. 2, Japan Concrete Institute, Tokyo, Japan, pp. 131-137.

Scheibe, M., and Rostasy, F. S., 1998, "Stress-Rupture Behavior of AFRP Bars in Concrete and Under Natural Environment," *Second International Conference on Composites in Infrastructure*, V. II, H. Saadatmanesh and M. R. Eshani, eds., University of Arizona, Tucson, AZ, pp. 138-151.

Seki, H.; Sekijima, K.; and Konno, T., 1997, "Test Method on Creep of Continuous Fiber Reinforcing Materials," *Proceedings of the Third International Symposium on Non-Metallic (FRP) Reinforcement for Concrete Structures (FRPRCS-3)*, V. 2, Japan Concrete Institute, Tokyo, Japan, pp. 195-202.

Sen, R.; Shahawy, M.; Sukumar, S.; and Rosas, J., 1998a, "Effect of Tidal Exposure on Bond of CFRP Rods," *Second International Conference on Composites in Infrastructure*, V. II, H. Saadatmanesh and M. R. Eshani, eds., University of Arizona, Tucson, AZ, pp. 512-523.

Sen, R.; Shahawy, M.; Rosas, J.; and Sukumar, S., 1998b, "Durability of Aramid Pretensioned Elements in a Marine Environment," *ACI Structural Journal*, V. 95, No. 5, Sept.-Oct., pp. 578-587.

Shield, C.; French, C.; and Hanus, J., 1999, "Bond of GFRP Rebar for Consideration in Bridge Decks," *Fourth International Symposium on Fiber Reinforced Polymer Reinforcement for Reinforced Concrete Structures*, SP-188, C. W. Dolan, S. H. Rizkalla, and A. Nanni, eds., American Concrete Institute, Farmington Hills, MI, pp. 393-406.

Shield, C.; French, C.; and Retika, A., 1997, "Thermal and Mechanical Fatigue Effects on GFRP Rebar-Concrete Bond," *Proceedings of the Third International Symposium on Non-Metallic (FRP) Reinforcement for Concrete Structures (FRPRCS-3)*, V. 2, Japan Concrete Institute, Tokyo, Japan, pp. 381-388.

Shield, C., Galambos, T., and Gulbrandsen, P., 2011, "On the History and Reliability of the Flexural Strength of FRP Reinforced Concrete Members in ACI 440.1R," *10th International Symposium on Fiber Reinforced Polymer Reinforcement for Concrete Structures*, SP-275, R. Sen, R. Seracino, C. Shield, and W. Gold, eds., American Concrete Institute, Farmington Hills, MI, pp. 1-18.

Sippel, T. M., and Mayer, U., 1996, "Bond Behavior of FRP Strands under Short-Term, Reversed and Cyclic Loading," *Proceedings of the Second International Conference on Advanced Composite Materials in Bridges and Structures (ACMBS-2)*, M. M. El-Badry, ed., Canadian Society for Civil Engineering, Montreal, QC, Canada, pp. 837-844.

Sonobe, Y.; Fukuyama, H.; Okamoto, T.; Kani, N.; Kimura, K.; Kobayashi, K.; Masuda, Y.; Matsuzaki, Y.; Mochizuki,

S.; Nagasaka, T.; Shimizu, A.; Tanano, H.; Tanigaki, M.; and Tenshigawara, M., 1997, "Design Guidelines of FRP Reinforced Concrete Building Structures," *Journal of Composites for Construction*, V. 1, No. 3, pp. 90-115. doi: 10.1061/(ASCE)1090-0268(1997)1:3(90)

Szerszen, M., and Nowak, A., 2003, "Calibration of Design Code for Buildings (ACI 318): Part 2—Reliability Analysis and Resistance Factors," *ACI Structural Journal*, V. 100, No. 3, May-June, pp. 383-391.

Taerwe, L., ed., 1995, "Non-Metallic (FRP) Reinforcement for Concrete Structures," *Proceedings of the Second International RILEM Symposium on Non-Metallic (FRP) Reinforcement for Concrete Structures (FRPRCS-2)*, Ghent, Belgium, 714 pp.

Taerwe, L., 1997, "FRP Activities in Europe: Survey of Research and Applications," *Proceedings of the Third International Symposium on Non-Metallic (FRP) Reinforcement for Concrete Structures (FRPRCS-3)*, V. 1, Japan Concrete Institute, Tokyo, Japan, pp. 59-74.

Takewaka, K., and Khin, M., 1996, "Deterioration of Stress-Rupture of FRP Rods in Alkaline Solution Simulating as Concrete Environment," *Advanced Composite Materials in Bridges and Structures*, M. M. El-Badry, ed., Canadian Society for Civil Engineering, Montreal, QC, Canada, pp. 649-664.

Tamura, T., 1993, "FiBRA," *Fiber-Reinforced-Plastic (FRP) Reinforcement for Concrete Structures: Properties and Applications, Developments in Civil Engineering*, V. 42, A. Nanni, ed., Elsevier, Amsterdam, pp. 291-303.

Tannous, F. E., and Saadatmanesh, H., 1999, "Durability of AR-Glass Fiber Reinforced Plastic Bars," *Journal of Composites for Construction*, V. 3, No. 1, pp. 12-19. doi: 10.1061/(ASCE)1090-0268(1999)3:1(12)

Teng, J.-G., ed., 2001, "FRP Composites in Civil Engineering," *Proceedings CICE 2001*, Hong Kong, China, V. 1 and 2.

Tepfers, R., 2002, "Test System for Evaluation of Bond Properties of FRP Reinforcement in Concrete," *Proceedings of the Third International Symposium on Bond in Concrete—From Research to Standards*, Budapest, Hungary, pp. 657-666.

Theriault, M., and Benmokrane, B., 1998, "Effects of FRP Reinforcement Ratio and Concrete Strength on Flexural Behavior of Concrete Beams," *Journal of Composites for Construction*, V. 2, No. 1, pp. 7-16. doi: 10.1061/(ASCE)1090-0268(1998)2:1(7)

Tighiouart, B.; Benmokrane, B.; and Gao, D., 1998, "Investigation of Bond in Concrete Member with Fiber Reinforced Polymer (FRP) Bars," *Construction and Building Materials Journal*, Dec., 10 pp.

Tighiouart, B.; Benmokrane, B.; and Mukhopadhyaya, P., 1999, "Bond Strength of Glass FRP Rebar Splices in Beams under Static Loading," *Construction & Building Materials*, V. 13, No. 7, pp. 383-392. doi: 10.1016/S0950-0618(99)00037-9

Tobbi, H.; Farghaly, A. S.; and Benmokrane, B., 2012, "Concrete Columns Reinforced Longitudinally and Transversally with Glass Fiber-Reinforced Polymers Bars," *ACI Structural Journal*, V. 109, No. 4, July-Aug., pp. 551-558.

Tokyo Rope, 2000, "CFCC, Carbon Fiber Composite Cable," *Product Circular* No. 991-2T-SA, Tokyo Rope Manufacturing Co., Tokyo, <http://www.tokyorope.co.jp/>

Tomosawa, F., and Nakatsuji, T., 1996, "Evaluation of the ACM Reinforcement Durability by Exposure Test," *Advanced Composite Materials in Bridges and Structures*, M. M. El-Badry, ed., Canadian Society for Civil Engineering, Montreal, QC, Canada, pp. 699-706.

Tomosawa, F., and Nakatsuji, T., 1997, "Evaluation of the ACM Reinforcement Durability by Exposure Test," *Proceedings of the Third International Symposium on Non-Metallic (FRP) Reinforcement for Concrete Structures (FRPRCS-3)*, V. 2, Japan Concrete Institute, Tokyo, Japan, pp. 139-146.

Toutanji, H., and Saafi, M., 2000, "Flexural Behavior of Concrete Beams Reinforced with Glass Fiber-Reinforced Polymer (GFRP) Bars," *ACI Structural Journal*, V. 97, No. 5, Sept.-Oct., pp. 712-719.

Tureyen, A. K., and Frosch, R. J., 2002, "Shear Tests of FRP Reinforced Concrete Beams without Stirrups," *ACI Structural Journal*, V. 99, No. 4, July-Aug., pp. 427-434.

Tureyen, A. K., and Frosch, R. J., 2003, "Concrete Shear Strength: Another Perspective," *ACI Structural Journal*, V. 100, No. 5, Sept.-Oct., pp. 609-615.

Uomoto, T., 2000, "Durability of FRP as Reinforcement for Concrete Structures," *Proceedings of the 3rd International Conference on Advanced Composite Materials in Bridges and Structures*, ACMB3-3, J. L. Humar and A. G. Razaqpur, eds., Canadian Society for Civil Engineering, Montreal, QC, Canada, pp. 3-17.

Uppuluri, V. S.; Bakis, C. E.; Nanni, A.; and Boothby, T. E., 1996, "Analysis of the Bond Mechanism in FRP Reinforcement Rods: The Effect of Rod Design and Properties," *Proceedings of the Second International Conference on Advanced Composite Materials in Bridges and Structures (ACMB3-II)*, Montreal, QC, Canada, pp. 893-900.

Vijay, P. V., and GangaRao, H. V. S., 1999, "Accelerated and Natural Weathering of Glass Fiber Reinforced Plastic Bars," *Fourth International Symposium on Fiber Reinforced Polymer Reinforcement for Reinforced Concrete Structures*, SP-188, C. W. Dolan, S. H. Rizkalla, and A. Nanni, eds., American Concrete Institute, Farmington Hills, MI, pp. 605-614.

Vijay, P. V.; GangaRao, H. V. S.; and Kalluri, R., 1998, "Hygrothermal Response of GFRP Bars under Different Conditioning Schemes," *Proceedings of the First International Conference (CDCC 1998)*, Sherbrooke, QC, Canada, pp. 243-252.

Wambeke, B., and Shield, C., 2006, "Development Length of Glass Fiber Reinforced Polymer Bars in Concrete," *ACI Structural Journal*, V. 103, No. 1, Jan.-Feb., pp. 11-17.

Wang, J., 1998, "Determination of the Shear Resistance of Concrete Beams and Slabs Reinforced with Fibre Reinforced Plastics," MS thesis, Carleton University, Ottawa, ON, Canada.

White, T. D., ed., 1992, "Composite Materials and Structural Plastics in Civil Engineering Construction," *Proceedings of the Materials Engineering Congress*, ASCE, Reston, VA, pp. 532-718.

Wicaksono, S., and Chai, G. B., 2013, "A Review of Advances in Fatigue and Life Prediction of Fiber-Reinforced Composites," *Journal of Materials Design and Applications*, V. 227, pp. 179-195.

Wu, W. P., 1990, "Thermomechanical Properties of Fiber Reinforced Plastic (FRP) Bars," PhD dissertation, West Virginia University, Morgantown, WV, 292 pp.

Yamaguchi, T.; Kato, Y.; Nishimura, T.; and Uomoto, T., 1997, "Creep Rupture of FRP Rods Made of Aramid, Carbon and Glass Fibers," *Proceedings of the Third International Symposium on Non-Metallic (FRP) Reinforcement for Concrete Structures (FRPRCS-3)*, V. 2, Japan Concrete Institute, Tokyo, Japan, pp. 179-186.

Ye, L. P.; Feng, P.; Zhang, K.; Lin, L.; Hong, W. H.; Yue, Q. R.; Zhang, N.; and Yang, T., 2003, "FRP in Civil Engineering in China: Research and Applications," *Proceedings of the Sixth International Symposium on FRP Reinforcement for Concrete Structures (FRPRCS-6)*, K. H. Tan, ed., Singapore, 1401 pp.

Yost, J.; Gross, S.; and Dinehart, D., 2003, "Effective Moment of Inertia for GFRP Reinforced Concrete Beams," *ACI Structural Journal*, V. 100, No. 6, Nov.-Dec., pp. 732-739.

Zaidi, A., and Masmoudi, R., 2008, "Thermal Effect on Fiber Reinforced Polymer Reinforced Concrete Slabs," *Canadian Journal of Civil Engineering*, V. 35, No. 3, Mar., pp. 312-320. doi: 10.1139/L07-110

Zaidi, A.; Masmoudi, R.; and Bouhicha, M., 2013, "Numerical Analysis of Thermal Stress-Deformation in Concrete Surrounding FRP Bars in Hot Region," *Construction & Building Materials*, V. 38, Jan, pp. 204-213. doi: 10.1016/j.conbuildmat.2012.08.047

Zhao, W.; Maruyama, K.; and Suzuki, H., 1995, "Shear Behavior of Concrete Beams Reinforced by FRP Rods as Longitudinal and Shear Reinforcement," *Proceedings of the Second International RILEM Symposium on Non-Metallic (FRP) Reinforcement for Concrete Structures (FRPRCS-2)*, Ghent, Belgium, pp. 352-359.

APPENDIX A—SLABS-ON-GROUND

Two of the most common types of construction for slabs-on-ground are discussed in this appendix: plain concrete slabs and slabs reinforced with temperature and shrinkage reinforcement.

A.1—Design of plain concrete slabs

Plain concrete slabs-on-ground transmit loads to the subgrade with minimal distress and are designed to remain uncracked under service loads. To reduce shrinkage crack effects, the spacing of construction joints, contraction joints, or both, is usually limited. For details of design methods of plain concrete slabs-on-ground, refer to ACI 360R.

A.2—Design of slabs with shrinkage and temperature reinforcement

When designing a slab with shrinkage and temperature reinforcement, it should be considered a plain concrete slab

without reinforcement to determine its thickness. The slab is assumed to remain uncracked when loads are placed on its surface. Shrinkage crack width and spacing are limited by a nominal amount of distributed fiber-reinforced polymer (FRP) reinforcement placed in the upper half of the slab. The primary purpose of shrinkage reinforcement is to control the width of any crack that forms between joints. Shrinkage reinforcement does not prevent cracking, nor does it significantly add to the flexural capacity of the slab. Increasing the thickness of the slab can increase the flexural capacity.

Although the slab is intended to remain uncracked under service loading, the reinforcement is used to limit crack spacing and width, permit the use of wider joint spacing, increase the ability to transfer load at joints, and provide a reserve strength after shrinkage or temperature cracking has occurred.

The subgrade drag method is frequently used to determine the amount of nonprestressed shrinkage and temperature reinforcement that is needed, but does not apply when prestressing or randomly distributed fibers are used (Portland Cement Association 1990). When using steel reinforcement, the drag equation is as follows

$$A_s = \frac{\mu L w_{slab}}{2 f_{s,allow}} \quad (A.2a)$$

where A_s is the cross-sectional area of steel per linear foot, in.² (mm² per linear meter); $f_{s,allow}$ is the allowable stress in steel reinforcement, psi (MPa), commonly taken as two-thirds to three-fourths of f_y ; μ is the coefficient of subgrade friction (1.5 is recommended for floors on ground [Portland Cement Association 1990]); L is the distance between joints, ft (m); and w is the dead weight of the slab, lb/ft² (N/m²), usually assumed to be 12.5 lb/ft² per in. of slab thickness (24 N/m² per mm).

Because of the lower modulus of the FRP reinforcement, the governing equation should be based on the strain rather than the stress level when designing shrinkage and temperature FRP reinforcement. At the allowable stress, the strain in steel reinforcement is approximately 0.0012; implementing the same strain for FRP will result in a stress of $0.0012E_f$, and Eq. (A.2a) can be written as

$$A_{f,sh} = \frac{\mu L w}{2(0.0012E_f)} \quad (A.2b)$$

Equation (A.2b) can also be used to determine joint spacing L for a set amount of reinforcement. No experimental data have been reported on FRP slab-on-ground applications; research is required to validate this approach.



American Concrete Institute
Always advancing

As ACI begins its second century of advancing concrete knowledge, its original chartered purpose remains “to provide a comradeship in finding the best ways to do concrete work of all kinds and in spreading knowledge.” In keeping with this purpose, ACI supports the following activities:

- Technical committees that produce consensus reports, guides, specifications, and codes.
- Spring and fall conventions to facilitate the work of its committees.
- Educational seminars that disseminate reliable information on concrete.
- Certification programs for personnel employed within the concrete industry.
- Student programs such as scholarships, internships, and competitions.
- Sponsoring and co-sponsoring international conferences and symposia.
- Formal coordination with several international concrete related societies.
- Periodicals: the ACI Structural Journal, Materials Journal, and Concrete International.

Benefits of membership include a subscription to Concrete International and to an ACI Journal. ACI members receive discounts of up to 40% on all ACI products and services, including documents, seminars and convention registration fees.

As a member of ACI, you join thousands of practitioners and professionals worldwide who share a commitment to maintain the highest industry standards for concrete technology, construction, and practices. In addition, ACI chapters provide opportunities for interaction of professionals and practitioners at a local level.

American Concrete Institute
38800 Country Club Drive
Farmington Hills, MI 48331
Phone: +1.248.848.3700
Fax: +1.248.848.3701

www.concrete.org



American Concrete Institute
Always advancing

38800 Country Club Drive
Farmington Hills, MI 48331 USA
+1.248.848.3700
www.concrete.org

The American Concrete Institute (ACI) is a leading authority and resource worldwide for the development and distribution of consensus-based standards and technical resources, educational programs, and certifications for individuals and organizations involved in concrete design, construction, and materials, who share a commitment to pursuing the best use of concrete.

Individuals interested in the activities of ACI are encouraged to explore the ACI website for membership opportunities, committee activities, and a wide variety of concrete resources. As a volunteer member-driven organization, ACI invites partnerships and welcomes all concrete professionals who wish to be part of a respected, connected, social group that provides an opportunity for professional growth, networking and enjoyment.

